An Obese Genotype Affects the Sphingolipid Signaling Pathway

by

Erin L. Burrows

A thesis
presented to the University of Waterloo
in fulfillment of the
thesis requirement for the degree of
Master of Science
in
Biology

Waterloo, Ontario, Canada, 2008

I hereby declare that I am the sole author of this thesis. This is a true copy of the thesis, including any required final revisions, as accepted by my examiners.

I understand that my thesis may be made electronically available to the public.

Abstract

Sphingolipids are important signaling molecules regulating cell growth, cell death and differentiation, thus making them important molecules in determining the fate of a cell and in the pathogenesis of chronic illnesses. The sphingolipid signaling pathway can be initiated by reactive oxygen species (ROS) and inflammatory molecules, both of which are believed to be upregulated in a state of obesity. The hypothesis tested in this dissertation is that due to the inflammatory state of obese animals, the sphingolipid pathway is altered, shifting the balance of pro- and anti-apoptotic proteins and contributing to the pathogenesis of diseases associated with an obese state. The specific aims were to compare, 1) key sphingolipid signaling enzymes; 2) levels of sphingolipid signaling molecules and 3) pro and anti-apoptotic protein levels, in hepatic and colonic tissues procured from lean and obese animals.

Obese animals are susceptible to various diseases, including colon cancer and hepatic steatosis. To assess the effect of obesity on sphingolipid signaling, and to provide insight as to the pathogenesis of diseases in a state of obesity, liver and colon tissues from Zucker obese female rats (fa/fa) were compared to tissues from their lean counterparts (Fa/fa or Fa/Fa Zucker rats). Enzyme analyses included an assay of sphingomyelinase (SMase) activity and quantification of ceramidase and sphingosine kinase-1 (SK1) protein expression by western blot. Also, sphingomyelin (SM), ceramide, ceramide-1 phosphate (C1P), sphingosine and sphingosine-1-phosphate (S1P) levels were determined by high-performance liquid chromatography (HPLC) -tandem mass spectroscopy (MS). Representative apoptotic proteins, Bax and Bcl-2 were quantified by western blot.

Obese liver demonstrates hepatic steatosis in the Zucker animal model. Among the major differences noted between obese and lean liver were significantly upregulated ceramidase, and downregulated SK1 and C1P levels ($P<0.05$), as well as a difference in ceramide and SM species composition. Bax was overexpressed while Bcl-2 level was lower in obese compared to lean liver ($P<0.05$). Taken together, the results indicate a shift toward higher apoptotic signaling in obese liver tissue and correspond with the diseased state of the steatotic liver.

Analysis of the sphingolipid pathway in colon revealed upregulation of ceramidase and downregulation of SK1 ($P<0.05$), similar to liver tissue. C1P levels were lower ($P<0.05$) but no changes were observed for ceramide, SM or sphingosine levels. A trend toward higher SMase activity

in obese colon was observed. Bax was overexpressed in obese colon tissue ($P< 0.05$), while Bcl-2 results were inconclusive.

The liver expressed lower level of molecules associated with sphingolipid signaling than the colons. This study is first to demonstrate tissue-specific differences in the sphingolipid signaling pathway, regardless of genotype. Nevertheless, overall the genotype of Zucker model was found to be a factor altering the expression levels of various sphingolipid enzymes and metabolites in both colon and liver. The findings of the present research provide incentive to further understand the role and modulation of sphingolipid signaling pathway in causation and prevention of chronic diseases prevalent in obese state.

Acknowledgements

I would like to thank my supervisor, Dr. Ranjana Bird, for the opportunity to be a part of her interesting research. I am especially grateful for the freedom I had in choosing my own project so that I could be passionate about what I was working on. I really appreciate your patience and trust in me.

I would also like to thank my co-supervisor, Dr. Matt Vijayan, for agreeing to take me on as a student for my final term. I really appreciate your support, guidance and advice while I finished my thesis and I cannot thank you enough for the extra time you had for me.

I would like to thank my committee members for agreeing to be part of my project: Dr. John Heikkila, Dr. Thomas Singer, and Dr. Heidi Engelhardt. Dr. Engelhardt, thank you for your open door and all your support. Also, a special thank you to Linda Zepf for having time for all my questions and concerns. Your kindness and optimism are much appreciated.

Thank you to Dr. Jacek Bielawski and the Lipidomics core at the Medical University of South Carolina for their services and cooperation.

All my lab colleagues thank you for your friendship and being a part of my research experience. I would especially like to thank Nita for being such a good teacher to me in the lab and being so patient to answer all my questions. I am very grateful to you for your help and the kindness you showed me when I first joined the lab. Annette, my confidante, thanks for all the great conversations and laughs both inside the lab and out.

Finally I would like to thank my family and friends for supporting me while I completed this project. Thanks to Mom, Dad, Kristen and Andrew. And last but not least, thanks to Melissa, Amy and Chris for helping me make the most of these last two years at Waterloo.

Table of Contents

List of Figures

List of Tables

Chapter 1
Introduction

1.1 Overview:

The objective of this thesis was to investigate the differences in the sphingolipid signaling pathway between lean and obese animals in liver and colon tissue for the purpose of investigating whether the sphingolipid pathway may be a contributing factor to the pathogenesis of hepatic steatosis and colon cancer in obese animals.

Sphingolipids are important signaling molecules regulating cell growth, cell death and differentiation, making them important molecules for determining the fate of cells. The sphingolipid signaling pathway can be initiated by reactive oxygen species (ROS) and inflammatory molecules. As obese animals are in a constant state of inflammation and are susceptible to various diseases, specifically hepatic steatosis and colon cancer, it is valuable to see if the sphingolipid signaling pathway is altered in this state and contributing to disease susceptibility. Any alteration of the sphingolipid pathway will result in a change in the balance between pro-apoptotic and anti-apoptotic proteins. The proteins that are involved in the sphingolipid signaling pathway, as well as key pro- and anti-apoptotic proteins, were compared in lean versus obese colon and liver. This provides insight into changes that occur to the sphingolipid pathway in a state of obesity and how these changes may contribute to the pathogenesis of various diseases.

The specific aims were to:

1) Analyze key sphingolipid signaling enzymes in lean versus obese animals.
2) Compare levels of sphingolipid signaling molecules in lean versus obese animals.
3) Analyze pro and anti-apoptotic protein levels in lean and obese animals.

Hypothesis: Due to the inflammatory state of obese animals, the sphingolipid pathway is altered, thus shifting the balance of pro- and antiapoptotic proteins and contributing to the pathogenesis of disease in an obese state.

The background information in the following sections describes the sphingolipid signaling pathway, obesity, hepatic steatosis, and colon cancer as it relates to this thesis.

1.2 Sphingomyelin and its Signaling Cascade

1.2.1 Sphingomyelin Pathway

Sphingolipids have emerged as important signaling molecules mediating cell proliferation, differentiation and apoptosis. The sphingomyelin signaling cascade, in particular, has received a lot of attention for its role in the pathology of several human diseases, including Alzheimer's disease, atherosclerosis, and a number of cancers. Sphingomyelin (SM) is a main phospholipid component of animal cell membranes. It is especially concentrated in membranous myelin sheaths of myelinated nerves. SM consists of sphingosine (a long, unsaturated fatty acid chain) attached to a fatty acid and choline (a polar head group) (Fig.1). The ceramide backbone of sphingolipids is generated in the endoplasmic reticulum, while the polar head groups are added in the golgi apparatus.

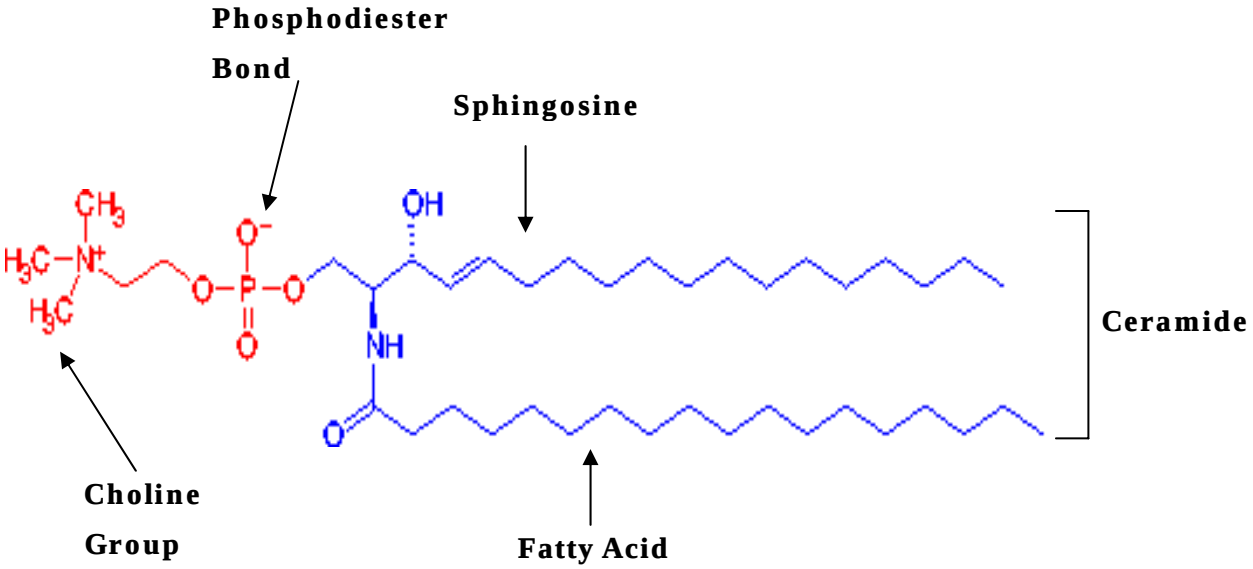

Figure 1: Structure of sphingomyelin

Most sphingolipids reside in membrane bilayers and are concentrated in lipid rafts (Levade, 2001). Due to its location, sphingomyelin was long believed to serve only structural roles, providing a barrier to the extracellular environment (Kolesnick, 2002). More recent studies have demonstrated the existence of a sphingomyelin signaling cascade, initiated when sphingomyelin becomes hydrolyzed into secondary messengers. Three main secondary messengers of sphingomyelin are now recognized: ceramide, sphingosine, and sphingosine-1-phosphate (S1P), though there are many other sphingolipid derivatives. The various conversions between molecules in the sphingolipid pathway are illustrated below (Fig. 2).

The pathway is initiated by the hydrolysis of the phosphodiester bond of sphingomyelin *via* the enzyme, sphingomyelinase (SMase). The action of SMase on sphingomyelin releases ceramide, a pro-apoptotic signaling molecule (discussed in section 1.3). Alternatively, ceramides can be formed by de novo synthesis, whereby the amino acid serine is condensed sequentially with two fatty acids by the actions of serine palmitoyl transferase and ceramide synthase. Ceramides can be converted back to SM by the transfer of phosporylcholine from the phospholipid phosphatidylcholine to ceramide *via* the enzyme SM synthase.

Once generated, ceramide may accumulate or may be transformed to other metabolites, including sphingosine. Ceramide is converted to sphingosine when it is deacetylated by ceramidase. Ceramide can also be phosphorylated to ceramide 1 phosphate (C1P) by the action of ceramide kinase (CerK). C1P can readily be converted back to ceramide by the action of phosphatidic acid phosphohydralase. Sphingosine can be converted back to ceramide via the enzyme ceramide synthase or can be further converted to the proliferative molecule, S1P, through phosphorylation via sphingosine kinase. This phosphorylation is easily reversible via the enzyme sphingosine-1-phosphate phosphatase, which dephosphorylates S1P back to sphingosine.

The metabolites that result from the action of sphingomyelinase play varied roles in cell signaling (discussed in Section 1.3). The relative levels of these molecules as well as the enzymes that convert them may be important indicators of the fate of cells in a given tissue type. A deeper knowledge of these molecules will be beneficial for understanding the role they play in several human diseases.

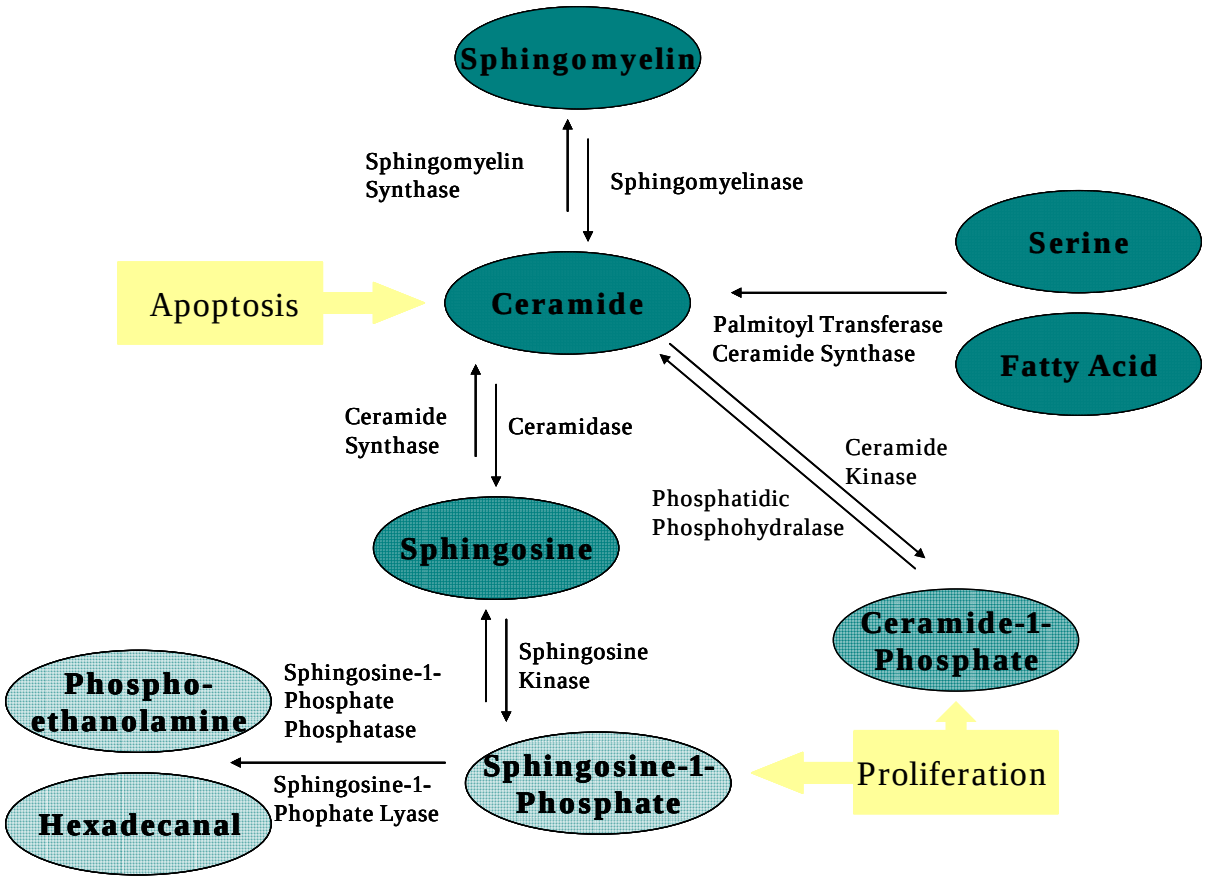

Figure 2: Schematic of sphingomyelin signaling cascade, showing the conversions between apoptotic signal ceramide and proliferative signals, SIP and C1P.

1.2.2 Sphingomyelinase

Sphingomyelinase, with its phospholipase C activity, initiates the sphingomyelin signaling pathway by hydrolyzing the phosphodiester bond of SM. Three distinct isoforms of SMase have been identified based on their pH optima: neutral SMase, acid SMase and alkaline SMase (Kolesnick, 2002). The pH affects the on-off rate of the substrate to SMase, rather than the catalytic activity of the enzyme (Schissel et al., 1998). Neutral SMase (pH optimum 7.4) and acid SMase (pH optimum 4.5-5.0) are similar in structure and function and are present in all cell types (Kolesnick, 2002), while alkaline SMase (optimal pH 9-9.5) is structurally distinct and is found only in the gastrointestinal tract (Cheng et al., 2002).

Alkaline SMase, discovered in 1969 by Nilsson, may be important in the digestion of dietary SM (Cheng et al., 2004). This belief is due to studies that indicate that dietary SM is not hydrolyzed by pancreatic juice, and SM digestion occurs where alkaline SMase levels are abundant – in the middle and lower small intestine (Cheng et al., 2002). This enzyme may play a protective role in colon carcinogenesis, as feeding mice with ceramide or SM reduced the number of aberrant crypt foci (Schmelz, et al., 1997; Schmelz et al., 1999). Furthermore, in human adenoma and colonic carcinoma, the activities of alkaline sphingomyelinase are reduced by 50% and 75%, respectively (Herervig et al. 1996).

Acid sphingomyelinase was long believed to be exclusively a lysosomal enzyme (Kolesnick, 2002). However, more recent studies have isolated acid SMase from secretory vesicles near plasma membranes (Grassme et al., 2001), and an acidic sphingomyelinase has been found to be secreted extracellularly from macrophages, fibroblasts and endothelial cells (Schissel et al., 2006; Marathe et al., 1998). Acidic SMase has also been observed in caveolae, microdomains rich in SM (Liu et al., 1995). In acidic SMase knockout mice, residual SMase activity remains (Horinouchi et al., 1995), demonstrating the existence of one or more distinct genes that must encode such enzymes. Neutral sphingomyelinase is indeed genetically distinct from acidic sphingomyelinase (Chatterjee, 1999). It is magnesium dependent and is considered a membrane-bound enzyme (Chatterjee, 1993).

Neutral and acidic SMases are activated by a wide range of stressors to increase cellular ceramide levels. Inducers of SMase include tumor necrosis factor alpha (TNF-α), interleukin-1 beta (IL-1β),

Fas ligand, as well as UV-exposure, free fatty acids, radiation and oxidative stress (Woodock, 2006; Ogretmen, 2006; Kolesnick, 2002). This ability of sphingomyelinase to convert stress signals into biochemical messengers is what makes it an important and interesting enzyme to be studied in many disease processes.

1.2.3 Ceramidase

Ceramidase (N-acylsphingosine deacylase) further participates in the modulation of the signal transduction pathway. It cleaves the N-acyl linkage of ceramide to produce sphingosine and a fatty acid (Tani et al., 1998). Ceramidase exists in mammals as a 55kDa precursor protein that can be cleaved to a mature 40kDa protein. Like sphingomyelinase, this enzyme can also be classified according to its optimal pH into acid and neutral and alkaline isoforms, coded for by different genes (Kolesnick, 2002; Xu et al., 2006).

Acid ceramidase is synthesized as a precursor polypeptide that is proteolytically processed into alpha and beta subunits (Park et al., 2006). With an optimal pH of 4.0-5.0, acid ceramidase is found mainly in lysosymes and cell membranes, though a portion of the enzyme may be secreted and other subcellular locations may exist (Park et al., 2006). A recently identified alkaline, ceramidase (Xu et al., 2006), has been found localized to the golgi complex. Overexpression of this enzyme can lead to sphingosine accumulation within cells. Neutral ceramidase is found in kidney and intestinal cells (Olsson et al., 2004). It has been postulated that this enzyme is necessary in the gastrointestinal tract to metabolize dietary and brush border ceramide (Olsson et al., 2004).

1.2.4 Sphingosine Kinase

Sphingosine kinase is responsible for the phosphorylation of sphingosine, yielding the sphingolipid metabolite, S1P. Two distinct isoforms of sphingosine kinase, SK1 and SK2, have been identified and cloned (Kahoma et al., 1998; Liu et al., 2000). SK1 can be stimulated by external stimuli, particularly growth and survival factors. Recognized inducers of SK1 include platelet-derived growth factor (PDGF) and TNF-α, among others (Olivera et al., 1999; Huang et al., 2007). It is well established that S1P produced by SK1 inhibits apoptosis and promotes cell growth and proliferation (reviewed in Maceyka et al., 2002).

Much less is known about SK2, though it appears to have a distinct physiological role from SK1. SIP derived from SK2 has been implicated in enhanced apoptosis and suppressed growth, which contrasts the proliferative effects of SK1-derived S1P (Liu et al., 2003; Igarashi et al., 2003). While the SKs appear to have distinct functions, the two enzymes have highly similar amino acid sequences and possess five evolutionarily conserved domains. SK2 differs from SK1 only in its amino terminus and central region (Maceyka et al., 2005).

One possible explanation for the differential effects of these isoenzymes is that S1P may have distinct functions depending on which compartment of the cell it is produced in, and SK1 and SK2 have been found to be located or translocated to different areas within the cell. SK1 has been shown to be predominantly cytosolic and can be translocated to the plasma membrane by growth factors (Speigel et al., 2003). S1P produced by the translocation of SK1 can activate the cell surface receptor G protein-coupled receptors, also known as the Edg receptors (reviewed in Young et al., 2006). SK2, on the other hand, is found in low levels in the cytosol and has been found to be mainly localized to the plasma membrane and endoplasmic reticulum (Maceyka et al., 2005). S1P made by SK2 does not transactivate the Edg receptors. Treatment with an inhibitor of G-coupled S1P receptor does not interfere with the ability of SK2 to induce apoptosis (Liu et al., 2003). Despite the opposing implications of S1P produced by these two different isozymes, SK1 is the more predominant isozyme and, therefore, S1P is regarded as a promoter of cell growth and differentiation.

1.3 Sphingolipids in Cell Death/Survival

1.3.1 Altered Bcl-2 Proteins and Apoptotic Signaling by Ceramide and Sphingosine

The primary products of sphingomyelinase, ceramide and sphingosine, mediate and trigger apoptosis, while S1P is considered to be a survival molecule, promoting proliferation. Ceramide plays a role in apoptotic signaling by altering the biophysical characteristics of cellular membranes. The turnover of sphingomyelin at the plasma membrane results in sphingolipid-rich domains known as lipid rafts, where there is a clustering of receptors and signaling molecules (Ohanian and Ohanian, 2001). In this way, ceramide influences membrane receptor signaling.

The role of ceramide in apoptosis is not fully defined, though some preliminary associations have been determined. Cellular targets for ceramide include cathepsin D, ceramide-activated protein

phosphatases (CAPPs), and the stress activated protein kinases (SAPKs) among others. Binding of ceramide to cathepsin D *in vitro* or in endosomes prompts autolytic cleavage of cathepsin to its active form (Kolesnick, 2002). While the function of cathepsin D is not clearly defined as of yet, ceramide-induced activation of cathepsin D has been shown to mediate activation of Bid, a pro-apoptotic Bcl-2 family member (Heinrich et al., 2004). In studies where cathepsin D was inhibited in apoptotic stimulated cells, cells were able to survive or delay death (Johansson et al., 2003; Diess et al., 1996).

Both protein phosphatase 1 (PP1) and protein phosphatase 2a (PP2a) are serine/threonine CAPPS that will induce growth arrest or apoptosis in response to a rise in ceramide levels (Kolesnick, 2002). There are several targets for CAPPs, including protein kinase C alpha (PKCα), Akt/protein kinase B (PKB) and Bax. PKC is involved in signal transduction, and growth/metabolic regulation (Chalfant et al., 2006). PKC has been implicated as an anti-apoptotic molecule and it has been proposed that inactivation of PKCα is important in inducing apoptosis (Gamard et al., 1996). Studies performed on Molt-4 Leukemia cells indicate that PP2a inactivates PKC by removing critical phosphates, thus allowing the induction of apoptosis (Chalfant and Hannun, 2006). CAPP also inactivates Akt/PKB by dephosphorylation. Inactivated Akt/PKB is responsible for phosphorylating substrates such as caspase 9, which has been proposed as a necessary step in apoptosis (Cardone et al., 1998).

PP2a has more recently been shown to activate the pro-apoptotic Bcl-2 family member, Bax, through dephosphorylation. This dephosphorylation of Bax by PP2a has been shown to be mediated by ceramide and leads to subsequent cytochrome c release, caspase activation, and apoptosis (Xin et al., 2006). Ceramide has also been implicated in upregulating other pro-apoptotic Bcl-2 family members, including Bid and Bad, while downregulating antiapoptotic Bcl-2 and Bcl-X_L (Zhang et al., 2006; Chalfant and Spiegel, 2005). Bcl-2 and Bcl-X_L prevent apoptosis by binding to Apaf-1, preventing Apaf-1 activation of caspase 9 (Hu et al., 1998). Furthermore, heterodimerization of Bcl-2 to Bax prevents apoptosis (Vincenzo et al., 1998). Thus the balance between these pro- and antiapoptotic proteins is an important determinant in the fate of the cell, while the ability of ceramide to alter this balance may be fundamental in its apoptotic signaling ability.

More recent studies have shown ceramide to activate a mixed lineage kinase (MLK). MLK lies upstream of the SAPK pathway, and ceramide has proven to activate this kinase both *in vitro* and *in vivo*, thereby activating pro-apoptotic Jun kinase (JNK) (Sathyanarayana et al., 2002). Though much

is known about the role of ceramides in apoptosis, research it still ongoing. Since ceramides act on a number of other targets, there could be many additional ways by which ceramides affect apoptosis.

Sphingosine's role in apoptosis is less established. Though sphingosine activates some of the same pathways as ceramide, it can positively and negatively affect kinase activities, and unlike ceramide, is not confined to membranes (Woodcock, 2006). Sphingosine has been demonstrated to inhibit PKC (Smith et al., 2000) and has been implicated in activating the SAPK/JNK pathway (Ruvolo et al., 2003). For these reasons, sphingosine is considered a pro-apoptotic molecule.

The apoptotic actions of ceramide are depicted in the following figure (Fig.3).

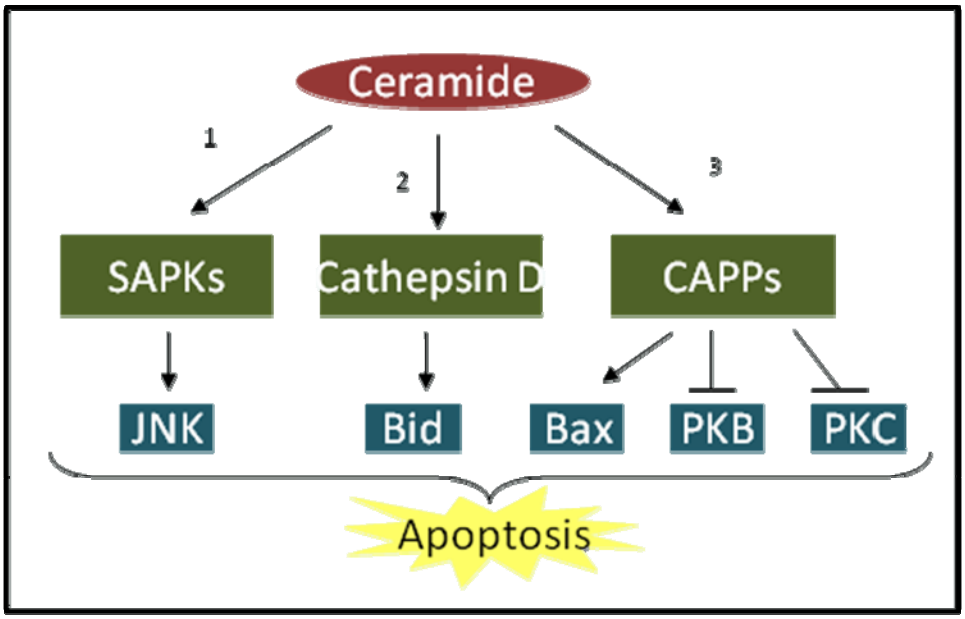

Figure 3: Apoptotic pathways of ceramide.

Ceramide can mediate apoptosis through: (1) the stress activated protein kinase (SAPKs), which activate pro-apoptotic Jun-kinase (JNK); (2) cleavage of cathepsin D to activate pro-apoptotic Bid; (3) ceramide-activated protein phosphatases (CAPPs) which mediate apoptosis through Bax activation, and inactivation of PKB and PKC.

1.3.2 Cell Survival Signaling by S1P and C1P

In contrast to ceramide and sphingosine, S1P has been implicated as a cell survival molecule. The metabolic conversion from ceramide/sphingosine to S1P is, therefore, capable of switching cells from an apoptotic state to a proliferative state. S1P has been found as an important signal in cell proliferation, induced by potent mitogens (Olivera and Spiegel, 1993). It has been shown to not only stimulate DNA synthesis, but also to cause an increase in cell division (Desai et el, 1992). Furthermore, S1P promotes cell survival and suppresses ceramide-mediated apoptosis (Cuvillier et al., 1996).

It has been established that cellular targets for S1P are the cell surface Edg family of G-protein coupled receptors (Lee et al., reviewed in Young et al., 2006). So far Edg 1, 3, 5, and 8 have been identified as receptors that bind S1P with high affinity and specificity (reviewed in Young et al., 2006). However, the biological functions of these receptors remain poorly understood. Preliminary work shows a possible role of these differentially expressed receptors in cell migration (Wang et al., 1999), though clearly this is an area for further research.

The intracellular targets for S1P have not yet been unequivocally determined, however, several enzymes and pathways have been identified. S1P has been shown to inhibit acid SMase in macrophages, thereby blocking the sphingomyelinase from producing pro-apoptotic ceramide and promoting cell survival (Gomez-Munoz et al., 2003). S1P may also promote proliferation by activating the mitogen-activated protein kinases (MAPKs), Erk-1 and Erk-2 (Cuvillier et al., 1996), proteins responsible for regulating cell growth and differentiation. As well, S1P activates phospholipase D (Desai et al., 1992). Phospholipase D and its product, phophatidic acid, are involved in enhancing cell proliferation and preventing cell cycle arrest (Foster and Xu, 2003). S1P counteracts ceramide-mediated cell death by inhibiting the JNK/SAPK pathway (Cuvillier et al., 1996).

Like S1P, C1P is an anti-apoptotic molecule, though the pathways and metabolic targets of C1P are not well characterized. It was identified over a decade ago but its biological importance has only just begun to be elucidated and appreciated. C1P is formed *via* phosphorylation of ceramide by ceramide kinase (CerK). CerK is a relative of SK1 catalyzing the formation of ceramide to C1P (Siguira et al., 2002). C1P was first described as a putative stimulator of cell proliferation and was shown to simulate

DNA synthesis in rat fibroblasts (Gomez-Munoz et al., 2005). C1P has been shown to block caspase3/caspase 9 pathway activation, thereby inhibiting apoptosis in macrophages (Gomez-Munoz et al., 2004). It has also been shown to upregulate BcL-X_L, an antiapoptotic member of the Bcl-2 family of proteins that is downregulated by ceramide (Gomez-Munoz et al., 2005).

Similarly to S1P, C1P has been shown to inhibit acid SMase. This has been demonstrated in both macrophages and cell homogenates, thereby preventing ceramide accumulation and apoptosis (Gomez-Munoz at al, 2004). Receptors for C1P remain unknown and instead it is suggested that C1P interacts with its targets such as acid SMase directly (Gomez-Munez at al, 2004). Other targets for C1P include PP1 and PP2a. While ceramide activates these protein phosphatases, C1P has been shown to inhibit these proteins *in vitro* (Chalfant, 2004). Inhibition of phosphatases PP1 and PP2a has been associated with activation of the proliferative Erk-1/Erk-2 pathway, increasing DNA synthesis and cell division (Doughetry et al., 2005). While further studies need to be carried to confirm the effects of C1P on protein phosphatases *in vivo*, this coincides with the survival effect of C1P.

It is clear that both C1P and S1P function distinctly to oppose pro-apoptotic ceramide signals. Since all the bioactive sphingolipids discussed are mutually convertible, the overall balance of these molecules is important. Future examination of the ceramide/sphingosine/S1P/C1P relationships, as well as the enzymes that produce and degrade these metabolites, should shed light on other cell death/survival pathways that are affected by this delicate balance.

1.4 Obese State and Disease

Obesity is a chronic disease characterized by an increase in body fat stores (Formiguera and Canton, 2004). Due to its prevalence, obesity is currently the most common metabolic disease in the world (Formiguera et al., 2004). The World Health Organization (WHO) has claimed it to be a world-wide epidemic of the 21st Century. Although obesity is considered a disease on its own and is directly related to mortality, part of its threat lies in the fact that it increases the risk for various other diseases, including cardiovascular disease, hypertension, dyslipidemia, type-2 diabetes and cancer, among others (Formiguera et al., 2004).

The sphingolipid pathway becomes an important area of study in obesity since it may be altered in an obese state, thus affecting the cell proliferation/death balance and contributing to the increased pathogenesis of certain diseases. Research is limited in this area. The only study to date compares adipose tissue of lean and obese mice and showed an overall decrease in SM and ceramide in obese mice compared to lean, with an increase in sphingosine and neutral and acidic SMase. Plasma levels of obese mice showed increased levels of sphingomyelin, ceramide, sphingosine and S1P, contributing to the proinflammatory phenotype of the obese adipose tissue (Samad et al., 2006).

1.4.1 Obesity, Hepatic Steatosis and Sphingolipid Metabolism

1.4.1.1 Biology of the Liver

The liver is the largest internal organ by percent weight in the human body and has crucial functions, including cholesterol production, intermediary metabolism, hormone synthesis, bile and urea production and drug detoxification. The functional cells of the liver are eosinophilic cells referred to as hepatocytes.

The liver is organized into structural units called lobules. Each lobule is centered around a terminal hepatic venule. Radiating from the central venule are plates of hepatocytes separated by wide vascular channels called sinusoids. Sinusoids carry blood from the terminal branches of the portal vein and hepatic artery, which bring nutrient rich blood from the gastrointestinal tract and oxygen rich-blood from the lungs, respectively (Young et al., 2000). Sinusoids thus allow blood to have intimate contact with hepatocytes, allowing for exchange of nutrients and metabolic products.

1.4.1.2 Sphingolipid Metabolism and Hepatic Steatosis in Obesity

Hepatic steatosis is a condition of the liver, defined as an excess of triglycerides in hepatocytes. This condition was long thought to be mainly a symptom of alcoholic liver disease. In recent years, however, steatosis has been found in the absence of alcohol abuse and led to the definition of a series of disorders ranging from nonalcoholic fatty liver (NAFL) to nonalcoholic steatohepatitis (NASH). Hepatic steatosis is associated with various factors including obesity, type II diabetes and

hyperlipidaemia (Raman and Allard, 2006). Insulin resistance has emerged as the most common disorder associated with hepatic steatosis (Angulo, 2002). Obesity and insulin resistance result in increased release of free fatty acids from adipocytes due to the activity of a hormone sensitive lipase. The elevated plasma levels of free fatty acids result in a higher influx of free fatty acids to the liver. Free fatty acids taken up by hepatocytes are metabolized by three different pathways: oxidation to form ATP, esterification to produce triglycerides for storage or incorporation into VLDL particles. Defects or changes in these pathways, such as increased esterification, decreased oxidation or faulty VLDL secretion can lead to hepatic steatosis (Browning and Horton, 2002).

Additionally, hepatic steatosis is linked to oxidative stress and inflammation (Chitturi and Farrell, 2001). Oxidative stress resulting from mitochondrial fatty acids oxidation, adipocytokines, and NF-kappaB-dependent inflammatory cytokine expression are all considered to be the potential factors leading to hepatocyte injury and inflammation in fatty liver disease (Duvnjak et al., 2007). Oxidative stress and inflammatory cytokines are known inducers of sphingomyelinase, activating the sphingolipid pathway. Despite this knowledge, there is limited research on hepatic steatosis and its affects on the sphingolipid signaling pathway. In a recent study, sphingomyelin was found to be downregulated in livers of obese mice compared to their lean counterparts (Yetukuri et al., 2007). As well, in a study comparing obese women with fatty livers to obese women with normal livers, it was found that both SMase and ceramide were significantly higher in adipose tissue in the fatty liver group (Kolac et al., 2007). It is clear that fatty liver disease does affect the sphingolipid pathway, but this is a novel area of research lacking conclusive results. It is therefore worthwhile to profile the sphingolipid pathway in this tissue, to clearly demonstrate how sphingolipid pathway is altered in an obese state/hepatic steatosis versus a normal lean state.

1.4.2 Obesity, Colon Cancer, and Sphingolipid Metabolism

1.4.2.1 Biology of the Colon

The mammalian colon, or large intestine, functions to store waste, absorb water, maintain water balance in the body and absorb vitamins, such as vitamin K. The large intestine can be divided into four distinct concentric layers: the mucosa, the submucosa; the muscularis externa; and the

adventita/serosa. The mucosa is the innermost layer of the digestive tract. Next is the submucosa consisting of dense connective tissue and functioning to vascularize and innervate the colon. The muscularis externa consists of muscular layers necessary for propelling waste through the large intestine. The adventitial layer consists of epithelial layers and a thin connective layer forming a serous membrane. In terms of colon cancer development, it is the mucosa that becomes the most important layer to examine.

The mucosa can be further divided into three layers: epithelium; lamina propria; and muscularis mucosa. A single layer of epithelial cells lines the entire surface of the mucosa. Beneath the epithelium lies the lamina propria, consisting of loose connective tissue. The epithelium protrudes down through the lamina propria in intestinal glands known as the crypts of Lieberkuhn (Young et al., 2000). It is within these glands where loss of proliferation control is attributed to colon cancer. A thin layer of smooth muscle tissue referred to as the muscularis mucosa lies beneath the lamina propria and keeps the mucosal surface and glands in a state of gentle agitation to expel contents of glandular crypts and improve contact between the epithelium and the contents of the lumen of the large intestine.

1.4.2.2 Cancer of the Colon

Colon cancer is one of the top five most common cancers in both men and women, resulting in 655,000 deaths per year worldwide (WHO, 2006). Colon cancer is defined by epithelial cells proliferating in an uncontrolled manner and invading the muscularis mucosa (Morson and Sobin, 1976). This form of cancer may develop sporadically, influenced by diet and lifestyle choices, or it may result from one of two inherited conditions; familial adenomatous polyposis or hereditary non-polyposis colorectal cancer. The colon will first demonstrate epithelial cell changes by the appearance of preneoplastic lesion, known as aberrant crypt foci, first discovered by Bird in 1987 (Bird, 1987).

In the occurrence of colon cancer, the appearance of aberrant crypt foci will be followed by the development of adenomatous polyps, before invading the mucosa as a carcinoma (Janne and Mayer, 2000). A series of molecular and histological changes are responsible for the progression of normal epithelial cells into colon carcinoma, including mutations to proto-oncogenes and tumor suppressor genes. A detailed progression of these events can be found in the Vogelstein model of colon carcinogenesis (Vogelstein et al., 1998). It is important to note that healthy epithelium in colonic

crypts is maintained by the balance between cell growth and cell death signals, and subtle changes to this balance occur prior to any neoplastic transformations (Shanmugathasin et al., 2000).

1.4.2.3 Obesity and Colon Cancer

It is well established in epidemiological data that obesity is related to an increased risk for colon cancer (reviewed by Gunter and Leitzmann, 2006). Current reasoning for this relationship lies in the fact that an obese state of chronic inflammation is linked to insulin resistance, hyperglycemia, oxidative stress and excess lipid storage. The increased concentrations of insulin may induce a mitogenic effect within colon cells, while exposure to excess glucose and fatty acids may induce alterations in cell signaling (Gunter and Leitzmann, 2006). As oxidative stress and inflammatory markers are inducers of the sphingolipid pathway, which is pivotal in determining cell fate, it also becomes an important area to consider in the relationship between obesity and colon cancer risk.

1.4.2.4 Sphingolipid Signaling and Colon Cancer

While links between obesity and sphingolipid signaling remain unclear, a particular link between colon cancer and sphingolipid metabolism has been identified. Changes in sphingomyelin metabolism are found to be associated with the development of tumors. Numerous studies have also looked at SK1 in the pathogenesis of colon cancer. It has been found that this enzyme is upregulated in colon tumor tissue and is necessary for promoting survival and proliferation of tumor cells (Kawamori et al., 2006; Kohno et al., 2006). Human colon cancers showed a greater than 50% decrease in ceramide levels compared to normal mucosa (Selzner et al., 2001). Furthermore, sphingosine-1 phosphate lyase, the enzyme which irreversibly degrades S1P, is downregulated in human colon cancer tissues compared to surrounding normal tissues, preventing degradation of the proliferative messenger (Oskouian et al., 2006). It appears that altering the sphingolipid pathway has important therapeutic potential, as increasing the ceramide levels in HT-29 colon cancer cells has been found to induce cell death, and adenoma size was decreased in rats that could not produce SK1 (De Stefanis et al., 2002; Kohno et al., 2006). As evidence linking sphingolipid signaling in colon cancer builds, it becomes valuable to assess what role obesity plays in this signaling pathway. If the sphingolipid pathway is altered by obesity in colon tissue, this may change the colonic environment in which tumors can develop.

1.4.3 Zucker Obese Animal Models

Zucker obese rats are commonly used as animal models for the study of obesity (see Fig. 4). They exhibit many of the characteristics common with human obesity, including hyperphagia, hyperglycemia and hyperinsulinemia. The Zucker obese rats (fa/fa) inherit their obesity as an autosomal recessive trait, as they are homozygous for nonfunctional leptin receptors compared to their lean counterparts (Zucker lean Fa/Fa or Fa/fa) (Zucker and Zucker 1961). Leptin is a hormone produced in adipose tissue that is responsible for regulating body weight and fat metabolism by signaling the hypothalamus to suppress appetite (Guyton et al., 2000). Nonfunctional leptin receptors result in the Zucker-obese rats overeating and becoming morbidly obese.

The obese Zucker rats are therefore an excellent model to use in this study as the tissues of this obese model can be compared to the lean tissues of an animal model within the same strain (Zucker lean).

Figure 4: Lean and obese Zucker rat

Chapter 2
Materials and Methods

2.1 Materials

Unless otherwise stated, all chemicals and reagents were purchased from Sigma Chemical Co., St. Louis, MO, USA.

2.2 Animals

Five-week-old female Ob (fa/fa) rats (n=14) and their lean (Fa/Fa) counterparts (n=12) were obtained from Charles River Laboratories (Wilmington, MA, USA). They were housed in suspended wire cages approximately 10 cm above sawdust bedding trays with a 12-h light/12-h dark cycle in the animal housing facility. Temperature and relative humidity were controlled at 22°C and 55%, respectively. All animals were acclimatized to these conditions for one week with free access to standard laboratory rodent chow and *ad libitum* drinking water until initiation of the experiment. All animals were cared for according to the guidelines of the Canadian Council on Animal Care and the protocol was approved by the University of Waterloo Animal Care committee.

2.3 Diet, Body Weights, Termination

The rats were fed synthetic diet AIN93. The rats remained on respective diets for nine weeks, after which, they were weighed, and terminated by CO_2 asphyxiation. Following termination, gross anatomy was observed and any pathologic abnormalities were recorded. Weights of liver, kidney, spleen, and heart tissues were recorded and the samples were frozen for biochemical analysis.

2.4 Sphingomyelinase Assay

The activity of neutral and acidic sphingomyelinases in liver and colon were measured using the Amplex Red Sphingomyelinase Assay Kit (Molecular Probes, Eugene, OR). Amplex Red reagent (10-acetyl-3, 7 dihydroxyphenoxazine) measures sphingomyelinase activity indirectly, as it is a sensitive fluorogenic probe for H_2O_2. First sphingomyelinase hydrolyses sphingomyelin to yield ceramide and phosphorylcholine. Then the added alkaline phosphatase hydrolyses phosphorylcholine to choline, which can then be oxidized by choline oxidase to yield butane and H_2O_2. Finally, H_2O_2, in the presence of horseradish peroxidase, reacts with Amplex Red reagent in a 1:1 stoichiometry to generate highly fluorescent resorufin.

The activity of neutral sphingomyelinase was analyzed using 250 μg of protein from each liver and colon sample diluted in 1x reaction buffer to make volume to 100 μL. The method was followed directly from the manufacturer's instructions. 100 μL of each sphingomyelinase diluted samples was added to a 96 well plate. To each well, 100 μL assay solution was added containing 100 μM Amplex Red, 2 U/ml HRP, 0.2 U/mL cholesterol oxidase, 8 U/mL alkaline phosphatase, 0.5 mM sphingomyelin (made in 2% Triton X-100) with 0.1 M Tris-HCl and 10 mM $MgCl_2$, pH 7.4. After 30 min incubation at 37° C, the fluorescence was measured using excitation at 545±10 nm and emission detection at 590±10 nm.

The activity of acidic sphingomyelinase was analyzed in a two-step reaction procedure. The sphingomyelinase containing samples were prepared using 250ug of protein from each sample diluted in a sodium acetate buffer (pH 5). 100 μL of each sample was added to the 96 well plate, and to each well was added 10μL of 5mM sphingomyelin solution. The plate was incubated for 1 h at 37 °C. The reaction was then placed on ice as the reaction mixture containing 100 μM Amplex Red, 2 U/ml HRP, 0.2 U/mL cholesterol oxidase, 8 U/mL alkaline phosphatase, with 100 mM Tris-HCl, pH 8 was added and further incubated at 37° C for 30 min. The fluorescence intensities were measured with a filter set for excitation and emission detection at 545±10 and 590±10 nm, respectively.

2.5 Tissue Lysate

Tissues were stored at -80°C. 0.25 g of liver (from left lobe) and colon tissue (scraped mucosa) were sliced over dry ice (to keep tissues frozen) and mixed with 2 mL of ice-cold RIPA buffer (50 mM

Tris-HCl, 1% NP-40, 0.25% Sodium deoxycholate, 150 mM NaCl, 1 mM EDTA, 1 mM NaF) with freshly added protease inhibitors (1 μg/mL of Aprotinin, Leupeptin, Trypsin Inhibitor, Sodium Orthovandate) and then homogenized on ice using PT2100 Polytron homogenizer. The mixture was transferred into the microcentrifuge tubes, and lipids and cell debris were removed by centrifugation at 13,000 rpm for 20 min at 0°C. The supernatant (lysate) was then collected from below the top lipid layer and aliquoted in small amounts in pre-chilled eppendorf tubes and stored in -20°C for further analysis.

2.6 Western Blot

Antibody acquisitions were as follows:

1. Rabbit polyclonal to SK1 in rat, human and mouse (Abgent Inc., San Diego, CA, USA; catalogue # AP7237c).
2. Goat polyclonal to ceramidase in rat, human and mouse (Santa Cruz Biotechnologies, Santa Cruz, CA, USA; catalogue # sc-28486).
3. Rabbit polyclonal to Bax and Bcl-2 in rat, human and mouse (Abcam Inc., Cambridge, MA, USA; catalogue #s ab7977 and ab7973, respectively).
4. Bovine Anti-goat IgG-HRP (Santa Cruz Biotechnologies, Santa Cruz, CA, USA; catalogue # sc-23500).
5. Goat Anti-rabbit IgG-HRP (Cell Signaling Technology Inc., Boston, MA, USA; catalogue # 7074).

2.6.1 Protein Assay

The Bio-Rad colorimetric protein assay, based on Bradford method, was used to determine the total protein content using bovine serum albumin as a standard. Protein solution was assayed in duplicates in 96 well plates and the absorbance was measured using Bio-Rad 3550-UV Microplate Reader at 595 nm.

2.6.2 Sodium Dodecyl Sulfate-Polyacrylamide Gel Electrophoresis (SDS-PAGE)

The protein samples were subjected to 10 % SDS-PAGE using the Mini-Protean-BioRad II apparatus (Bio-Rad Laboratories Ltd, Carlsbad, CA, USA). A linear range was done for each protein of interest

(using samples containing 10, 25, 50, 75, 100, 150, 200 ug of protein) to determine the optimal amount of protein to load for each antibody. 50 μg of protein was added to each sample for all antibodies with the exception of sphingosine kinase, which required 100 μg of protein for each liver sample and 150 μg of protein for each colon sample for optimal detection. Liver samples were mixed with equal volume of 2x SDS Laemmli buffer (Sigma Chemical). Colon samples were mixed with 0.25 homogenate volume of 5x Laemmli buffer to decrease total sample size. All samples were boiled for 5 min at 90°C. Then the equal protein samples were loaded in 15-well gels and the proteins separated in SDS-PAGE at 120V for 90 min. As the colon samples for SK1 were too large, the lean samples and obese samples were run separately in 10-well gels. A positive control (liver) was included in these gels to minimize background and account for gel-to-gel variability.

2.6.3 Western Blot

Proteins were transferred from gels onto methanol soaked 0.45 μm PVDF membranes (Pall Corp. FL, USA.) The Trans-Blot Semi-Dry transfer cell system (Bio-Rad Laboratories Ltd, Carlsbad, CA, USA) at 20V for 30 min was used for SK1 immunoblots. For all other blots, transfer was completed using the Mini-Trans-Blot Electrophoretic Transfer Cell (Bio-Rad Laboratories Ltd, Canada) at 100V for 60 min. The gels were stained with Coomassie Brilliant Blue to confirm proper transfer. SK1 blots were washed briefly in 10% TBS-T solution and were incubated in TBS-T containing bovine serum albumin (5%) blocking buffer for 1 h at room temperature to block non-specific binding, then probed with SK1 primary antibodies for 1 h at room temperature, followed by overnight incubation at 4°C.

Blots for ceramidase, Bax, and Bcl-2 also followed the above protocol except the blocking was carried out in TBS-T containing 5% skim milk for 1 h at room temperature and overnight at 4°C. Blots were then incubated in their respective primary antibodies for 2.5 h at room temperature. After incubation in primary antibody, all immunoblots were washed three times with TBS-T and then incubated with peroxidase conjugated secondary antibodies in a 1% blocking solution for 1.5 h. After washing three times in TBS-T, the blots were incubated for five minutes with ECL plus (Amersham Biosciences Canada, GE Healthcare Bio-Sciences Inc.,Quebec, Canada) and developed using X-ray film (Fisher Scientific Company, Ottawa, ON, Canada). Finally, densitometric analysis was conducted using AlphaEaseFC software. The membranes were stained with Ponceau-S to confirm equal loading and were used to normalize the integrated density values for quantification. Densitometry analysis was performed using a Visible Imaging System equipped with AlphaEaseFC

software (Alpha Innotech, San Leandro, CA). The blots for liver samples were washed in TBS-T and reprobed with beta-actin as a secondary control for equal loading. For colon membranes, ponceau staining alone was used as control as beta-actin does not show up consistently in colon samples.

2.7 Sphingolipid Quantitative Analysis

Sphingomyelin, ceramide, ceramide-1 phosphate, sphingosine and sphingosine-1-phosphate were analyzed by high-performance liquid chromatography (HPLC) -tandem mass spectroscopy (MS) by the lab of Dr. J Beilawski (Lipidomic Core, Medical University of South Carolina, Charleston, SC). A detailed description of the method can be found in the journal of Methods (Beilawski et al., 2006). Briefly, 0.5 grams of each liver and colon sample were homogenized in tissue buffer and fortified with internal standards, 17-sphingosine, 17-S1P, 18C17-SM and 17C16-ceramide. Protein concentration was determined in each sample (Bio-Rad Protein Assay) and then sphingolipids were extracted using a solution of iso-propanol: water: ethyl acetate (30:10:60). Samples were centrifuged for 10 min at 4000 rpm and supernatants collected. Organic extracts were evaporated under N_2 gas and were reconstituted in methanol containing 0.2% formic acid. Samples were then analyzed using TSQ 7000 LC/MS system. Quantitative analysis is based on calibration curves generated by spiking bovine serum albumin with known amounts of target synthetic standards and an equal amount of internal standard. The calibration curves are generated by plotting the peak area ratios of sphingolipid to the respective internal standards against concentration using a linear regression model.

2.8 Statistical Analysis

Statistical analysis of the data was performed using SPSS statistical software (SPSS Inc., Chicago, IL, USA). A comparison between lean and obese groups was performed and differences were determined using independent samples t-test, at a significance level of $P < 0.05$. Statistical analysis between tissue types was determined using paired samples t-test, at a significance level of $P<0.05$.

Chapter 3
Results

3.1 Animal weights

Body mass of obese rats were significantly higher than their lean counterparts (Table 1).

Table 1: Body mass of lean and obese rats[a]

	Lean	Obese
Body mass (g) :	269.75±6.27	552.83±15.43*

[a] means± s.e.m. at time of termination (9 weeks); * significantly different from the lean control group ($P<0.05$; Lean group, N=12; Obese group, N=14).

3.2 Lean and Obese Liver Tissue Results

3.2.1 Liver observations

Obese Zucker livers were significantly larger than the lean livers. Furthermore, obese Zucker liver tissue appeared pale and creamy colored compared to the darker red of the lean livers. Shown below is previous liver histology from Zucker obese and lean control rats (Fig.5). Obese Zucker liver shows lipid accumulation within the hepatocytes demonstrating hepatic steatosis, while the lean liver shows normal liver histology.

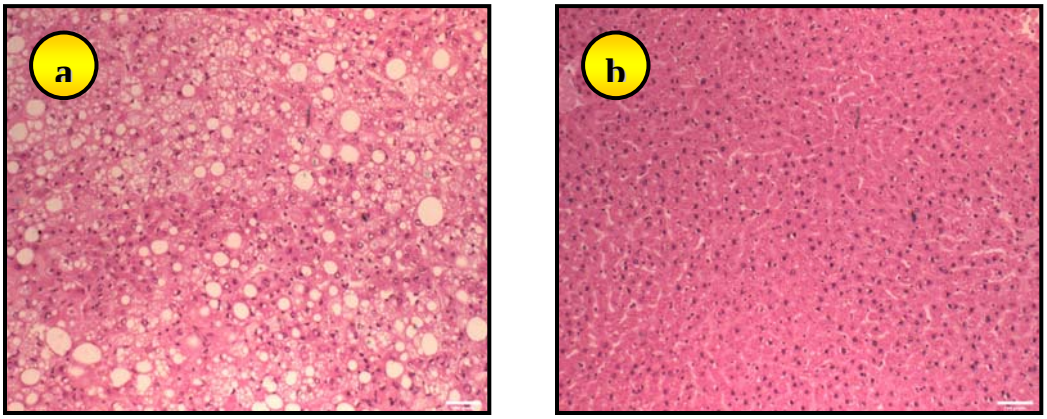

Figure 5: Haematoxylin and eosin stained liver histology of: (a) Zucker obese rat liver tissue; (b) Zucker lean rat liver tissue.

After termination, a segment of liver was fixed in a buffered formalin solution. Transverse sections (4µm) were stained with haematoxylin (staining the nuclei black) and eosin (staining the cytoplasm pink). Obese liver (a) shows lipid accumulation in hepatocytes, and lean liver (b) shows normal liver histology.
(Nita Modi, and Ranjana Bird, unpublished).

3.2.2 Sphingomyelinase Activity in Liver

There were no significant differences in acidic and neutral sphingomyelinase levels in lean and obese liver tissue (Figs. 6 and 7).

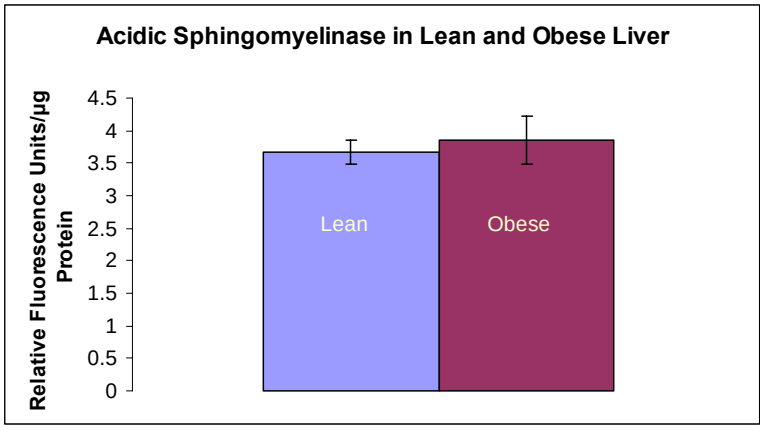

Figure 6: Acidic sphingomyelinase in lean and obese liver tissue.

Mean sphingomyelinase levels (N=6 per group) are expressed in relative fluorescence units per µg protein ± s.e.m. See materials and methods for details.

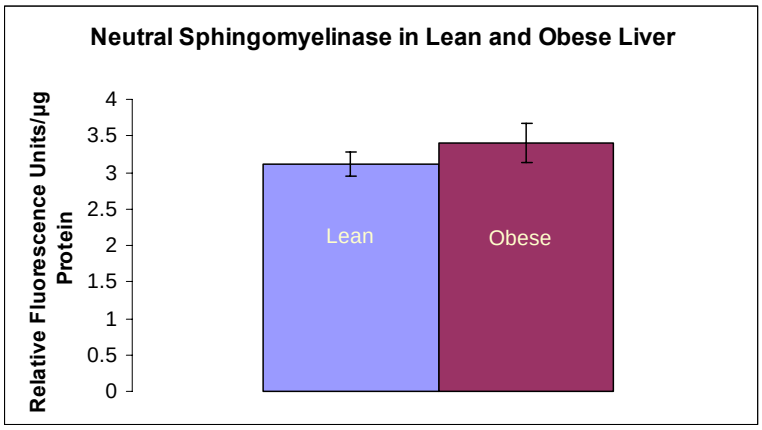

Figure 7: Neutral sphingomyelinase in lean and obese liver tissue.

Mean sphingomyelinase levels (N=6 per group) are expressed in relative fluorescence units per µg protein ± s.e.m. See materials and methods for details.

3.2.3 Ceramidase Expression in Liver

Ceramidase bands were observed at a band size of 55kDa for both lean and obese liver tissue. This band size is consistent with the ceramidase 55kDa precursor protein. Ceramidase protein expression is significantly higher in obese liver tissue compared to the lean tissue (Fig. 8).

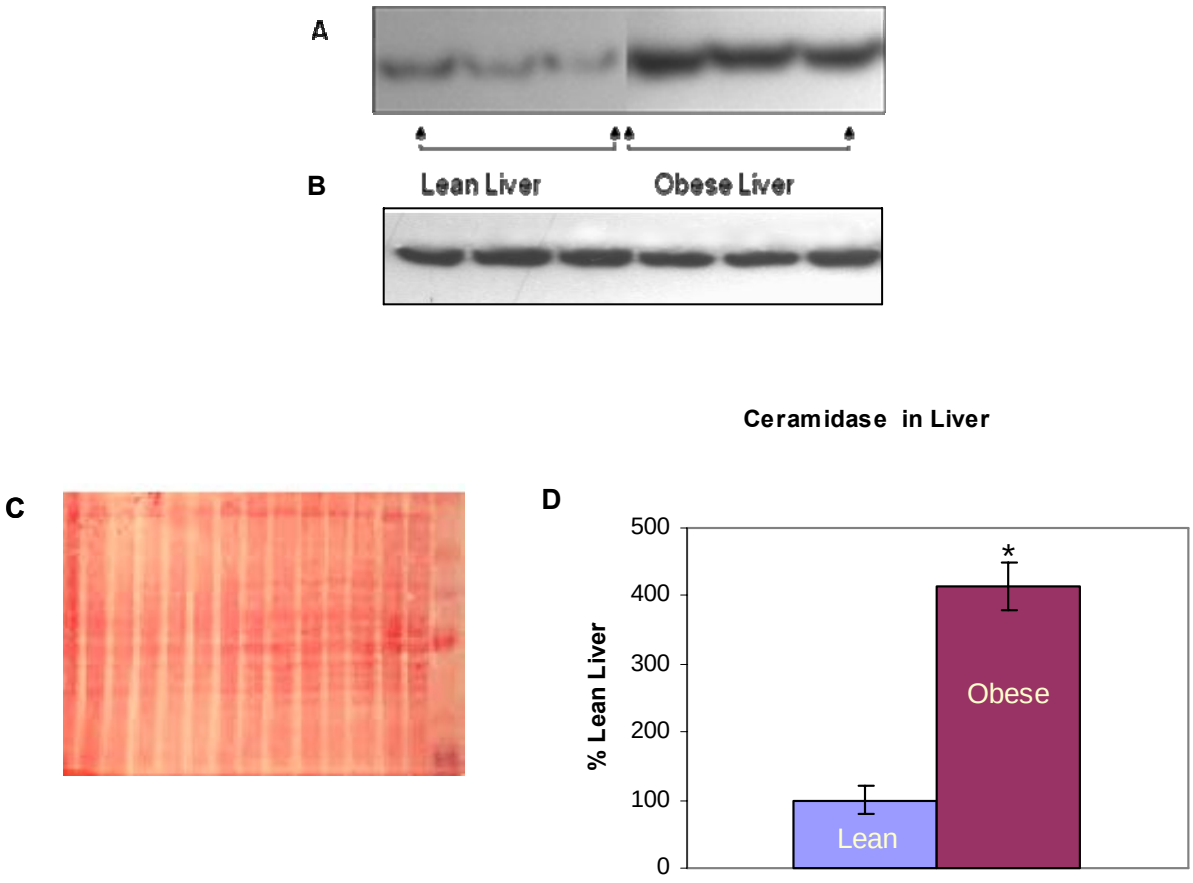

Figure 8: Western blot for ceramidase in lean and obese liver and ponceau stain.

3 representative bands from each group (A) are shown with beta-actin control bands (B). Samples containing 50 µg of protein were separated by 10% SDS-PAGE and transferred onto PVDF membranes. Following incubation with primary anti-ceramidase at a1:200 dilution and secondary HRP-conjugated anti-goat at a 1:10 000 dilution, the blots were developed on X-ray film using ECL-Plus substrate. Membranes were then stained with Ponceau-S for equal loading control (C). Bar graphs (D) represent mean levels of ceramidase in lean and obese liver. All ceramidase bands were normalized to their respective ponceau bands; *significantly different from lean group ($P<0.05$; $N=6$).

3.2.4 Sphingosine Kinase Expression in Liver

Sphingosine kinase bands were observed at the predicted band size of 43 kDa for both lean and obese liver tissue. A second band appeared just below the 43 kDa mark in obese liver tissue that was not observed in lean tissue. SK1 protein expression is significantly higher in lean liver tissue compared to the obese tissue (Fig. 9).

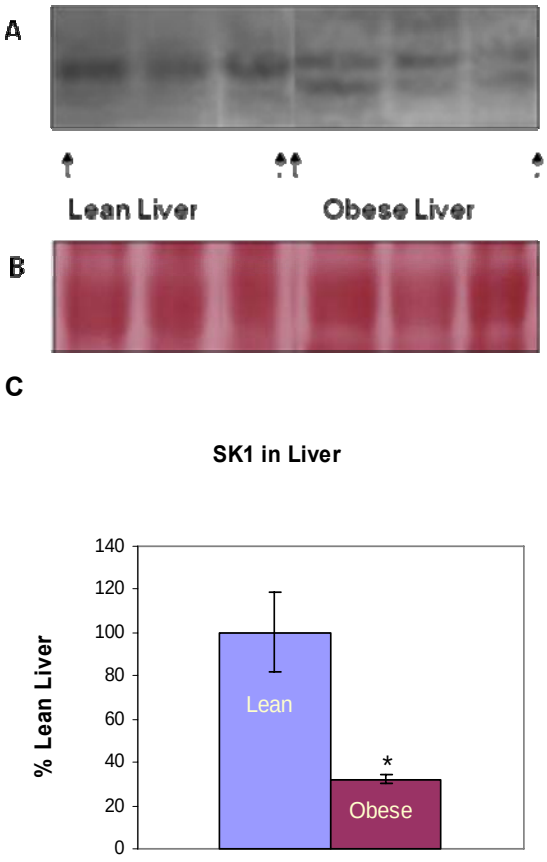

Figure 9: Western blot for SK1 in lean and obese liver.

3 representative bands from each group (A) are shown with representative bands from their respective ponceau stains (B). A second band is observed in obese liver, while only a single band appears for lean liver. Samples containing 100 µg of protein were separated by 10% SDS-PAGE gel and transferred onto PVDF membranes. Following incubation with primary anti-SK1 at a1:500 dilution and secondary HRP-conjugated anti-rabbit at a 1:3000 dilution, the blots were developed on X-ray film using ECL-Plus substrate. Membranes were then stained with Ponceau-S for equal loading control. Bar graphs (C) represent expression levels of SK1 in lean and obese liver, expressed as percentage lean liver. For obese liver, only the upper band that appeared at the expected 43 kDa mark was quantified. All SK1 expression bands were normalized to ponceau bands; *significantly different from lean group ($P<0.05$; $N=6$).

3.2.5 Bcl-2 Expression in Liver

Bcl-2 bands were observed at the predicted band size of 30 kDa for both lean and obese liver tissue. Lean liver tissue shows greater Bcl-2 levels than the obese liver. Bcl-2 protein expression is significantly higher in lean liver tissue compared to obese (Fig. 10).

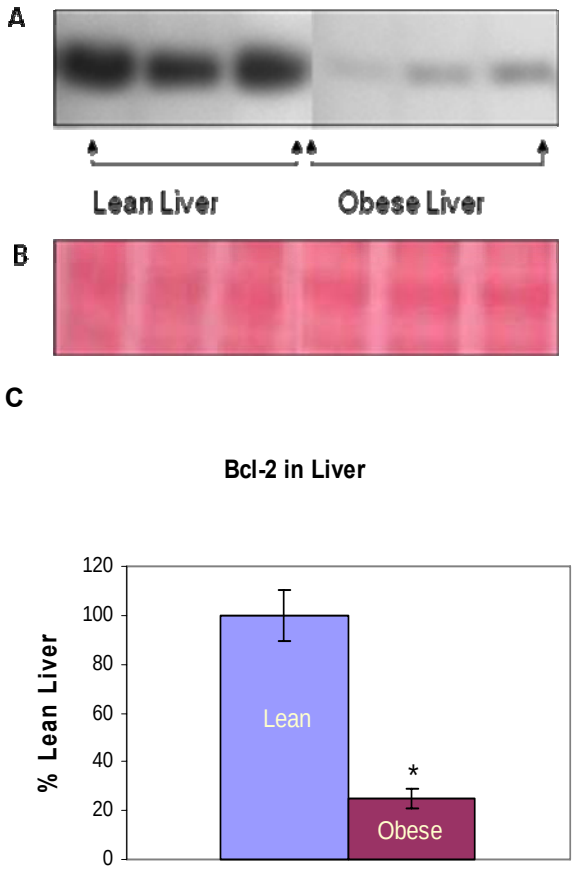

Figure 10: Western blot for Bcl-2 in lean and obese liver.

3 representative bands from each group (A) are shown with representative bands from their respective ponceau stains (B). Samples containing 50 µg of protein were separated by 10% SDS-PAGE gel and transferred onto PVDF membranes. Following incubation with primary anti-Bcl-2 at a1:500 dilution and secondary HRP-conjugated anti-rabbit at a 1:3000 dilution, the blots were developed on X-ray film using ECL-Plus substrate. Membranes were then stained with Ponceau-S for equal loading control. All Bcl-2 expression bands were normalized to ponceau bands. Bar graphs (C) represent expression levels of Bcl-2 in lean and obese liver, expressed as percentage lean liver; *significantly different from lean group ($P<0.05$; N=6).

3.2.6 Bax Expression in Liver

Bax bands were observed at the predicted band size of 21 kDa for both lean and obese liver tissue. Faint bands also appeared at the 42kDa mark, as predicted by antibody specifications, as Bax regularly forms homodimers. Bax protein expression is significantly higher in obese liver tissue compared to lean (Fig. 11).

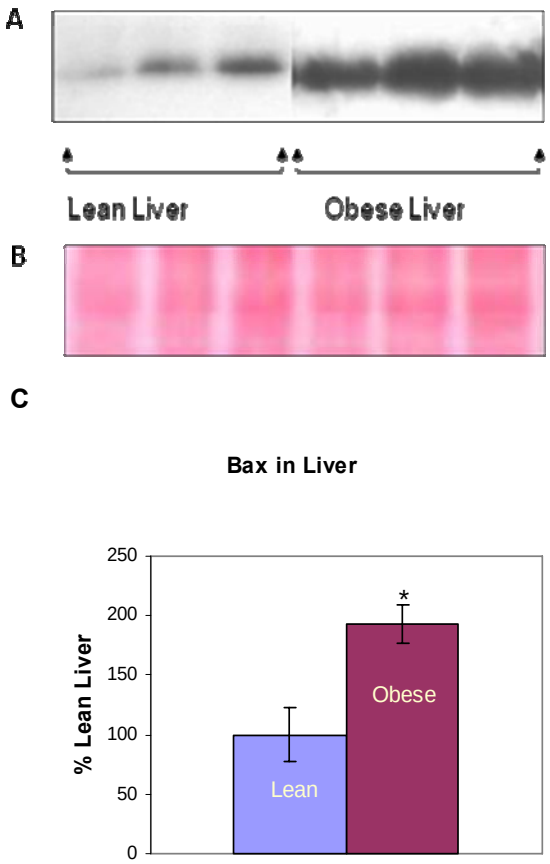

Figure 11: Western blot for Bax in lean and obese liver.

3 representative bands from each group (A) are shown with representative bands from their respective ponceau stains (B). Samples containing 50 µg of protein were separated by 10% SDS-PAGE gel and transferred onto PVDF membranes. Following incubation with primary anti-Bax at a1:500 dilution and secondary HRP-conjugated anti-rabbit at a 1:3000 dilution, the blots were developed on X-ray film using ECL-Plus substrate. Membranes were then stained with Ponceau-S for equal loading control. All Bax expression bands were normalized to ponceau bands. Bar graphs (C) represent expression levels of Bax in lean and obese liver, expressed as percentage lean liver; *significantly different from lean group ($P<0.05$; $N=6$).

3.2.7 Sphingomyelin Content in Liver

LC-MS (liquid chromatography-mass spectroscopy) analysis results show that various species of SM are altered in obese liver tissue compared to lean. SM species differ in the number of carbons and number of double bonds in their fatty acid chain. C16-SM is significantly higher in obese liver while C22- and C24-SM levels are significantly lower in obese liver (Fig. 12). C22:1-, C26- and C26:1- SM are also significantly lower in obese liver tissue compared to lean (Fig. 13).

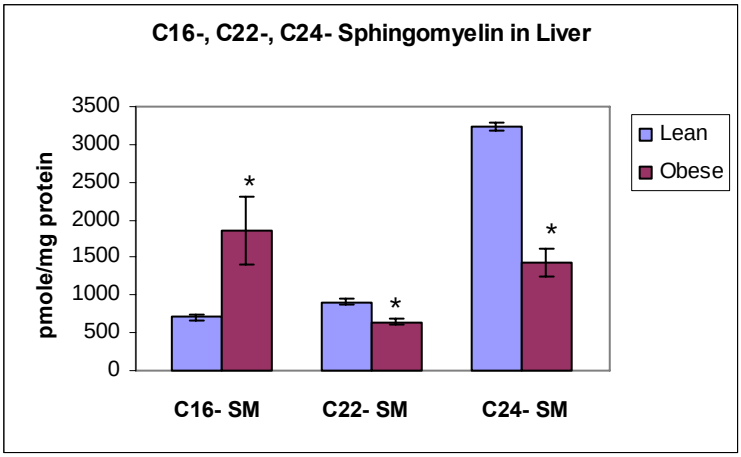

Figure 12: C16, C22 and C24 sphingomyelin levels in lean and obese liver tissue

SM levels are shown in pmole/mg protein ± s.e.m.; *significantly different from lean group ($P<0.05$; $N=5$). SMs were quantified by HPLC-MS. 18C17-SM was used as an internal standard. After sphingolipid extraction, samples containing 1mg of protein were analyzed using TSQ 7000 LC/MS system.

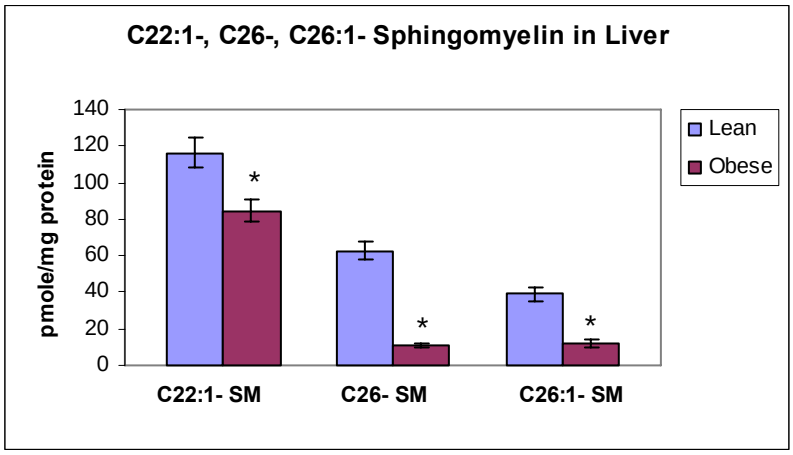

Figure 13: C22:1, C26, C26:1 sphingomyelin levels in lean and obese liver tissue

SM levels are shown in pmole/mg protein ± s.e.m.; *significantly different from lean group ($P<0.05$; $N=5$). SMs were quantified by HPLC-MS. 18C17-SM was used as an internal standard. After sphingolipid extraction, samples containing 1mg of protein were analyzed using TSQ 7000 LC/MS system.

Other SM species, C14-, C18-, C18:1-, C20-, C20:1- and C24:1- SM, did not differ significantly between the two groups. Calculation of total SM shows lower SM content in obese liver tissue although this difference is not significant with the present sample size.

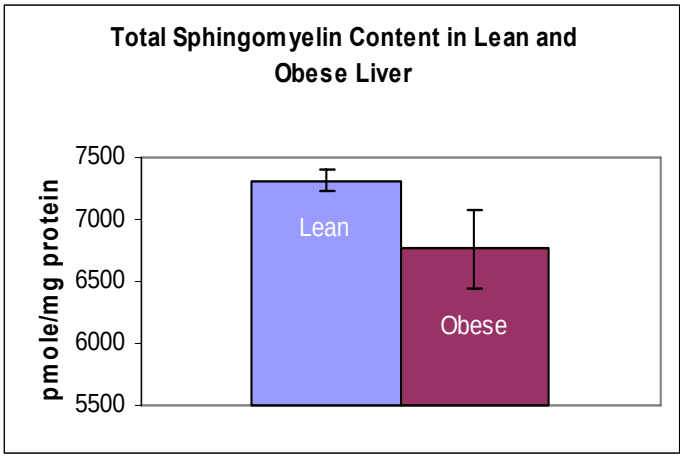

Figure 14: Total sphingomyelin content in lean and obese liver tissue

SM levels are shown in pmole/mg protein ± s.e.m. N=5 per group. SMs were quantified by HPLC-MS. 18C17-SM was used as an internal standard. After sphingolipid extraction, samples containing 1mg of protein were analyzed using TSQ 7000 LC/MS system.

The relative differences in SM species compositions between the lean and obese livers are depicted in the following stacked graph (Fig. 15).

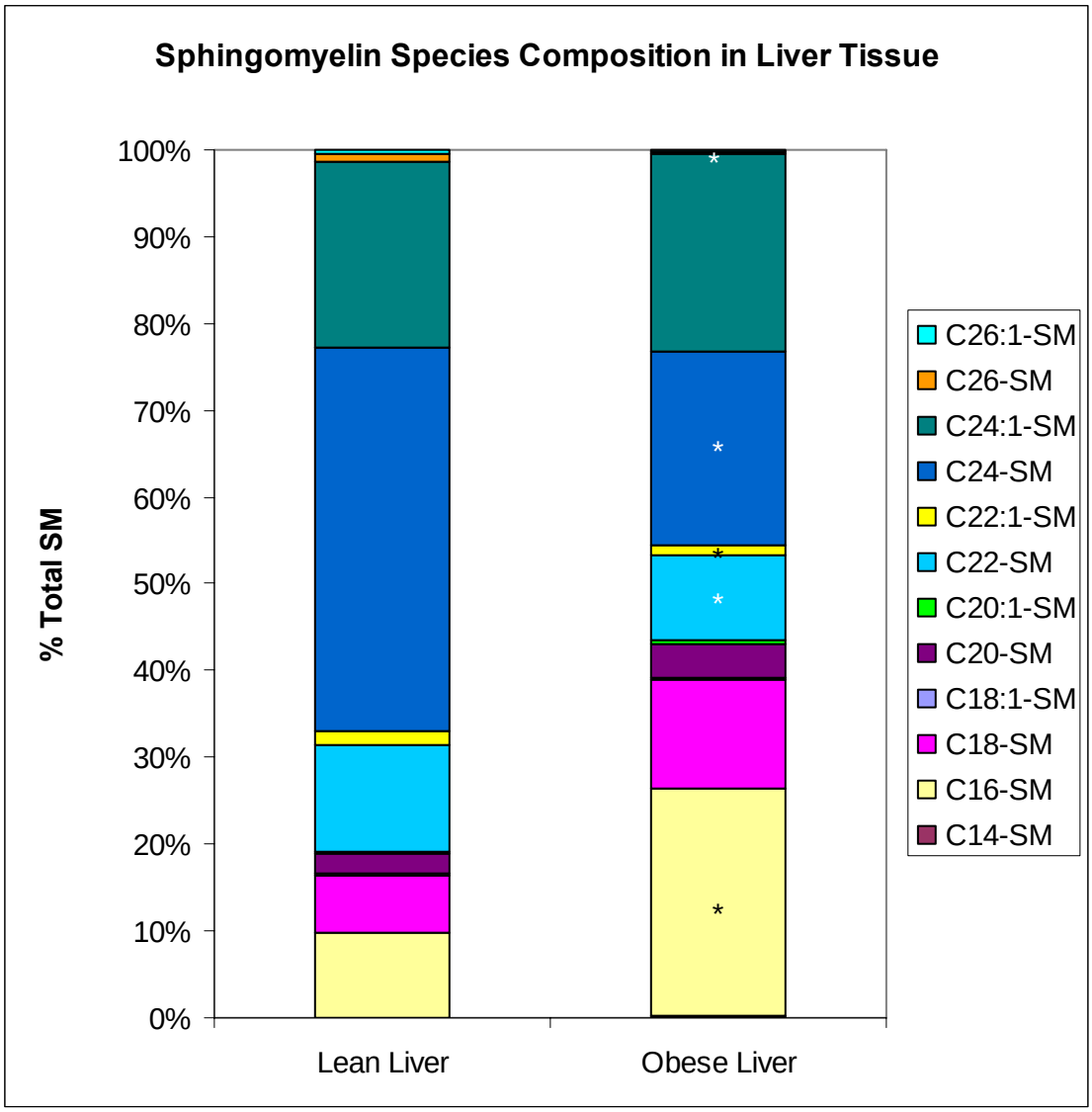

Figure 15: Sphingomyelin species composition in lean versus obese liver tissue

SM species levels are shown as a percentage of total SM content in this stacked graph; *significantly different from lean group ($P<0.05$; $N=5$). Significant differences can be observed for C16-, C22-, C22:1-, C24-, and C26-SM. Note that significant differences were also observed for C26:1-SM, but the levels of this species were too low to be visible in this figure.

3.2.8 Ceramide Content in Liver

LC-MS analysis shows that various ceramide species are significantly altered in obese liver tissue compared to lean. Ceramide species differ in the number of carbons and number of double bonds in their fatty acid chain. C16-ceramide is significantly lower in obese tissue, while C22-, C24:1-ceramides are higher in obese tissue (Fig. 16). C18-, C20- and C24:0- ceramide levels are also significantly higher in an obese state (Fig. 17).

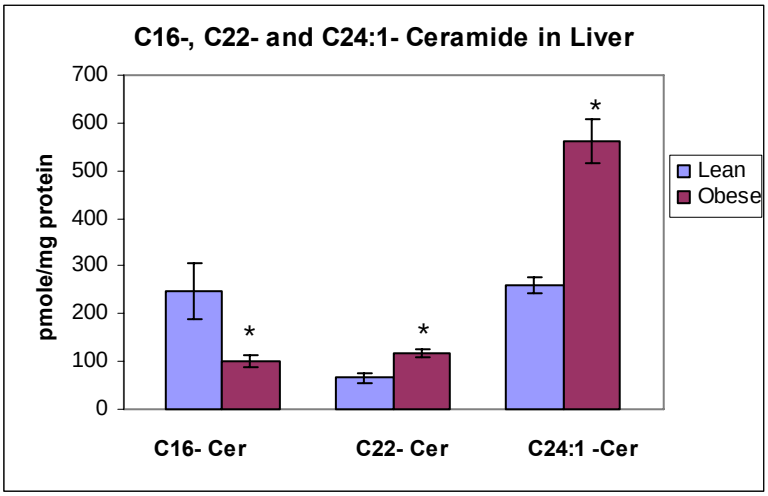

Figure 16: C16, C22 and C24:1 ceramide levels in liver tissue

Ceramide levels are shown in pmole/mg protein ± s.e.m.; *significantly different from lean group ($P<0.05$; N=5). Ceramides were quantified by HPLC-MS. 17C16-ceramide was used as an internal standard. After sphingolipid extraction, samples containing 1mg of protein were analyzed using TSQ 7000 LC/MS system.

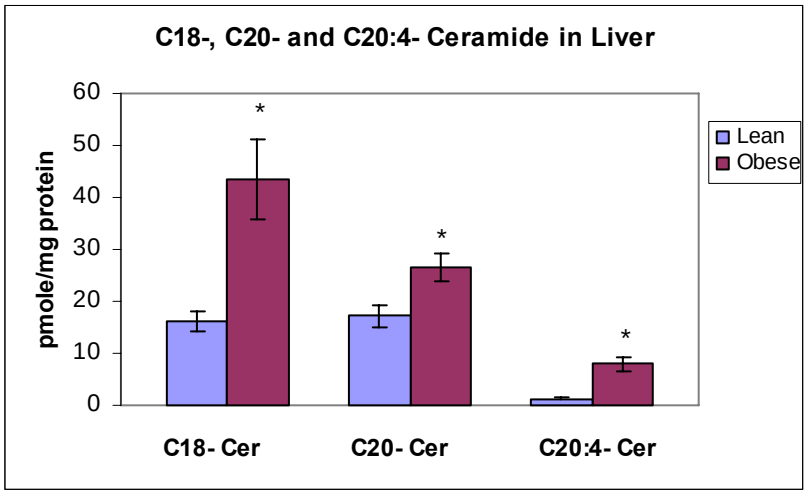

Figure 17: C18, C20 and C20:4 ceramide levels in lean and obese liver tissue

Ceramide levels are shown in pmole/mg protein ± s.e.m.; *significantly different from lean group ($P<0.05$; N=5).. Ceramides were quantified by HPLC-MS. Internal standard 17C16-ceramide was used. After sphingolipid extraction, samples containing 1mg of protein were analyzed using TSQ 7000 LC/MS system.

Levels of C18:1, C14, C20:1, C22:1, C24, C26, and C26:1 ceramide did not differ significantly between lean and obese groups. Total ceramide content was found to be higher in obese liver compared to lean liver but differences were not statistically significant (Fig.18).

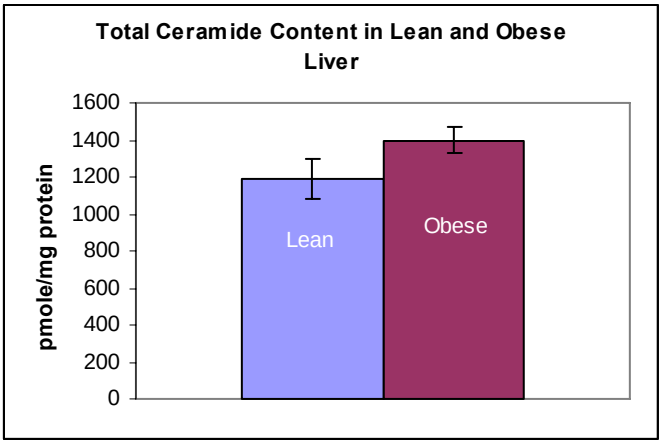

Figure 18: Total ceramide content in lean and obese liver tissue

Ceramide levels are shown in pmole/mg protein ± s.e.m. N=5 per group. Ceramides were quantified by HPLC-MS. 17C16-ceramide was used as an internal standard. After sphingolipid extraction, samples containing 1mg of protein were analyzed using TSQ 7000 LC/MS system.

The relative differences in ceramide species compositions between the lean and obese livers are depicted in the following stacked graph (Fig. 19).

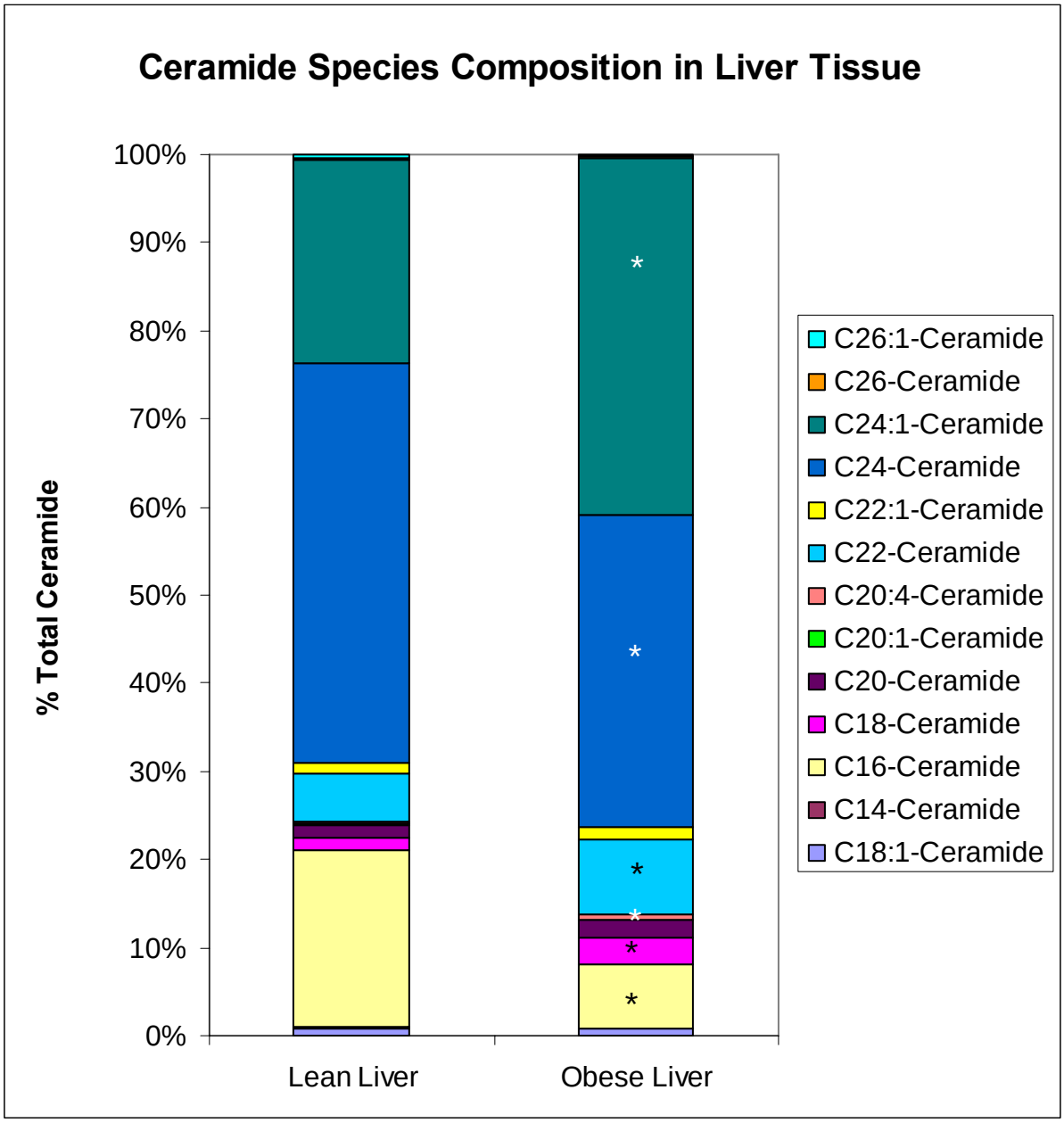

Figure 19: Ceramide species composition in lean versus obese liver tissue

Ceramide species levels are shown as a percentage of total ceramide content in this stacked graph; *significantly different from lean group ($P<0.05$; $N=5$). Significant differences can be observed for C16-, C18-, C20-, C22-, C24-, and C24:1-ceramide.

3.2.9 Ceramide-1-Phosphate Content Liver

LC-MS analysis shows that two C1P species are significantly altered in obese liver tissue compared to lean. C18- and C18:1- C1P levels are both significantly lower in an obese state (Figs.20 and 21). C16-C1P is lower in obese tissue, although not significantly. All other C1P species are below detection level. Total C1P levels show that total C1P is significantly lower in obese liver tissue (Fig. 22).

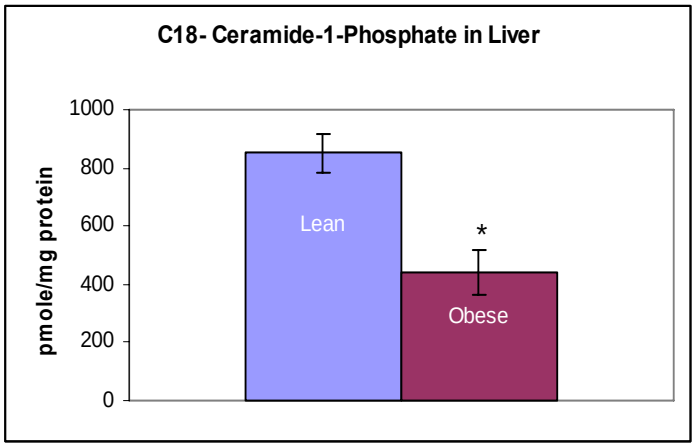

Figure 20: C18- ceramide-1-phosphate in lean and obese liver tissue

Ceramide levels are shown in pmole/mg protein ± s.e.m.; *significantly different from lean group ($P<0.05$; N=5). C1P is quantified by HPLC-MS. After sphingolipid extraction, samples containing 1mg of protein were analyzed using TSQ 7000 LC/MS system.

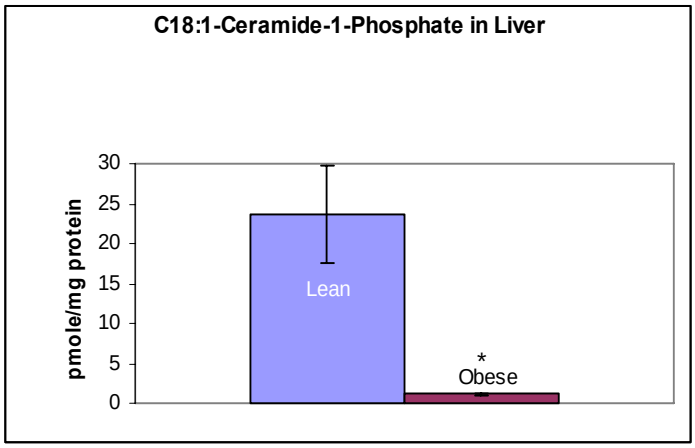

Figure 21: C18:1- ceramide-1-phosphate in lean and obese liver tissue

Ceramide levels are shown in pmole/mg protein ± s.e.m.; *significantly different from lean group (P<0.05; N=5).C1P is quantified by HPLC-MS. After sphingolipid extraction, samples containing 1mg of protein were analyzed using TSQ 7000 LC/MS system.

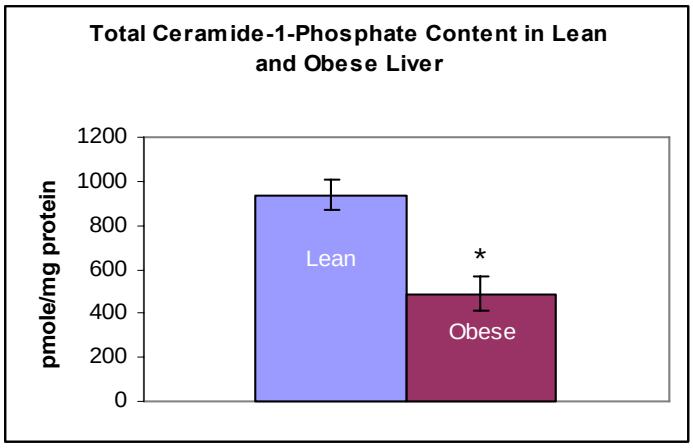

Figure 22: Total ceramide-1-phosphate content in lean and obese liver tissue

Ceramide levels are shown in pmole/mg protein ± s.e.m.; *significantly different from lean group (P<0.05; N=5). C1P is quantified by HPLC-MS. After sphingolipid extraction, samples containing 1mg of protein were analyzed using TSQ 7000 LC/MS system.

3.2.10 Sphingosine Content in Liver

LC-MS analysis shows that sphingosine is higher in obese liver compared to lean though the two groups do not differ significantly for N=5 per group. (Fig. B1 in appendix).

3.2.11 Sphingosine-1-Phosphate Content in Liver

S1P levels were below detection level in LC-MS analysis in liver. 17C-S1P was used as an internal standard. Samples containing 1mg of protein were analyzed using TSQ 7000 LC/MS system. S1P is the only sphingolipid undetectable in the 1mg samples used; therefore S1P must exist at much lower levels compared to other sphingolipids. Only 1-2 samples per group had detectable levels of S1P so statistical analysis could not be completed. It is inconclusive whether S1P levels differ significantly between lean and obese groups in liver.

3.3 Lean and Obese Colon Tissue Results

3.3.1 Sphingomyelinase Activity in Colon

Sphingomyelinase levels did not differ significantly between groups (Figs. 24 and 25).

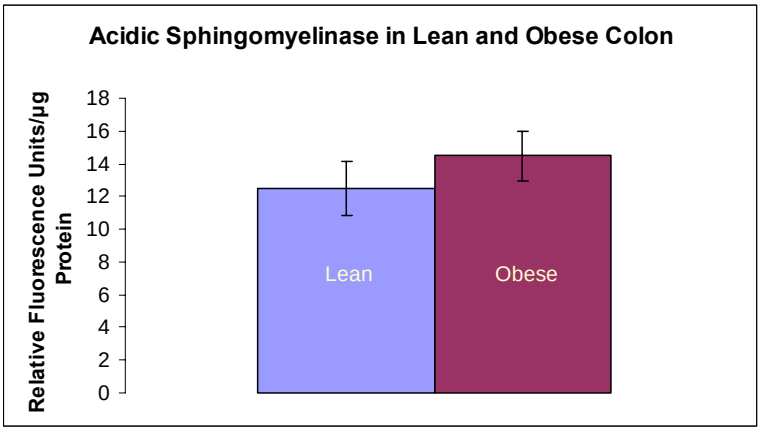

Figure 23: Acidic sphingomyelinase in lean and obese colon tissue

Mean sphingomyelinase levels (N=6 per group) are expressed in relative fluorescence units per µg protein ± s.e.m. See materials and methods for details.

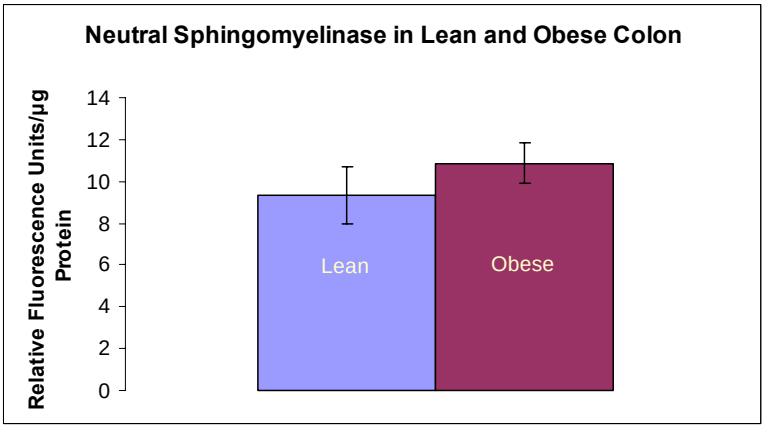

Figure 24: Neutral sphingomyelinase in lean and obese colon tissue

Mean sphingomyelinase levels (N=6 per group) are expressed in relative fluorescence units per µg protein ± s.e.m. See materials and methods for details.

3.3.2 Ceramidase Expression in Colon

Ceramidase bands were observed at a band size of 40kDa for both lean and obese liver tissue. This band size demonstrates that the ceramidase in colon is present as the mature 40kDa subunit ceramidase protein. Ceramidase protein expression is significantly higher in obese colon tissue compared to lean colon tissue (Fig. 25).

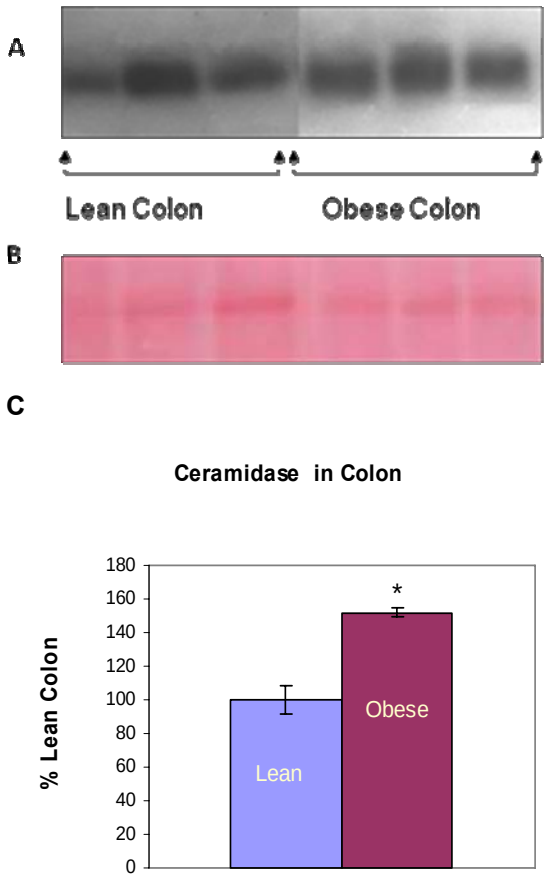

Figure 25: Western blot for ceramidase in lean and obese colon.

3 representative bands from each group (A) are shown with representative bands from their respective ponceau stains (B). Samples containing 50 µg of protein were separated by 10% SDS-PAGE gel and transferred onto PVDF membranes. Following incubation with primary anti-ceramidase at a1:200 dilution and secondary HRP-conjugated anti-goat at a 1:10,000 dilution, the blots were developed on X-ray film using ECL-Plus substrate. Membranes were then stained with Ponceau-S for equal loading control. Bar graphs (C) represent mean levels of ceramidase in lean and obese colon. All ceramidase bands were normalized to their respective ponceau bands; *significantly different from lean group ($P<0.05$; $N=6$).

3.3.3 Sphingosine Kinase Expression in Colon

Sphingosine kinase bands were observed at the predicted band size of 43 kDa for both lean and obese liver tissue. A wider band or possible doublet band is observed for both groups. However, altering the running time or gel concentration during electrophoresis did not help achieve band separation so the wide bands were quantified entirely. SK1 protein expression is significantly lower in obese colon tissue (Fig.26).

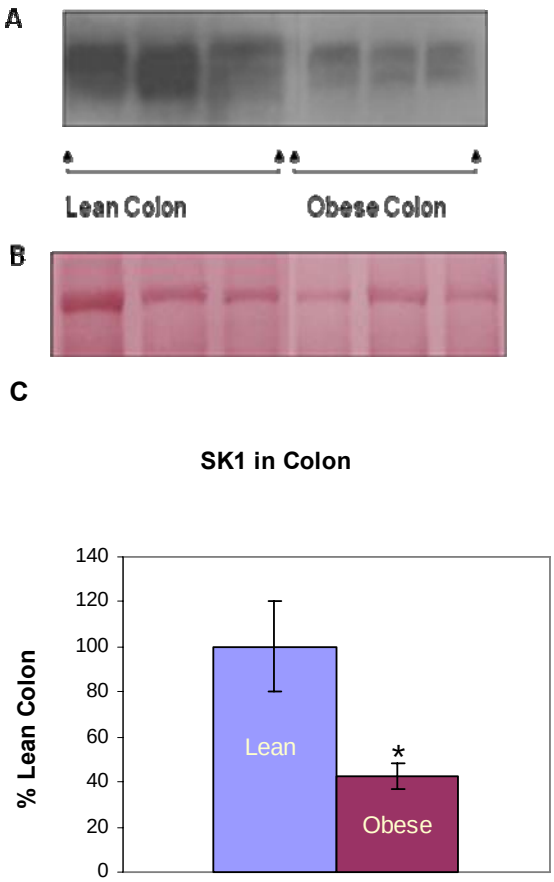

Figure 26: Western blot for SK1 in lean and obese colon.

3 representative bands from each group (A) are shown with representative bands from their respective ponceau stains (B). Samples containing 150 µg of protein were separated by 10% SDS-PAGE gel and transferred onto PVDF membranes. Following incubation with primary anti-SK1 at a1:500 dilution and secondary HRP-conjugated anti-rabbit at a 1:3000 dilution, the blots were developed on X-ray film using ECL-Plus substrate. Membranes were then stained with Ponceau-S for equal loading control. All SK1 expression bands were normalized to ponceau bands. Bar graphs (C) represent expression levels of SK1 in lean and obese colon, expressed as percentage lean colon; *significantly different from lean group ($P<0.05$; $N=6$).

3.3.4 Bcl-2 Expression in Colon Tissue

Bcl-2 bands were observed at the twice the predicted band size of 30 kDa for both lean and obese colon tissue, appearing at the 60kDa mark. As this band size is unpredicted by antibody specifications, it may not represent Bcl-2 and may be demonstrating cross reactivity of the antibody. Putative Bcl-2 protein expression is significantly higher in obese colon tissue (Fig.27).

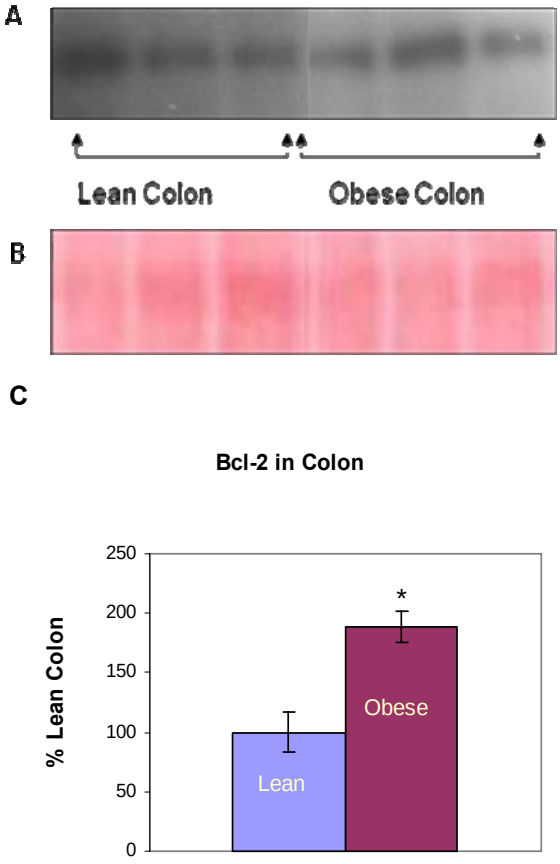

Figure 27: Western blot for Putative Bcl-2 in lean and obese colon.

3 representative bands from each group (A) are shown with representative bands from their respective ponceau stains (B). Samples containing 50 µg of protein were separated by 10% SDS-PAGE gel and transferred onto PVDF membranes. Following incubation with primary anti-Bcl-2 at a1:500 dilution and secondary HRP-conjugated anti-rabbit at a 1:3000 dilution, the blots were developed on X-ray film using ECL-Plus substrate. Membranes were then stained with Ponceau-S for equal loading control. All Bcl-2 expression bands were normalized to ponceau bands. Bar graphs (C) represent expression levels of putative Bcl-2 in lean and obese colon, expressed as percentage lean colon; *significantly different from lean group ($P<0.05$; N=6).

3.3.5 Bax Expression in Lean versus Obese Colon Tissue

Bax bands were observed at an expected band size of 42 kDa for both lean and obese liver tissue, demonstrating that Bax proteins are present as homodimers in colon tissue. Bax protein expression is significantly higher in obese colon tissue (Fig. 28).

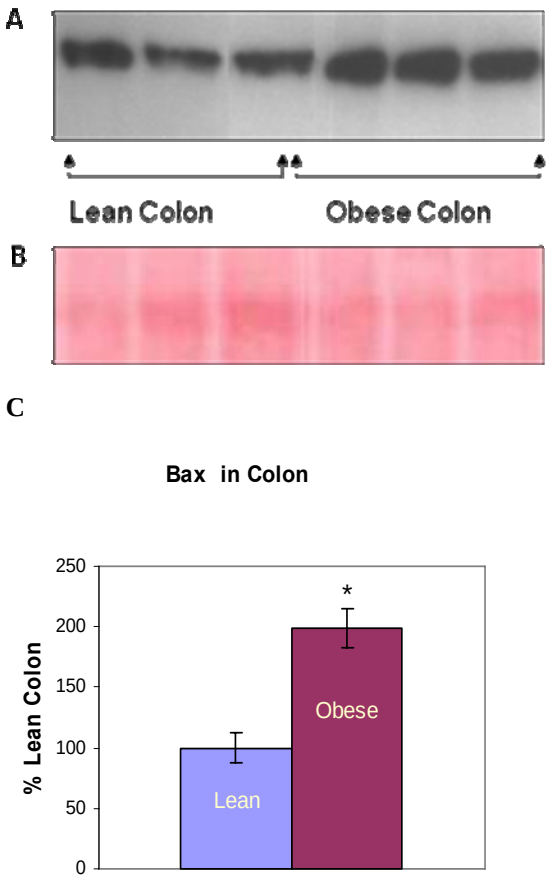

Figure 28: Western blot for Bax in lean and obese colon.

3 representative bands from each group (A) are shown with representative bands from their respective ponceau stains (B). Samples containing 50 µg of protein were separated by 10% SDS-PAGE gel and transferred onto PVDF membranes. Following incubation with primary anti-Bax at a1:500 dilution and secondary HRP-conjugated anti-rabbit at a 1:3000 dilution, the blots were developed on X-ray film using ECL-Plus substrate. Membranes were then stained with Ponceau-S for equal loading control. All Bax expression bands were normalized to ponceau bands. Bar graphs (C) represent expression levels of Bax in lean and obese colon, expressed as percentage lean colon; *significantly different from lean group ($P<0.05$; $N=6$).

3.3.6 Sphingomyelin Content in Colon

No significant differences in sphingomyelin species are observed between lean and obese colon tissue. (Fig. B2 in appendix).

Unlike liver tissue, no differences are observed in SM species composition between lean and obese colon (Fig. 29).

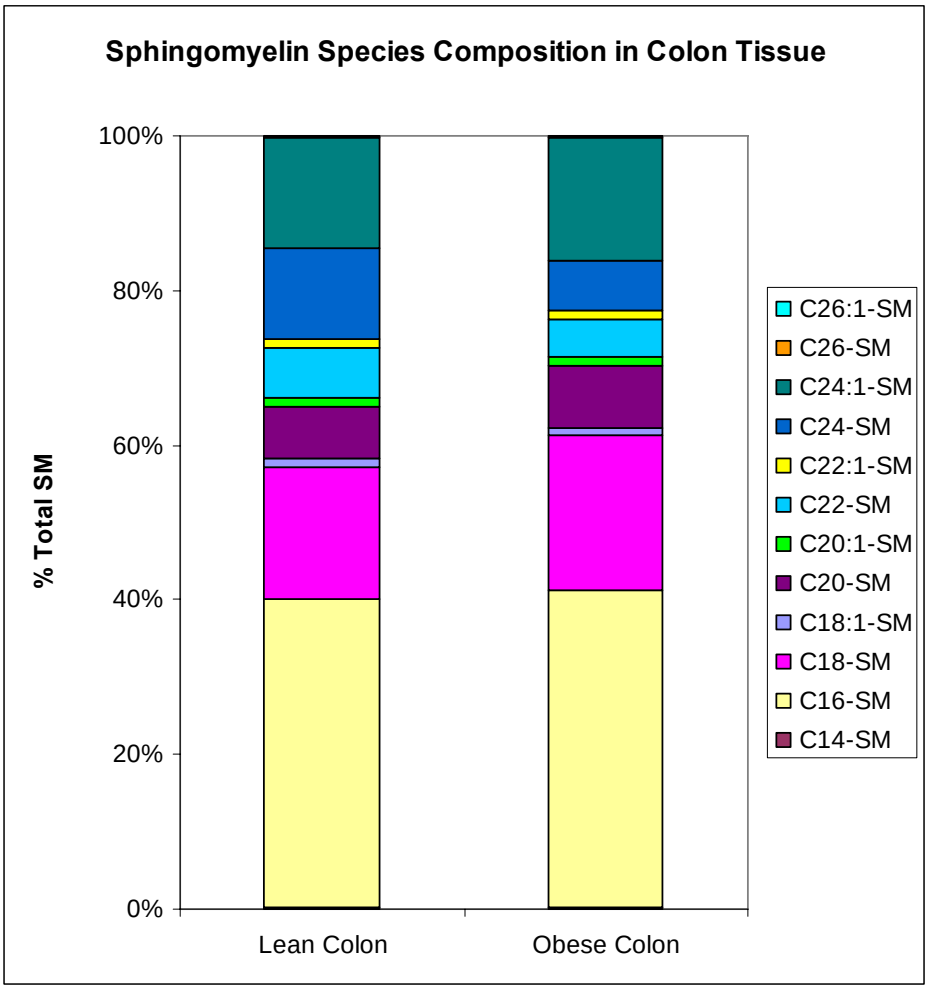

Figure 29: Sphingomyelin species composition in lean versus obese colon tissue

SM species levels are shown as a percentage of total SM content in this stacked graph. No significant differences between groups are observed.

3.3.7 Ceramide Content in Colon

C24:1 ceramide is significantly higher in obese colon tissue compared to lean (Fig. 30). No significant differences were observed for any other ceramide species in colon tissue. Total ceramide levels were higher in obese tissue, though not significantly (Fig. B3 in appendix).

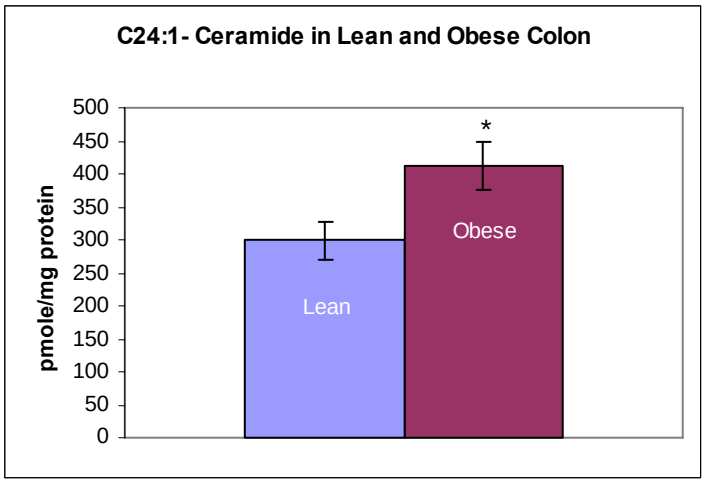

Figure 30: C24:1 ceramide levels in lean and obese colon

Ceramide levels are shown in pmole/mg protein ± s.e.m; *significantly different from lean group ($P<0.05$; N=5)**.**Ceramides were quantified by HPLC-MS. Internal standard 17C16-ceramide was used. After sphingolipid extraction, samples containing 1mg of protein were analyzed using TSQ 7000 LC/MS system.

The relative differences in ceramide species compositions between the lean and obese colons are depicted in the following stacked graph (Fig. 31).

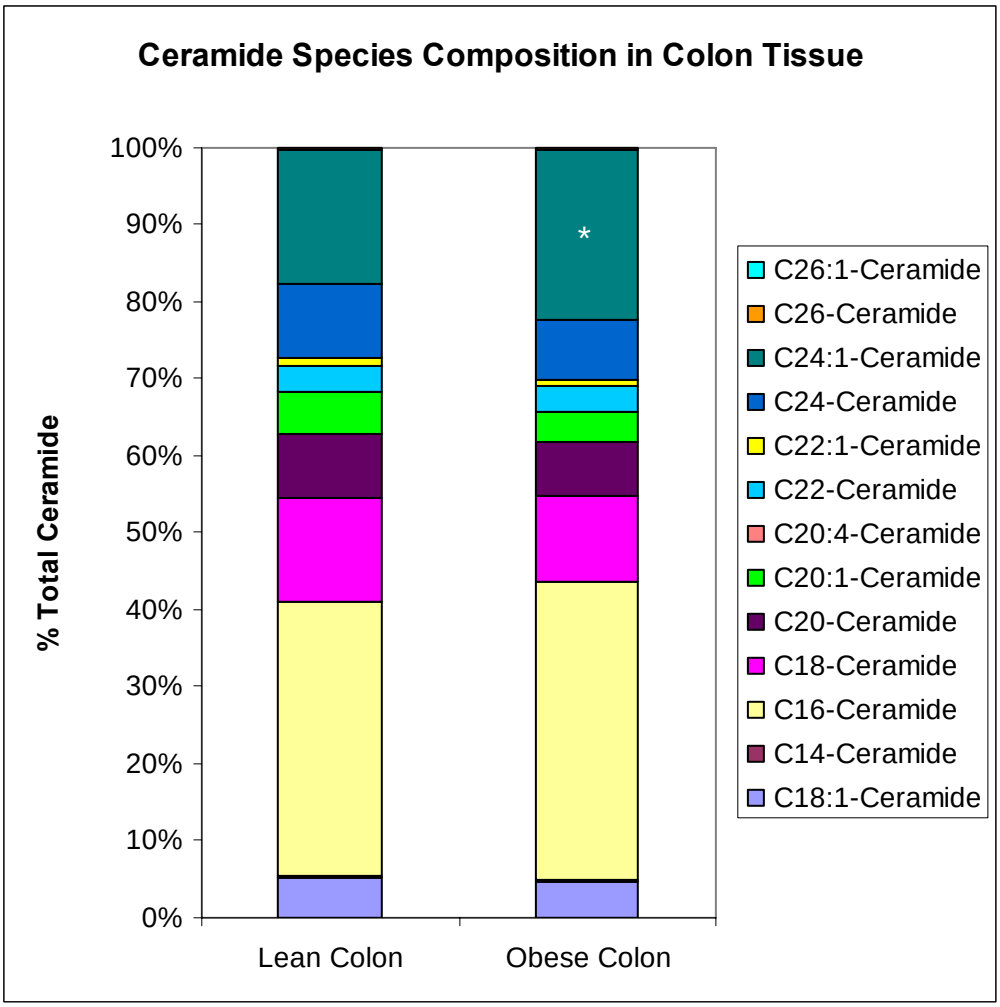

Figure 31: Ceramide species composition in lean versus obese colon tissue

Ceramide species levels are shown as a percentage of total ceramide content in this stacked graph:*significantly different from lean group ($P<0.05$; $N=5$). Significant differences can be observed only for C24:1-ceramide.

3.3.8 Ceramide-1-Phosphate Content in Colon

LC-MS analysis shows that only two C1P species are detectable in colon, C18- and C16-C1P. C18-C1P levels are significantly lower in an obese state (Fig.32). C16-C1P is lower in obese tissue, although not significantly. All other C1P species are below detection level. Total C1P levels show that total C1P is significantly lower in obese colon tissue (Fig. 33).

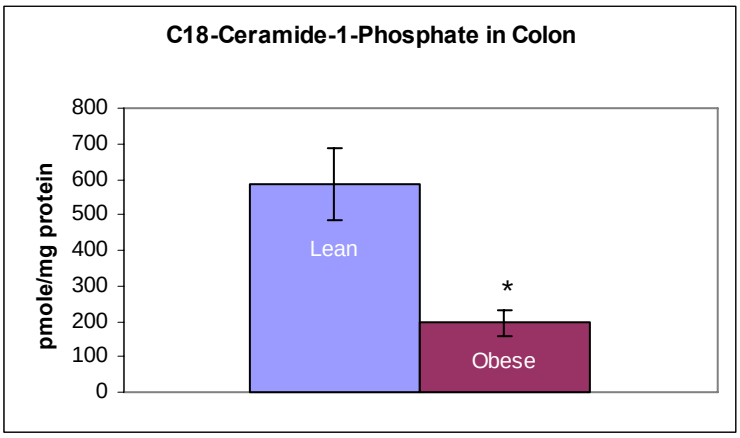

Figure 32: C18- ceramide-1-phosphate in lean and obese colon tissue

Ceramide-1-phosphate levels are shown in pmole/mg protein ± s.e.m.;*significantly different from lean group ($P<0.05$; N=5). C1P is quantified by HPLC-MS. After sphingolipid extraction, samples containing 1mg of protein were analyzed using TSQ 7000 LC/MS system.

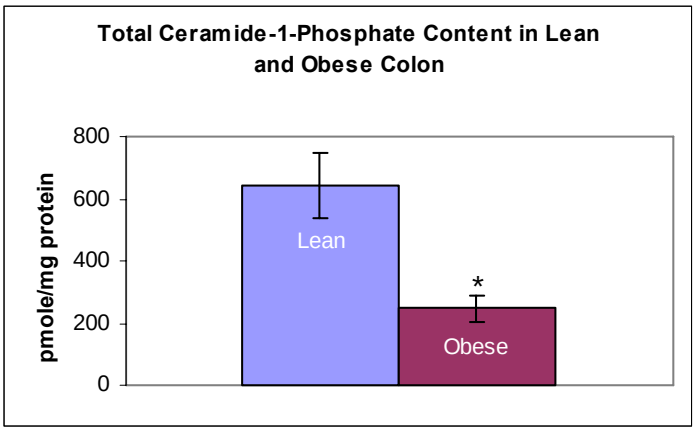

Figure 33: Total ceramide-1-phosphate content in lean and obese colon tissue

Ceramide-1-phosphate levels are shown in pmole/mg protein ± s.e.m.;*significantly different from lean group ($P<0.05$; N=5). C1P is quantified by HPLC-MS. After sphingolipid extraction, samples containing 1mg of protein were analyzed using TSQ 7000 LC/MS system.

3.3.9 Sphingosine Content in Colon

LC-MS analysis shows that sphingosine is higher in obese colon tissue compared to lean though the two groups do not differ significantly for N=5 per group (Fig. B4 in appendix).

3.3.10 Sphingosine-1-Phosphate in Colon

S1P levels were below detection level in LC-MS analysis in colon. 17C-S1P was used as an internal standard. Samples containing 1mg of protein were analyzed using TSQ 7000 LC/MS system. S1P is the only sphingolipid undetectable in the 1mg samples used; therefore S1P must exist at much lower levels compared to other sphingolipids. Only 1-2 samples per group had detectable levels of S1P so statistical analysis could not be completed. It is inconclusive whether S1P levels differ significantly between lean and obese groups in colon.

3.4 Tissue Specific Differences

3.4.1 Sphingomyelinase Activity in Liver versus Colon

Comparisons between liver and colon tissue show that sphingomyelinase activity differs significantly between tissues. Sphingomyelinase activity is higher in lean colon tissue compared to liver tissue (Fig.34), as well as in obese colon tissue compared to liver tissue (Fig.35).

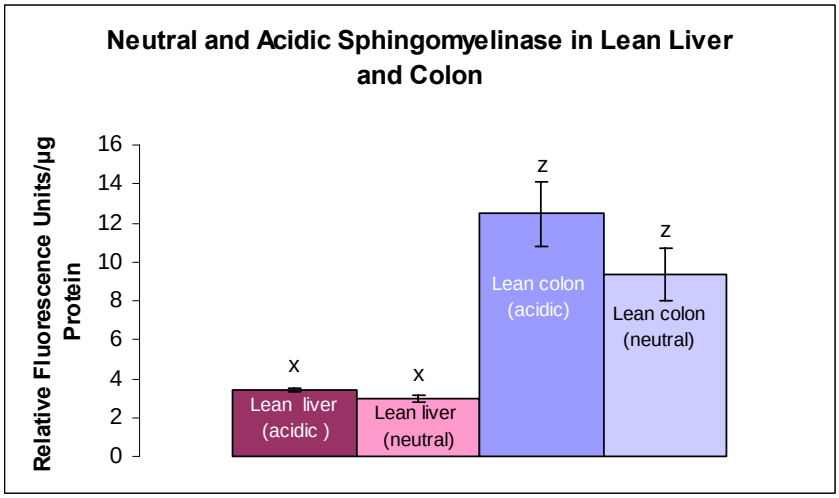

Figure 34: Neutral and acidic sphingomyelinase activity in lean liver and colon

Mean sphingomyelinase levels are expressed in relative fluorescence units per µg protein ± s.e.m.; values without a common letter (^{x,,z}) differ significantly ($P<0.05$, $N=6$). See materials and methods for details.

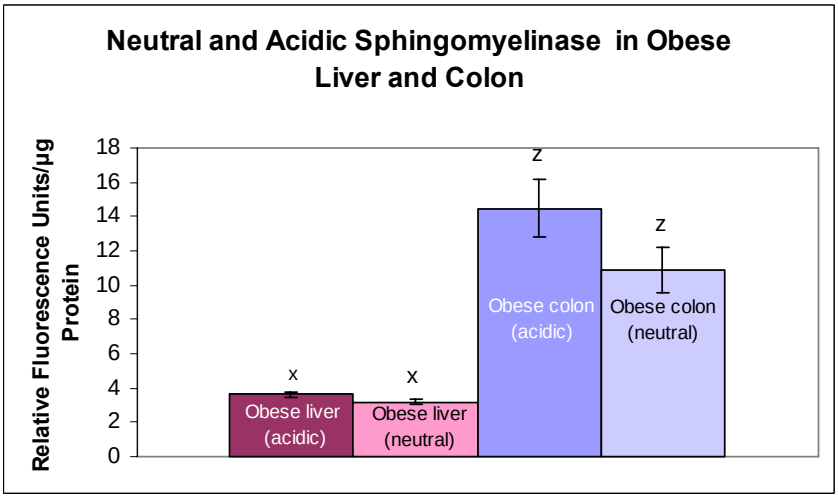

Figure 35: Neutral and acidic sphingomyelinase activity in obese liver and colon

Mean sphingomyelinase levels are expressed in relative fluorescence units per µg protein ± s.e.m.; values without a common letter (^{x,,z}) differ significantly ($P<0.05$, $N=6$). See materials and methods for details.

3.4.2 Sphingolipids in Liver versus Colon

LC-MS results showed that there are tissue specific differences between sphingolipids. A paired-samples t-test was run for each sphingolipid, comparing liver and colon tissue from the same rat.

3.4.2.1 Sphingomyelin Content in Liver versus Colon

Total sphingomyelin levels are significantly higher in colon tissue compared to liver tissue (Figs.36 and 37).

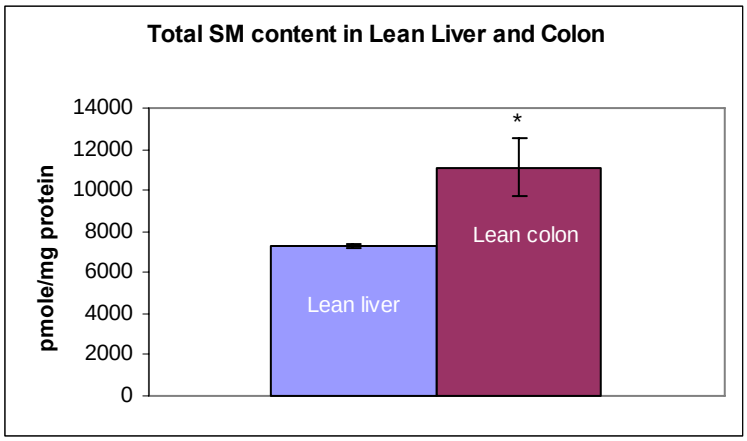

Figure 36: Total sphingomyelin content in lean liver and colon tissue

SM levels are shown in pmole/mg protein ± s.e.m.;*significantly different from lean group ($P<0.05$; $N=5$). SMs were quantified by HPLC-MS. 18C17-SM was used as an internal standard. After sphingolipid extraction, samples containing 1mg of protein were analyzed using TSQ 7000 LC/MS system.

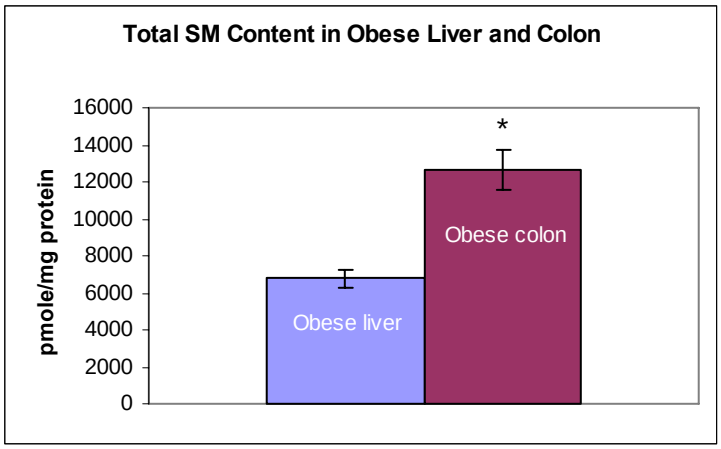

Figure 37: Total sphingomyelin content in obese liver and colon

SM levels are shown in pmole/mg protein ± s.e.m.;*significantly different from lean group ($P<0.05$; $N=5$). SMs were quantified by HPLC-MS. 18C17-SM was used as an internal standard. After sphingolipid extraction, samples containing 1mg of protein were analyzed using TSQ 7000 LC/MS system.

A shift in SM species composition can be observed between liver and colon tissue as illustrated in the stacked graph below (Fig. 38).

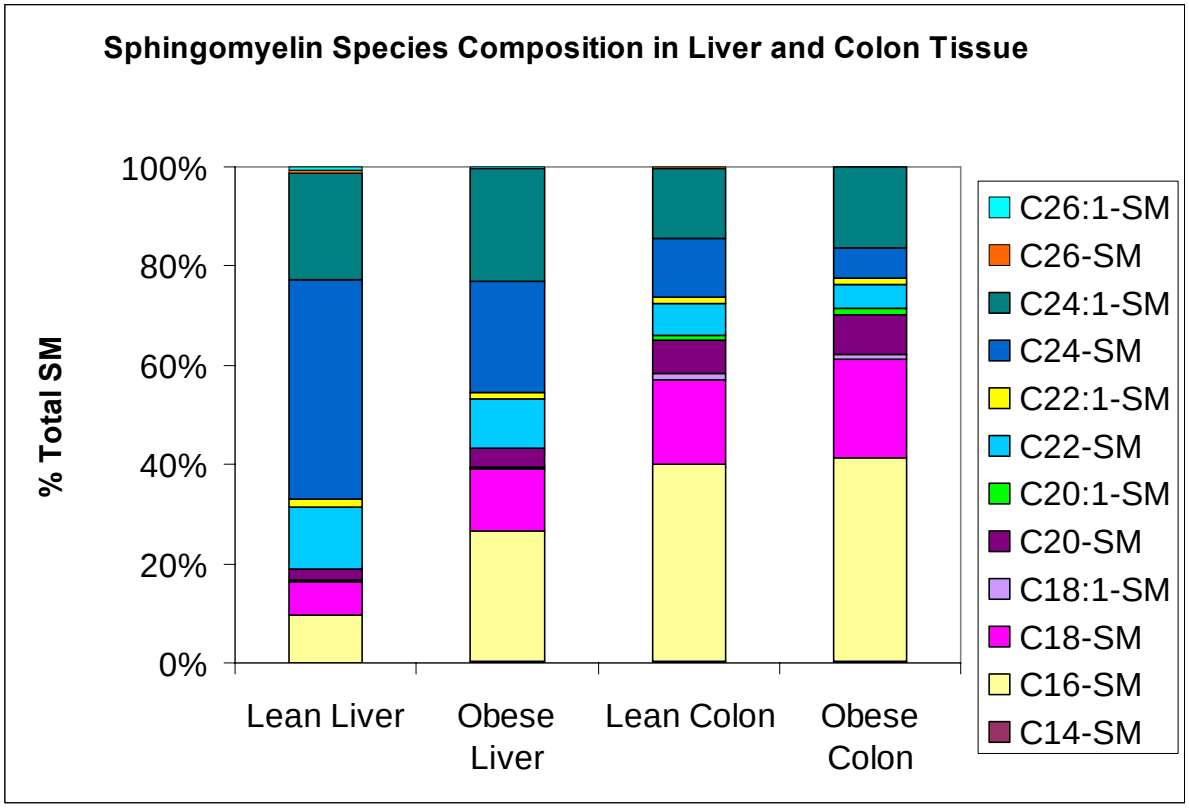

Figure 38: Sphingomyelin species composition in liver and colon tissue

This graph provides a qualitative visualization of differences in SM species between tissue types. SM species levels are shown as a percentage of total SM content in this stacked graph.

3.4.2.2 Ceramide Content in Liver versus Colon

Comparison of ceramide content in liver and colon finds that total ceramide is significantly higher in colon tissue (Figs. 39 and 40).

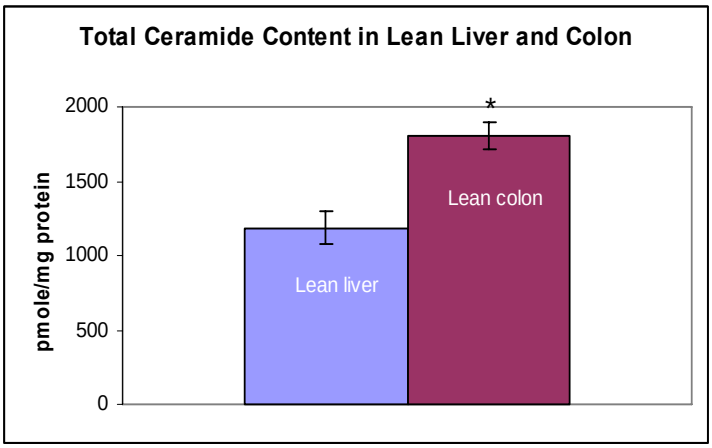

Figure 39: Total ceramide content in lean liver and colon

Ceramide levels are shown in pmole/mg protein ± s.e.m.;*significantly different from lean group ($P<0.05$; N=5). Ceramides were quantified by HPLC-MS. 17C16-ceramide was used as an internal standard. After sphingolipid extraction, samples containing 1mg of protein were analyzed using TSQ 7000 LC/MS system.

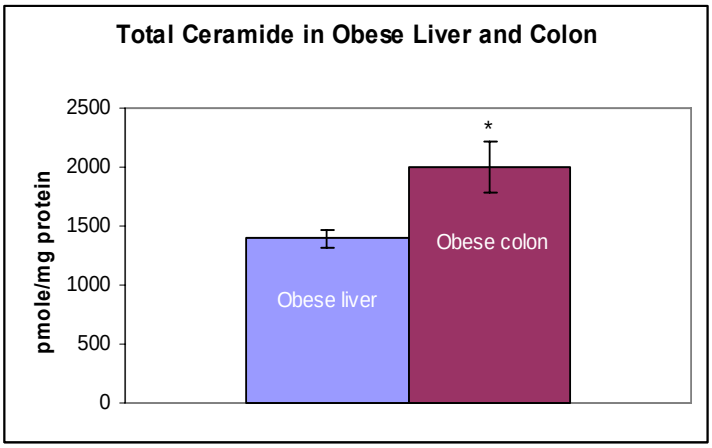

Figure 40: Total ceramide content in obese liver and colon

Ceramide levels are shown in pmole/mg protein ± s.e.m.;*significantly different from lean group ($P<0.05$; N=5). Ceramides were quantified by HPLC-MS. 17C16-ceramide was used as an internal standard. After sphingolipid extraction, samples containing 1mg of protein were analyzed using TSQ 7000 LC/MS system.

A shift in SM species composition can be observed between liver and colon tissue as illustrated in the stacked graph below (Fig.41).

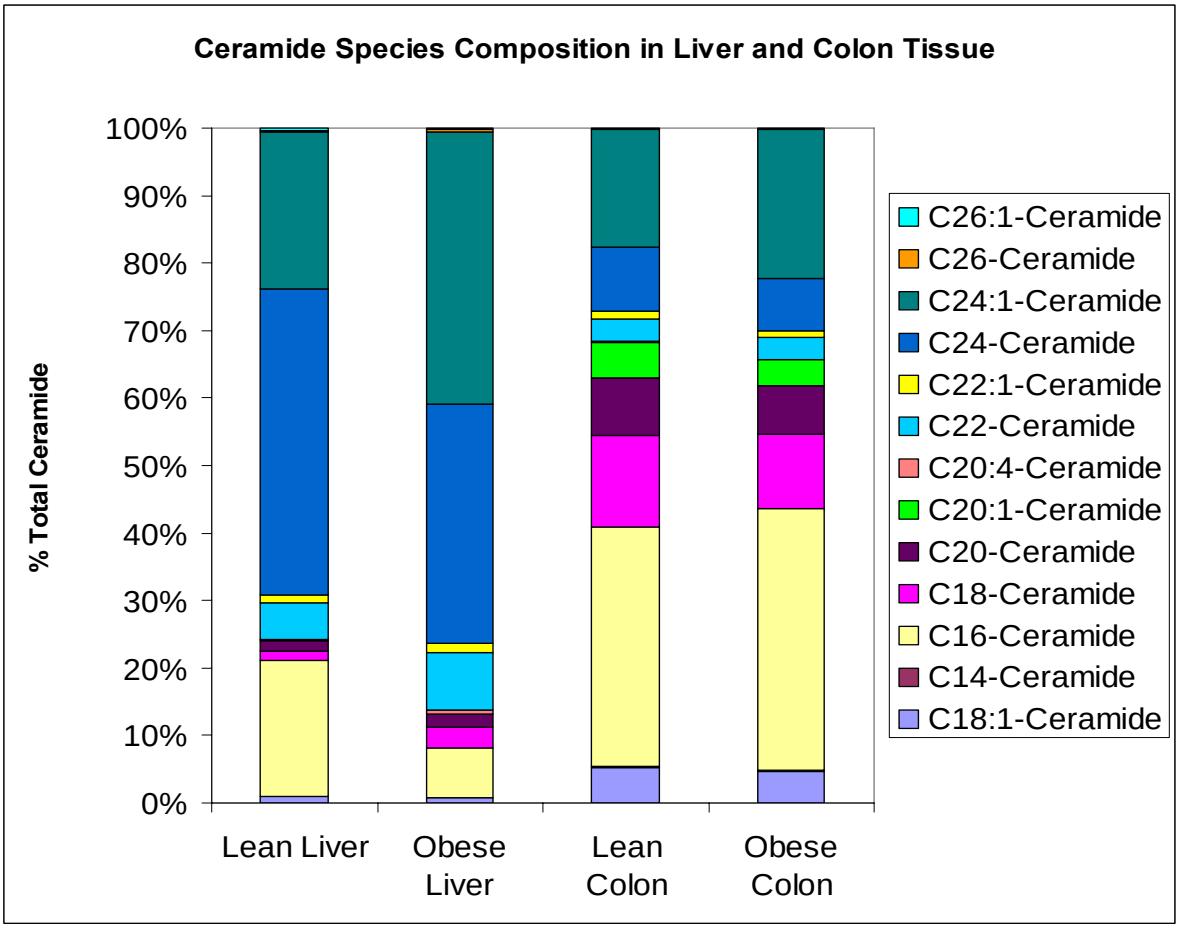

Figure 41: Ceramide species composition in liver and colon tissue

This graph provides a qualitative visualization of differences in ceramide species between tissue types. Ceramide species levels are shown as a percentage of total ceramide content in this stacked graph.

3.4.2.3 Sphingosine Content in Liver versus Colon

Sphingosine levels do not differ significantly in comparing liver and colon tissue (Figs. B5 and B6 in appendix).

3.4.2.4 Ceramide-1-Phosphate in Liver versus Colon

C1P levels are significantly lower in colon compared to liver (Figs.42 and 43).

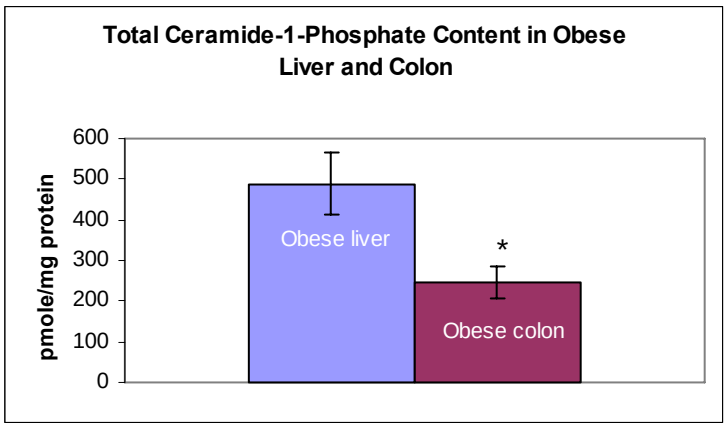

Figure 42: Total ceramide-1-phosphate content in lean liver and colon

Ceramide-1-phosphate levels are shown in pmole/mg protein ± s.e.m.;*significantly different from lean group ($P<0.05$; N=5). C1P is quantified by HPLC-MS. After sphingolipid extraction, samples containing 1mg of protein were analyzed using TSQ 7000 LC/MS system.

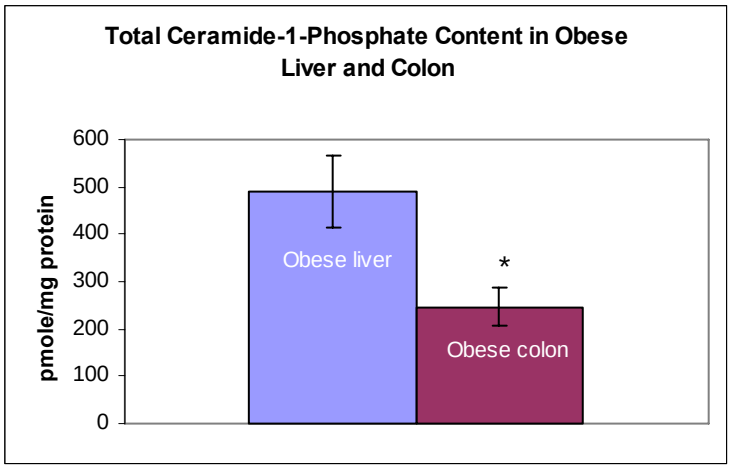

Figure 43: Total ceramide-1-phosphate content in obese liver and colon

Ceramide-1-phosphate levels are shown in pmole/mg protein ± s.e.m. .;*significantly different from lean group ($P<0.05$; N=5). C1P is quantified by HPLC-MS. After sphingolipid extraction, samples containing 1mg of protein were analyzed using TSQ 7000 LC/MS system.

Chapter 4
Discussion

In this study, an obese genotype impacted the sphingolipid signaling pathway in both liver and colon. To our knowledge, this is the first study comparing sphingolipid signaling in obese versus lean liver and colon tissue. The results show a clear tissue-specific alteration in sphingolipid signaling leading to the proposal that this pathway may be involved in the pathogenesis related to obesity.

4.1 Liver tissue

4.1.1 Sphingolipid Signaling Pathway in Liver Tissue

This study was undertaken to determine if the sphingolipid pathway is altered in a state of obesity in hepatic steatotic liver. It was hypothesized that the pro-inflammatory environment of the diseased fatty liver would result in an upregulation of the sphingolipid signaling pathway. Quantifying sphingolipids as well as the key sphingolipid enzymes did show notable differences in the sphingolipid pathway between obese and lean liver.

The liver is a complex and multi-functional organ and liver disease is a serious occurrence commonly linked to obesity. Zucker obese rats exhibit hepatic steatosis demonstrated by an accumulation of lipids in their hepatocytes (Figure 5). This may be attributed to insulin resistance and increased release of free fatty acids from adipose tissue (Angulo, 2002; Browning and Horton, 2002). In addition, hepatic steatosis is linked to oxidative stress and inflammation, and both reactive oxygen species and inflammatory molecules have been reported as being present in higher levels in a state of obesity (Bohlen, 2004; Chitturi et al., 2001). It is also well established that the sphingolipid signaling pathway is activated under conditions of cellular stress, including induction of SMase by TNF-α, IL-1β, free fatty acids, and ROS (Woodock, 2006; Ogretmen, 2006; Kolesnick, 2002).

When SMase activity was compared between obese and lean liver tissue, there was a trend toward a higher level of SMase in obese liver tissue. While both neutral and acidic SMase activity was found to be higher in obese tissue compared to lean in all repetitions of the assay, the differences were not

statistically significant. With the increased levels of inflammatory molecules and reactive oxygen species in obese tissue, it is interesting that there are not more significant differences in SMase activity between groups; however, many factors may contribute to the results obtained. Firstly, it should be noted that the animals in this study were not induced in any way to activate the pathway, and rather were in a steady state level of obesity. In studies looking at activation of SMase, inducers such as TNF-α or ROS are added in excess amounts. It cannot be expected that a steady state level of cellular stressors would affect the sphingolipid pathway to the same extent as shocking the cells with excess amounts of these molecules. Secondly, the enzyme assay is limited in that it only measures the level of available enzyme waiting to be stimulated. Thus enzyme that is already active or being used up is not being accounted for. Furthermore, it does not take into account turnover rate of the enzyme or the level of available substrate.

LC-MS quantification of SM shows a trend toward lower SM levels in obese liver tissue compared to lean. There are many different biological species of SM, distinguished by the number of carbon atoms and number of double bonds in their fatty acid chain. When individual SM species were compared between obese and lean liver, it was found that several species of SM are significantly lower in the obese tissue (Figs. 12 and 13). Specifically, long chain C22-, C22:1-, C24-, C26-, and C26:1- sphingomyelins were lower in obese liver tissue suggesting that either the longer chain SMs are being hydrolyzed to ceramide by activated SMase in obese tissue or that lean and obese rats simply differ in the composition of SMs present in their hepatocyte membranes. If the latter were true, it would be expected that with five species of SM lower in obese tissue, other species of SM must be present at higher levels, but in fact, only one SM species, C16-SM was found to be higher in obese liver tissue (Fig.12). While this does suggest a shift in SM species between lean and obese groups, it is possible that the longer chain SMs are being hydrolyzed by active SMase, thus explaining their lower levels in obese tissue.

Though the level of total SM is not significantly lower in the obese group, a very small sample size was used (N=5) (Fig.14). A larger sample size would help clarify if there are significant differences between SM levels in lean and obese liver tissue. It must also be noted that the sphingolipid pathway is not a stagnant one. While SM hydrolysis may be occurring, SM synthesis can also be taking place within the cells, resulting in SM regeneration, and perhaps certain species of SM are generated more frequently. The trend toward lower SM in obese liver coincides with a recent study that found SM to be downregulated in livers from obese mice compared to their lean counterparts (Yetukuri, 2007).

The hydrolysis of SM by SMase results in ceramide production. Examining ceramide content in lean and obese groups shows further sphingolipid differences. While there is a trend toward higher ceramide levels in obese liver tissue, total ceramide content is not significantly higher in obese tissue (Fig.18). Once again, a larger sample size would be more conclusive in deciding if total ceramide is significantly higher in obese liver, though the small sample size used here is still enough to see differences amongst ceramide species between groups.

Like SM, ceramide can be divided into species depending on the number of carbon atoms and double bonds are present in the fatty acid chain. When the various species were compared between groups, it was found that C22-, C24:1-, C18-, C20-, and C24:0-ceramide were present at higher levels in obese tissue (Figs. 16 and 17). Interestingly, C16-ceramide is significantly lower in obese tissue (Fig.16). The upregulation of some species and downregulation of anther indicates a shift in ceramide species composition (Fig.19). This supports a recent finding showing higher ceramide concentration in livers of obese mouse compared to a lean mouse (Yetukuri et al, 2007). Specifically, the mouse study showed that C18- and C16-ceramide were the most abundant ceramide species and were upregulated in obese liver. These upregulated ceramide species correlated with same chain length triacylglyerol, suggesting that accumulation of reactive ceramide species increase in the liver of the obese mice proportionally to the accumulation of triacylglycerol, which is a characteristic of hepatic steatosis (Yetukuri et al., 2007). In our analysis, we found that C16, C24 and C24:1-ceramides were the most abundant in liver tissue, and perhaps this can be linked to the chain length of triacylglycerols present in rat tissue that differ from those found in the mouse model. It is interesting to note the shift in abundant ceramide species observed between the obese mouse model and the rat used in our study. While the upregulation of C18-ceramide in obese liver is similar between the two models, the C16-ceramide concentration was downregulated in rat obese liver tissue unlike the mouse tissue (Yetukuri et a., 2007). However, this coincides with our finding that C16-SM is significantly higher in obese liver tissue suggesting that less C16-SM is being hydrolyzed by SMase to produce C16-ceramide.

The production and accumulation of ceramide is important in generating an apoptotic signal within the cell. The trend toward higher ceramide levels and altered ceramide species in obese tissue may contribute to the pathogenesis of the steatotic liver. Of course, other sphingolipid signaling molecules in the pathway must be examined as well so as to determine the overall balance in signaling molecules. Ceramide, once generated, has many fates within a cell. It can be converted back to SM, deacetylated to sphingosine, or phosphorylated to C1P. Ceramide can be phosphorylated by CerK to

form C1P. Quantification of C1P shows that C18- and C18:1-C1P (figures) are significantly downregulated in obese liver, as well as total C1P levels (figure). All longer chain species of C1P were below detection level. This downregulation of C1P is important as C1P opposes apoptotic ceramide activity. An overall depression in C1P indicates that the obese liver cells are receiving less stimulation for survival and proliferation.

Ceramide can also be prevented from accumulating in the cell via conversion to sphingosine. Ceramidase deacetylates ceramide, producing sphingosine. When this enzyme was analyzed by western blot, it was found that ceramidase expression was significantly higher in obese liver. In liver tissue, ceramidase bands were observed at a size of 55kDa, consistent with the expected size of ceramidase precursor protein. Ceramidase is synthesized as a 55kDa lysosomal protein. This protein can be cleaved into two subunits, alpha and beta, of 13kDa and 40 kDa respectively (Bernardo et al., 1995). Little is known about inducers of ceramidase, however, it has been suggested that platelet derived growth factor (PDGF) and insulin-like growth factor (IGF) can activate ceramidase, leading to sphingosine production (Suzuki et al., 2004). Ceramidase overexpression in obese liver tissue may indicate the tissue trying to compensate for high ceramide levels in the active sphingolipid pathway. Ceramidase may play a protective role by converting ceramide to sphingosine. While sphingosine is considered like ceramide to be an apoptotic signaling molecule, it is also the necessary substrate for SK1 and the production of S1P. Thus sphingosine is an important intermediary, signaling for apoptosis while being readily available to be converted to a mitogenic signaling molecule. In fact, a study examining the role of ceramide in apoptosis found that overexpression of acid ceramidase protected cells from TNF-α-induced apoptosis, demonstrating the ceramidase expression may help shift the balance between intracellular ceramide and S1P levels towards cell survival (Strelow et al., 2000).

LC-MS analysis of sphingosine revealed that there is a trend toward upregulation of sphingosine in obese tissue, although the results do not differ significantly. Though sphingosine is a bioactive lipid itself, capable of apoptotic signals, it can be converted back to ceramide via ceramide synthase, or as previously mentioned, it can be phosphorylated to S1P by SK1.

In contrast to SMase and ceramidase, SK1 expression was found to be downregulated in obese liver, by approximately 60%. SK1 phosphorylates sphingosine to produce S1P, an important mediator of cell growth and differentiation. SK1 is a 43 kDa protein though a second band can be

observed just below the 43 kDa mark in obese liver tissue. This could be demonstrating cross-reactivity of a non-specific antibody with other proteins, as three other bands of various sizes were observed in western blotting with polyclonal anti-SK1 in liver tissue. For further SK1 analysis, a highly purified antibody is recommended to yield cleaner results. The decreased expression of SK1 in steatotic liver tissue may indicate lower levels of S1P being produced, and this further verifies the idea that in hepatic steatotic tissue there is a shift toward apoptosis, induced by the change in balance between sphingolipid signaling enzymes.

LC-MS analysis of S1P showed that S1P levels were below detection level, meaning the levels of S1P for most samples were below 0.1 pmole/mg protein. S1P is normally at very low levels in vivo. Sphingosine-1- phosphatase can remove the phosphate, regenerating sphingosine or sphingosine-1-phosphate lyase can act to irreversibly degrade S1P. Together, these two enzymes control S1P levels. A study comparing S1P levels in various rat tissues found that S1P is the lowest in the liver (Yatomi, 1997) and this can be attributed to high levels of sphingosine-phosphate lyase (Veldhoven and Mannaerts, 1991). The low levels of S1P will increase only when SK1 is upregulated, induced by a diverse number of growth stimuli, including PDGF (Olivera et al., 1999; Olivera and Spiegel, 1993). Since it is clear in obese liver tissue that SK1 is downregulated, S1P levels would remain at a very low level.

4.1.2 Apoptotic Proteins in Liver Tissue

This portion of the study was carried out to assess representative apoptotic proteins that are known to be affected by the sphingolipid pathway. A rise in ceramide levels will mediate apoptosis through PP2a. PP2a can activate pro-apoptotic Bax through dephosphorylation, leading to membrane permeation and subsequent cytochrome c release and apoptosis (Xin et al., 2006). Furthermore, ceramide has been implicated in the downregulation of anti-apoptotic Bcl-2. Bcl-2 binds to Bax and prevents Bax from initiating apoptosis at the mitochondrial membrane. PP2a may also play a role in ceramide induction of Bcl-2. PP2a activated by ceramide can dephosphorylate Bcl-2, rendering it inactive as an anti-apoptotic protein (Ruvolo et al., 1999).

Analysis of Bax and Bcl-2 proteins by western blot showed that both are altered in obese liver tissue. The western blot for Bax showed proteins at the 21kDa level, and a faint band at the 42kDa

level, consistent with the tendency of Bax to form dimers (Gross et al., 1998). Densitometric analysis of the 21kDa bands showed that Bax is upregulated in obese tissue by approximately 100% (Fig.11). Analysis of Bcl-2 found that Bcl-2 protein expression is approximately 75% lower in obese tissue (Fig.10). The altered levels of these two proteins in liver tissue suggest an increase in pro-apoptotic signals in obese liver tissue and is consistent with the diseased state of the steatotic liver tissue. Hepatocyte apoptosis is closely associated with steatosis. Increased expression of death receptors in obese livers sensitizes these cells to pro-apoptotic stimuli, thereby triggering excessive hepatocyte apoptosis and inflammation (Canbay et al., 2005). The altered levels of Bcl-2 and Bax observed in this portion of the study support the notion that steatotic liver is primed for apoptosis (Canbay et al., 2005). It is possible that the altered sphingolipid signaling pathway is closely linked to the observed upregulation of Bax and downregulation of Bcl-2. As there are many other proteins involved in mediating apoptosis, further investigation is required to assess the role of these proteins in triggering cell death in steatotic liver. Furthermore, ceramide is not the only factor regulating the Bcl-2 family of proteins, so it cannot be assumed that these enzymes depend solely on the sphingolipid pathway. However, this study demonstrates that downstream effector proteins of the sphingolipid signaling pathway are altered in obese rats leading to the proposal that sphingolipid pathway and Bcl-2 proteins play a role in the pathogenesis of hepatic steatosis.

4.1.3 Summary of the Sphingolipid Pathway in Liver Tissue

Sphingolipids are important molecules mediating apoptotic and mitogenic cellular responses. The dynamic balance between apoptotic ceramide and sphingosine and anti-apoptotic S1P and C1P will determine the proliferative or apoptotic fate of the cells (Reviewed in Chalfant and Spiegel, 2005; Ohanian and Ohanian, 2005). As these molecules are inter-convertible, the enzymes responsible for the catabolism and metabolism of these signalers are also important. Significant differences in sphingolipid enzymes and metabolites were found between obese and lean liver tissue (see Fig.44).

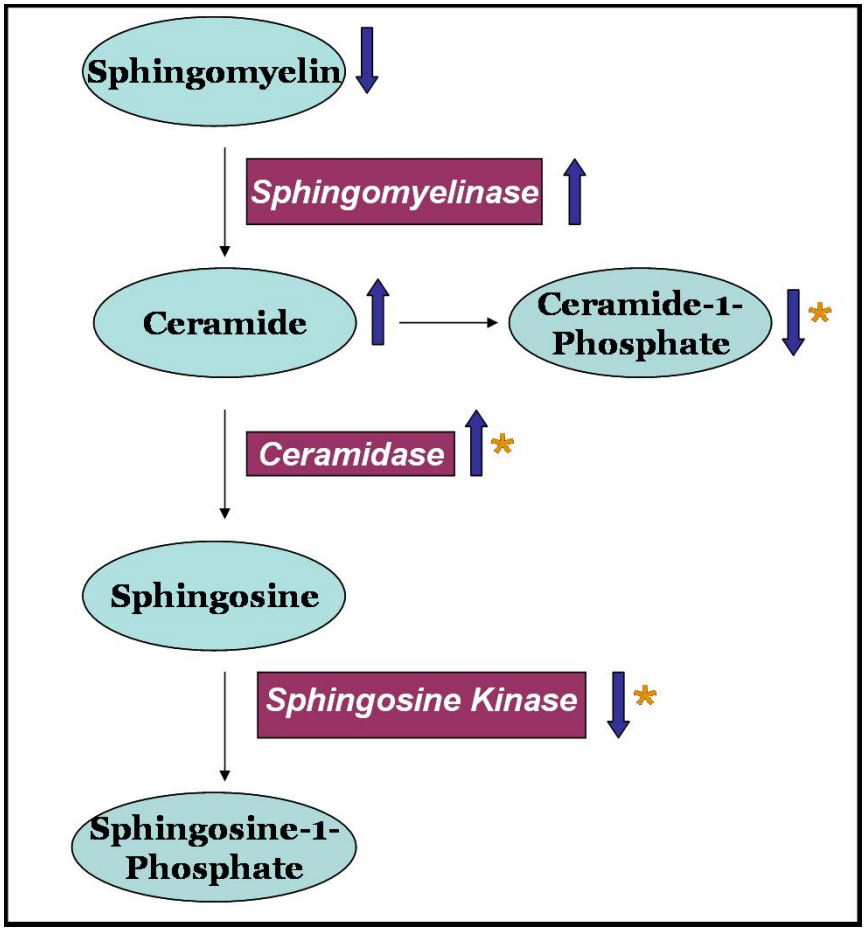

Figure 44: Summary of sphingolipid signaling changes in obese liver tissue

Arrows depict the observed trends of the sphingolipid enzymes and metabolites in obese liver tissue; * depicts significant changes observed (t-test, $P<0.05$); note that significant changes between SM and ceramide species observed are not depicted in this figure.

Obese liver tissue differs significantly from lean liver tissue in its SM and ceramide composition, highlighting a shift in the fatty acid tail length in obese liver sphingolipids. The tail length of sphingolipids may have important biological implications in sphingolipid signaling, thus this is an area of much needed research. Overall the results demonstrate that in obese steatotic liver tissue, SM and C1P were present at lower levels, while ceramide was present at a higher level. Also, ceramidase protein expression was significantly higher, while SK1 expression was significantly lower. The changes in the levels of these enzymes in obese tissue suggest that the sphingolipid pathway is altered in obese animals.

The overall trend in the pathway appears to be shifting the balance in sphingolipid molecules away from survival signals (S1P and C1P) and toward stronger apoptotic (ceramide) signals. Expression levels of Bax and Bcl-2, showing upregulation and downregulation, respectively, also supports this shift toward apoptosis. The alteration of these two downstream proteins that can be regulated by ceramide levels suggest that the sphingolipid pathway and apoptotic proteins are working together to increase apoptotic sensitivity in the obese liver. The altered sphingolipid pathway in an obese state thus may be contributing to the pathogenesis of hepatic steatosis. Taken together, the results of this study suggest that the steatotic liver is more sensitive to apoptosis (Canbay et al., 2005), while future studies may help clarify the mode of action of sphingolipids in the pathogenesis of hepatic steatosis.

4.2 Sphingolipid Signaling in Colon Tissue

The colon is an organ which is highly proliferative with a constant turnover of cells. It is sensitive to cancer development and colon cancer is one of the leading types of cancer worldwide. Epidemiological data suggests that obesity is a risk factor for colon cancer. The Zucker obese rat model used in this study has proven to be more sensitive to carcinogen-induced colon cancer than its lean counterpart (Weber et al., 2000). This study was carried out to examine if the proinflammatory phenotype of the obese animal model may activate and alter the sphingolipid pathway prior to any disease development.

Signal transduction of the pathway may begin with activation of SMase, hydrolyzing SM to ceramide. Enzyme activity analysis of SMase shows a trend toward higher SMase activity in the obese colon. In all repetitions of the assay, SMase activity was higher in the obese tissue compared to the lean tissue, although the differences were not statistically significant. LC-MS analysis of SM showed that there are no significant differences between SM levels in obese and lean colon. This indicates that the same level of substrate is available for SMase in both obese and lean tissue. Furthermore, no differences were observed when various species of SM were compared, showing that the total SM levels in each group are composed of relatively the same species (Fig.29).

Analysis of the SMase metabolite, ceramide, showed also that although total levels were slightly higher in obese colon tissue, the difference was not statistically significant. However, when individual species were compared between groups, one particular species was significantly upregulated. C24:1-ceramide was found to be higher in obese colon tissue (Fig.30). This particular species was also

upregulated in obese liver, indicating that this species of ceramide is more likely to be produced in obese tissue, either by SMase hydrolysis of C24:1-SM or by de novo synthesis. Although changes in total ceramide levels between groups were not seen, it must be noted that ceramide can be converted to less potent metabolites through glycosylation (to glycosylceramides), acetylation (to acylceramides) or to sphingosine via the action of ceramidase. Alternatively, ceramide can be phosphorylated by ceramide kinase to produce C1P.

C1P signaling opposes ceramide signaling and functions to protect cells from apoptosis. LC-MS analysis shows that total levels of C1P were lower in obese tissue (Fig.33). Only two species of C1P, C16- and C18-ceramide, were detectable in colon tissue, and of these, C18-cermide species differed significantly between groups (Fig.32). The lower levels of C1P in obese tissue suggest that ceramide is not being shunted toward C1P in the sphingolipid pathway and that there is less of a survival signal present in obese tissue from this metabolite.

To examine another route for ceramide in the signaling pathway, western blot analysis was performed to examine ceramidase protein expression. Acid-ceramidase antibody reacted with proteins 40kDa in size, indicating that ceramidase is present as a mature beta subunit in colon tissue. Quantification of the western blot showed that this enzyme is significantly upregulated by approximately 50% in obese colon (Fig.25). Known inducers of ceramidase include PDGF and IGF-1 (Suzuki et al., 2004). Overexpression of this enzyme has been shown to protect cells from stress-induced apoptosis, most likely by helping prevent ceramide accumulation and push the pathway toward S1P production (Strelow et al., 2000). The observed upregulation of ceramidase in obese colon tissue suggests that more of this enzyme is present to convert ceramide to sphingosine, and this may be a protective response to help prevent excess ceramide accumulation in the obese colon.

The product of ceramidase, sphingosine, was quantified by LC-MS. This analysis showed that there are no differences between sphingosine levels in lean and obese colon tissue. Compared to ceramide, sphingosine is considered to be a less potent inducer of apoptosis. As there were no differences observed between groups, and sphingosine levels were relatively low compared to other sphingolipids, it is clear that sphingosine is not accumulating in colon cells. Sphingosine is an important metabolite in the sphingolipid pathway, as it is the substrate for S1P production. Sphingosine can also be converted back to ceramide via the enzyme ceramide synthase.

To assess the production of S1P from sphingosine in colon tissue, SK1 was analyzed by western blot. SK1 was found to be significantly lower in obese tissue, by approximately 50%. As SK1 is necessary in the phosphorylation of sphingosine, it is clear that less enzyme is available in obese colon tissue to produce S1P. Western blot does not take into account the activity of the enzyme. So even though there are lower levels of SK1, no definite conclusions can be made about how much S1P is being produced in each tissue type. Also, as in liver tissue, S1P levels were too low to be detected by the LC-MS method used in this study. As mentioned earlier, S1P is normally present at very low levels in cells, and S1P will only accumulate if SK1 is stimulated by inducers such as PGDF (Olivera et al, 1999; Olivera and Spiegel, 1993). S1P is irreversibly degraded by S1P-lyase or is dephosphorylated by sphingosine-1-phosphatase. These two enzymes are active *in vivo* to keep S1P consistently at low levels, unless SK1 is induced. The downregulation of SK1 in obese colon tissue and the low levels of S1P suggest that the pathway may be shifting away from proliferative/mitogenic signaling.

4.2.1 Apoptotic Proteins in Colon Tissue

Bcl-2 and Bax were analyzed in order to assess if these proteins were altered in the colon of obese rats. As these proteins are downstream of the sphingolipid signaling pathway, it was valuable to see if any alterations occurred at this level in the apoptotic signaling process. Western blot analysis of Bax showed the protein at a band size of 42kDa, consistent with the tendency of the 21kDa Bax to form homodimers (Gross et al., 1998). Bax forms strong dimers and even though western blotting was carried out under denaturing conditions, antibody specifications indicated that it is common for this antibody to react with the dimerized form of the protein. Densitometric analysis showed that Bax is 100% upregulated in obese colon compared to lean. Bax induces apoptosis by permeating the mitochondrial membrane, allowing cytochrome c release, and subsequent apoptosis through activation of caspases. This upregulation of Bax suggests that the tissue may be primed for apoptosis. Bax is normally located in the cytosol and upon activation migrates to the mitochondrial membrane and stimulates the apoptotic process. The higher level of Bax along with altered sphingolipid pathway may increase the sensitivity of obese colon tissue to apoptosis and disease progression.

Western blot using Bcl-2 antibody showed bands at a size of 60kDa in all repetitions of this blot in colon tissue. This is twice the predicted band size for Bcl-2 as it is a 26kDa protein (Chao et al., 1998). Bcl-2 commonly forms dimers with other Bcl-2 family proteins, and is also capable of forming homodimers and oligodimers. Both monomeric and dimerized Bcl-2 are capable of interacting with activated Bax protein (Zhang et al., 2004). However; competition analysis showed that the formation of a Bax/Bcl-2 heterodimer is favored and this interaction inhibits Bcl-2 homodimerization (Zhang et al., 2004). It is interesting then that Bcl-2 appears to be present as homodimers in tissue that also has upregulated Bax levels. However, it cannot be said with certainty that the 60kDa bands observed do represent Bcl-2 homodimers or any other Bcl-2 dimer, as western blotting was carried out under denaturing conditions. The bands could also be demonstrating cross-reactivity of this antibody with another protein and remains to be characterized. Recent information on the polyclonal antibody used does reveal that the antibody has demonstrated non-specific binding at 37 and 45kDa and has been suggested to react to other Bcl-2 family members. Perhaps this may explain the unpredicted band size observed in our analysis (Abcam, 2007). All that can be concluded from this portion of the study is that Bax is significantly upregulated in obese colon tissue, while further analysis is required to confirm changes in Bcl-2 levels.

4.2.2 Summary of the Sphingolipid Pathway in Colon Tissue

Bioactive sphingolipids are important mediators of cell proliferation, differentiation, and programmed cell death. In the colon, cell turnover occurs at a rapid pace to maintain healthy colonic epithelium. An alteration in the sphingolipid pathway has been implicated in the etiology of colon cancer and studies examining sphingolipid enzymes and metabolites in colonic tumor tissue have exploded in recent years (Reviewed by Segui et al., 2006). Investigation of the pathway in obese colon tissue showed that elements of the pathway are altered in a state of obesity, prior to any cancer development (Fig.45).

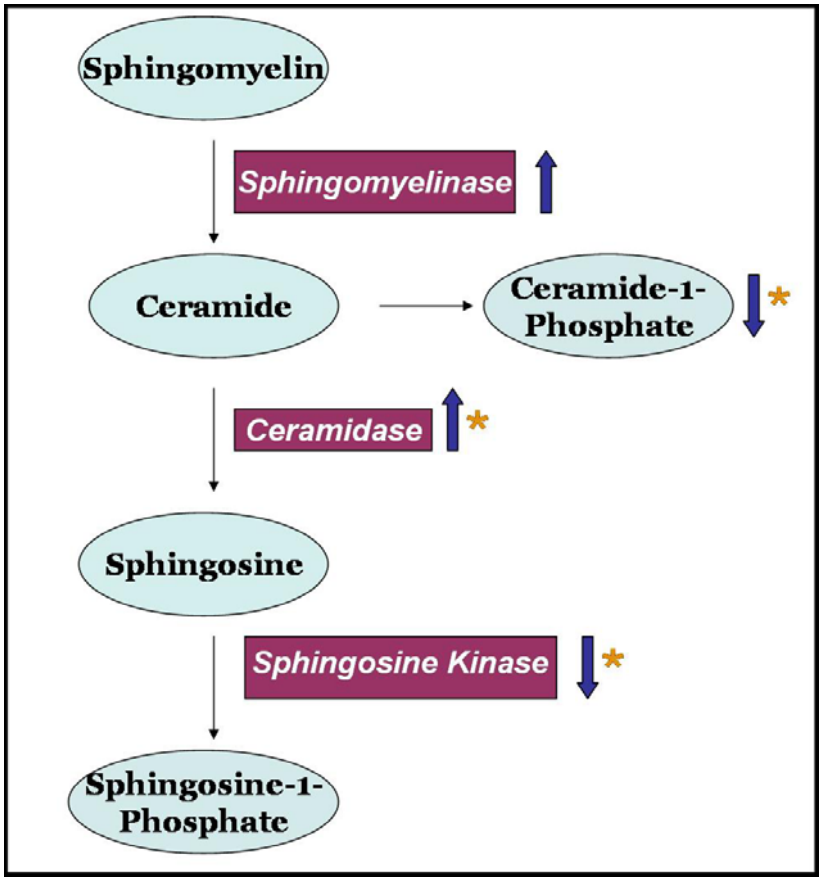

Figure 45: Summary of sphingolipid signaling changes in obese colon tissue

Arrows depict the observed trends of the sphingolipid enzymes and metabolites in obese colon tissue; * depicts changes that were statistically significant (t-test, $P<0.05$); note that significant changes between SM and ceramide species are not depicted in this figure.

The obese genotype has a significant effect on sphingolipids and their enzymes. Most notably altered in obese colon tissue were ceramidase, SK1 and C1P levels. Unlike the liver, there were no considerable shifts in ceramide and SM species compositions between groups, and overall there were fewer notable differences between obese and lean groups in colon tissue compared to liver tissue. The overall trends observed in the sphingolipid pathway remain consistent in both tissue types; ceramidase is upregulated while sphingosine kinase is downregulated. Again, since this study did not quantify the activity levels of the enzymes, it can only be noted that the available levels of this enzymes are altered in obese tissues. C1P levels are also downregulated in both tissue types, demonstrating that less of this survival signaling molecule is available in obese tissue. This, in concurrence with the lowered SK1 levels may suggest a shift toward apoptotic signaling. However,

without any noticeable differences in ceramide levels in colon tissue, this is merely a speculation and remains to be validated. The pro-apoptotic Bax demonstrated significant upregulation in obese colon tissue, providing further evidence that obese colon tissue is more prone to apoptosis, and that the sphingolipid metabolites may work in concert with apoptotic proteins. While the significance of the alterations in the sphingolipid pathway cannot be explicitly portrayed in this study, the important finding is that the sphingolipid pathway is altered in an obese state and this may have valuable implications in the etiology of colon cancer.

Numerous studies have looked at the sphingolipid pathway in colon tumor tissue. Findings include a significant reduction in ceramide levels in colon carcinomas compared to healthy mucosa, and an overexpression of SK1 in malignant colon cells (Selzner et al., 2001; Kawamori et al., 2006). Ceramidase enzyme may also have an important role in cancer development, as ceramidase inhibition resulted in ceramide accumulation and induction of cell death in colonic tumor cells (Selzner et al., 2001). These findings implicate low ceramide levels and dysfunctions in the sphingolipid pathway in the pathogenesis of colon carcinogenesis. It has previously been established that Zucker obese rats are more sensitive to azoxymethane-induced colon carcinoma (Weber et al., 2000). If in fact obese colon tissue has a shifted apoptotic balance due to its aberrant sphingolipid pathway, it is quite possible that this shift exposes a link between obesity and colon cancer development. Whether this shift creates an environment more susceptible to apoptosis or an environment more conducive to cell survival remains to be determined. However, it is clear that induced tumors are more likely to develop in the environment of obese colon tissue compared to lean colon tissue. Thus a likely hypothesis is that altered sphingolipid pathway in obese colon tissue contributes to an environment more sensitive to colon carcinogenesis. This, along with the knowledge that malignant cells have altered sphingolipid profiles compared to normal mucosa, provide strong value to further investigate the sphingolipid pathway and apoptotic state of obese colon tissue in the pathogenesis of colon carcinoma.

4.3 Tissue Specific Differences between Liver and Colon Tissue

Liver and colon have completely different functions and thus differ histologically. In comparing sphingomyelinase activity and sphingolipid levels between liver and colon tissue, it is clear that there are tissue specific differences in the sphingolipid pathway. Both isoforms of SMase, neutral and acidic, were found to be upregulated in colon tissue compared to liver tissue (Figs. 34 and 35).

Interestingly, SMase substrate, SM, is also at higher levels in colon tissue. This indicates that per milligram of colon tissue, there is more SM present for hydrolysis by SMase. Comparison of ceramide levels in colon and liver also show that ceramide is upregulated in colon tissue. This implies that the active SMase is resulting in greater ceramide production in colon tissue. Ceramide can also be produced by de novo synthesis; however, the upregulated SM and higher SMase activity in colon suggest that SM hydrolysis likely accounts for at least part of the high ceramide production seen in this tissue.

Closer examination of ceramide and SM shows that there is a shift in species composition for both sphingolipids between tissue types (Figs. 38 and 41). Varying carbon chain length and number of double bonds in the fatty acid chain of ceramide and SM may have important biological implications. However, as little is known about the biological importance of varying fatty acid chain length in these sphingolipids this is an excellent area for future research.

Other comparisons of the pathway between tissue types show a trend toward lower sphingosine in colon compared to liver, as well as significantly lower C1P levels. The downregulation in this portion of the pathway demonstrate that the colon tissue may be accumulating ceramide and producing less of a proliferative signal in the form of C1P. Taken together, the results of this portion of the study indicate that colon tissue is subjected to stronger apoptotic signals than liver tissue, as suggested by the higher SMase activity, higher ceramide, and lower C1P levels. These tissue-specific differences may be accounted for by the fact that the colon has relatively higher cell turnover, therefore requiring cell death signals (Deschner et al., 1987). In both animals and humans, apoptosis occurs in colonic crypts and villi unrelated to a known stimulus and may function to regulate the number of colonic cells (Johnson, 2006). As ceramide can mediate programmed cell death, there may be more of a requirement for production of this sphingolipid in colon tissue than in liver tissue. Thus the differences observed in SMase activity and ceramide levels in liver and colon may be indicative of the sphingolipid pathway's ability to influence cell turnover.

4.4 Conclusions and Future Directions

The sphingolipid pathway can be activated in various situations of cellular stress. To establish whether inflammation and reactive oxygen species that are associated with a state of obesity could alter the sphingolipid signaling pathway, key enzymes and bioactive sphingolipids were assessed in obese Zucker rats. As obese livers demonstrate hepatic steatosis, and obese colons are more sensitive to colon cancer, these two tissue types were selected for analysis. The results of this study demonstrate an obese genotype can significantly alter elements of the sphingolipid signaling pathway in both tissue types.

Key findings include the following:

- Higher expression of ceramidase and lower expression of SK1, as well as a trend toward higher SMase activity in obese steatotic liver compared to lean liver.
- Lower C1P levels and a trend toward a higher ceramide levels in obese liver.
- An increase in Bax levels and decrease in Bcl-2 levels in the obese liver. Taken together with sphingolipid pathway analysis, these results show for the first time a trend toward increased sphingolipid apoptotic signaling in obese liver tissue and are consistent with the pathological state of steatotic liver.
- A shift in SM and ceramide species composition in obese liver compared to lean liver. Alteration in the carbon tail chain length of fatty acids in sphingolipids may have important biological implications, thus this is an area for future research.
- An upregulation of ceramidase and downregulation of SK1 in obese colonic tissue, same as in liver tissue.
- Lower C1P levels in obese colon tissue.
- An increase in Bax protein levels in obese colonic tissue. Bcl-2 results were inconclusive.

- An upregulation of SMase activity and an upregulation of ceramide and SM levels in colon tissue compared to liver. These results indicate tissue-specific differences in the sphingolipid pathway.

In conclusion, an obese genotype does affect the sphingolipid pathway in both liver and colon tissue and this may have important implications in the pathogenesis of both hepatic steatosis and colon cancer.

Future studies must be designed using larger sample size to further explore the differences in sphingolipid signaling in an obese state. An expansion on the sphingolipid enzymes and molecules examined would also help elucidate differences. Furthermore, an investigation into sphingolipid species differences is necessary to determine whether or not variations in fatty acid tail composition of ceramide and sphingomyelin have a structural or functional effect. To further investigate the role of sphingolipid signaling in the pathogenesis of colon cancer in a state of obesity, it would be prudent to analyze sphingolipid signaling during the growth of the colonic tumor in obese and lean animal models.

This is a novel and exciting area of research. Further investigation and analysis of the sphingolipid pathway in obese liver and colon, as well as a deeper understanding of the activation and regulation of this pathway should elucidate the effect of obesity and the role of sphingolipid signaling in the pathogenesis of hepatic steatosis and colon cancer.

Bibliography

Angulo, P. (2002). Nonalcoholic fatty liver disease. *N Engl J Med*. 346:1221-1231.

Basu, S., Bayoumy, S., Zhang, Y., Lozano, J., Kolesnick, R. (1998). BAD enables ceramide to signal apoptosis via Ras and Raf-1. *J Biol Chem*.273:30419-30426

Bernardo, K., Hurwitz, R., Zenk, T., Desnick, R.J., Ferlinz, K., Schuchman, E.H., Sandhoff, K. (1995). Purification, characterization, and biosynthesis of human acid ceramidase. *J Biol Chem*. 270(19):11098-102.

Bird, R.P. (1987). Observation and quantification of aberrant crypts in the murine colon treated with a colon carcinogen: preliminary findings. *Cancer Lett*. 37(2):147-51.

Bohlen, G. (2004). Mechanisms for early microvascular injury in obesity and type II diabetes. *Current Hypertensive Reports*. 6(1): 60-65.

Canbay, A., Gieseler, R. K., Gores, G. J., Gerken, G. (2005).The relationship between apoptosis and non-alcpholic fatty liver disease: an evolutionary cornerstone turned pathogenic. *Gastroenteral*. 43(2):211-7.

Cardone, M.H., Roy, N., Stennicke, H.R. (1998). Regulation of cell death protease caspase-9 by phosphorylation. *Science*. 282:1318-1321.

Chalfant, C. E. (2004). Ceramide Kinase. *Lipids: Sphingolipid Metabolizing Enzymes*. Kerala, India: Research Signpost. 17-31.

Chalfant, C. E., Spiegel, S. (2005). Sphingosine-1-phosphate and ceramide-1- phosphate: expanding roles in cell signaling. *J Cell Sci*. 118: 4605–4612.

Chalfant, C., Hannun, Y. (2006). The role of serine/threonine protein phosphatases in ceramide signalling. Eurekah Bioscience collection.Online.Landes Bioscience.2006 Mar 28. <http://www.ncbi.nlm.nih.gov/books/bv.fcgi?rid=eurekah.section.4230>

Chatterjee, S. (1993).Neutral sphingomyelinase. *Adv Lipid Res*.26:25-48.

Chatterjee, S., Han, H., Rollins, S., Cleveland, T. (1999).Molecular cloning, characterization, and expression of a novel human neutral sphingomyelinase. *J Biol Chem*.274:37407-37412.

Cheng, Y., Nilsson, A., Tomquist, E., Duan, R.D. (2002). Purification, characterization, and expression of rat intestinal alkaline sphingomyelinase. *Journal of Lipid Research*. 43:316-324.

Cheng, Y., Ohlsson, L., Duan, R.D. (2004). Psyllium and fat in diets differentially affect the activities and expressions of colonic sphingomyelinases and caspase in mice. *British Journal of Nutrition*. 91(005):715-723.

Chitturi, S., Farrell, G.C. (2001). Etiopahtogenesis of nonalcoholic steatohepatitis. *Semin Liver Dis*.21(1):27-41.

Cuvillier, O., Pirianov, G., Kleuser, B., Vanek, P., Coso, O., Gutkind, S., Spiegel, S.(1996). Suppression of ceramide-mediated cell death by sphingosine-1-phosphate. *Nature*. 381: 800-803.

De Stefanis, D., Reffo, P., Bonelli, G., Baccino, F., Sala, G., Ghidoni, R., Codogno, P., Isidoro, C. (2002). Increase in ceramide level alters the lysomal targeting of cathepsin D prior to onset of apoptosis in HT-29 colon cancer cells. *J Biol Chem*. 383(6):989-999.

Deiss, L.P., Galinka, H., Berissi, H., Cohen, O., Kimchi, A. (1996). Cathepsin D protease mediates programmed cell death induced by interferon-gamma, Fas/APO-1 and TNF-alpha. *EMBO J*. 15:3861-3870.

Desai, N.N., Zhang, H., Olivera, A., Mattie, M.E., Spiegel, S.(1992). Sphingosine-1-phosphate, a metabolite of sphingosine, increases phosphatidic acid levels by phospholipase D activation. *J Biol Chem*. 267(32):23122-23128.

Deschner, E.E. (1987).Cell turnover and colon tumor development. *Prev Med*.16(4): 580-585.

Dougherty, M. K., Muller, J., Ritt, D. A., Zhou, M., Zhou, X. Z., Copeland,
T. D., Conrads, T. P., Veenstra, T. D., Lu, K. P., Morrison, D. K. (2005). Regulation of Raf-1 by direct feedback phosphorylation. *Mol Cell*. 17, 215-224.

Formiguera, X., Canton, A. (2004).Obesity: epidemiology and clinical aspects. *Best Pract Res Clin Gastroenterol*.18(6):1125-1146.

Foster, D. A., Xu, L. (2003). Phospholipase D in cell proliferation and cancer. *Mol Cancer Res*. 1 (11): 789-800.

Gamard, C.J., Dbaibo, G.S., Liu, B., Obeid, L.M., Hannun, Y.A.(1997). Selective involvement of ceramide in cytokine-induced apoptosis. Ceramide inhibits phorbol ester activation of nuclear factor kappa B. *J Biol Chem*.272:16474-16481.

Gómez-Muñoz, A., Duffy, P.A, Martin, A., O'Brien, L., Byun, H.S., Bittman, R., Brindley, D.N. (1995). Short-chain ceramide 1-phosphates are novel stimulators of DNA synthesis and cell division: antagonism by cellpermeable ceramides. *Mol Pharmacol*. 47:883–889.

Gómez-Muñoz, A., Kong, J., Salh, B., Steinbrecher, U. (2003). Sphingosine-1- phosphate inhibits sphingomyelinase and blocks apoptosis in macrophages. *FEBS Lett*. 539:56–60.

Gómez-Muñoz, A., Kong, J.Y., Salh, B., Steinbrecher, U.P. (2004). Ceramide-1- phosphate blocks apoptosis through inhibition of acid sphingomyelinase in macrophages. *J Lipid Res*. 45: 99–105.

Grassme, H., Schwarz, H., Gulbins, E. (2001). Molecular mechanisms of ceramide-mediated CD95 clustering. *Biochem Biophys Res Commun*.284:1016-1030.

Gross, A., Jockel, J., Wei, M.C., Korsmeyer, S.J. (1998). Enforced dimerization of BAX results in its translocation, mitochondrial dysfunction and apoptosis. *EMBO J*. 17:3878:3885.

Gunter, M., Leitzmann, M. (2006). Obesity and colorectal cancer: epidemiology, mechanisms and candidate genes. *J Nut Biochem*.17(3):145-156.

Guyton, A.C., Hall, J.E. (2000). Textbook of Medical Physiology 10th Edition. W.B. Saunders. 807.

Heinrich, M., Neumeyer, J., Jakob, M., Halla, C., Tchikov, V., Winoto-Morbach, S., Wickel, M., Schneider-Brachert, W., Trauzold, A., Hethke, A., Schutze, S. (2004). Cathepsin D links TNF-induced acid sphingomyelinase to Bid-meidated caspase-9 and -3 activation. *Cell Death Differ*.11:550-563.

Hertervig, E., Nilsson, A., Nyberg, L., Duan, R.D. (1996). Alkaline sphingomylinase activity is decreased in human colorectal carcinoma. *Cancer*.79:448-453.

Horinouchi, K., Erlich, S., Perl, D., Ferlinz, K., Bisgaier, C., Sandhoff, K., Desnick, R., Stewart, C., Schuman, E. (1995). Acid sphingomyelinase deficient mice: a model of types A and B Niemann-Pick disease. *Nat Genet*.10:288-293.

Huang, J.R., Seasholtz, T.M., Chang, J.W., Smith, J.M., Walsh, C.T., Brown, J.H.(2007). Tumor necrosis factor-alpha-stimulated cell proliferation is mediated through sphingosine kinase-dependent Akt activation and cyclin D expression. *J Biol Chem*. 282(2):863-870.

Igarashi, N., Okada, T., Hayashi, S., Fujita, T., Jahangeer, S., Nakamura, S. (2003). Sphingosine kinase 2 is a nuclear protein and inhibits DNA synthesis. *J Biol Chem*.278(47):46832-46839.

Janne, P.A., Mayer, R.J. (2000). Chemoprevention of colorectal cancer. *New England Journal of Medicine.* 342(26):1960-8.

Johansson, A.C., Steen, H., Ollinger, K., Roberg, K. (2003). Cathepsin D mediates cytochrome c release and caspase activation in human fibroblast apoptosis induced by staurosporine. *Cell Death Differ*.10(11):1253-9.

Johnson, L.R. (2006). Physiology of the gastrointestinal tract 14th Edition. Burlington MA: Elsevier Academic Press.

Kahoma, T., Olivera, A., Edsall, L., Nagiec, M.M., Dickson, R., Spiegel, S. (1998). Molecular cloning and funcitonal characterization of murine sphingosine kinase. *J Biol Chem*.273(37):23722-23728.

Kawamori, T., Osta, W., Johnson, K.R., Pettus, B.J., Bielawki, J., Tanaka, T., Wargovich, M.J., Reddy, B.S., Hannun, Y.A., Obeid, L.M., Zhou, D. (2006). Sphingosine kinase 1 is up-regulated in colon carcinogenesis. *FASEB J*. 20(2):386-8.

Kohno, M., Momoi, M., Oo, M.L., Paik, J., Lee, Y., Venkataraman, K, Ai Y, Ristimaki A.P., Fyrst H, Sano H, Rosenberg D, Saba J.D., Proia R.L., Hla T. (2006).Intracellular role for sphingosine kinase 1 in intestinal adenoma cell proliferation. *Mol Cell Biol*.26(19):7211-7223.

Kolak, M., Westerbacka, J., Velagapudi, V.R., Wagsater, D., Yetukuri, L., Makkonen, J., Rissanen, A., Hakkinen A.M., Lindell, M., Bergholm, R., Hamsten, A., Eriksson, P., Fisher, R.M., Oresic, M., Yki-Jarvinen, H. (2007). Adipoase tissue inflammation and increased ceramide content characterize subjects with high liver fat content independent of obesity. *Diabetes*. 56(8):1960-8.

Kolesnick, R. (2002). The therapeutic potential of modulating the ceramide/sphingomyelin pathway. *Journal of Clinical Investigation.*110(1):3-8.

Lee, M.J., Van Brocklyn, J.R., Thangada, S., Liu, C.H., Hand, A.R., Menzeleev, R., Spiegel, S., Hla, T. (1998). Sphingosine-1-phosphate as a ligand for the G protein-coupled receptor EDG-1.*Science*.279(5356):1552-1555.

Levade, T., Auge, N., Veldman, R.J., Cuvillier, O., Negre-Salvayre, A., Salvayre, R. (2001). Sphingolipid Mediators in Cardiovascular Cell Biology and Pathology. *Circ Res*. 89:957-968.

Liu, H., Sugiura, M., Nava, V.E., Edsall, L.C., Kono, K., Poulton, S., Milstien, S., Kohama, T., Spiegel, S. (2000). Molecular cloning and functional characterization of a novel mammalian sphingosine kinase type 2 isoform. *J Biol Chem*. 275(26): 19513-19520.

Liu, H., Toman, R.E., Goparaju, S.K., Maceyka, M., Nava, V.E., Sankala, H., Payne, S.G., Bektas, M., Ishii, I., Chun, J., Milstien, S., Spiegel, S. (2003). Sphingosine kinase type 2 is a putative BH3-only protein that induces apoptosis. *J Biol Chem*.278(41):40330-40336.

Liu, P., Anderson, R. (1995). Compartmentalized production of ceramide at the cell surface. *J Biol Chem*.270:27179-27185.

Maceyka, M., Payne, S., Milstien, S., Spiegel, S. (2002). Sphingosine kinase, sphingosine-1-phosphate and apoptosis. *Biochim Biophys Acta*.1585(2-3):193-201.

Maceyka, M., Sankala, H., Hait, N.C, Stunff, H., Liu, H., Toman, R., Collier, C., Zhang, M., Satin, L.S., Merrill, A.H., Milstien, S., Spiegel, S. (2005). Sphk1 and Sphk2, Sphingosine kinase isoenzymes with opposing functions in sphingolipid metabolism. *J Biol Chem*.280(44):37118-37129.

Marathe, S., Schissel, S.L., Yellin, M.J., Beatini, N., Mintzer, R. Williams, K.J., Tabas, I. (1998). Human vascular endothelial cells are a rich and regulatable source of secretory sphingomyelinase. Implications for early atherogenesis and ceramide-mediated cell signalling. *J Biol Chem*. 273(7):4081-4086.

Morson, B., Sobin, L. (1976).Histological typing of intestinal tumours. International histological classification of tumours, no 15. WHO: Geneva.

Ogretem B.(2006).Sphingolipids in cancer: regulation of pathogenesis and therapy. *FEBS Lett*. 580:5467–5476.

Ohanian, J., Ohanian, V. (2001).Sphingolipids in mammalian cell signaling. *Cell Mol Life Science*. 58:2053-2068.

Olivera, A., Edsall, L., Poulton, S., Kazlauskas, A., Spiegal, S.(1999). Platelet-derived growth factor-induced activation of sphingosine kinase requires phophorylation of the PDGF receptor tyrosine residue responsible for binding of PLCγ. *FASEB J*. 13:1593-1600.

Olivera, A., Spiegel, S. (1993). Sphingosine-1-phosphate as second messenger in cell proliferation induced by PDGF and FCS mitogens. *Nature*.365(6446):557-560.

Olsson, M., Duan R.D., Ohlsson, L., Nilsson, A.(2004). Rat intestinal ceramidase: purification, properties and physiological relevance. *Am J Physiol Gastrointest Liver Physiol*. 287:929-937.

Osawa, Y., Uchinami, H., Bielawski, J., Schwabe, R.F., Hannun, Y.A. (2005).Roles for C16-ceramide and sphingosine-1-phosphate in regulating hepatocyte apoptosis in response to tumor necrosis factor-alpha. *J Biol Chem*. 280(30):27879-87.

Oskouian, B., Sooriyakumaran, P., Borowsky, A. D., Crans, A., Dillard-Telm, L., Tam, Y.Y., Bandhuvula, P., Saba, J.D. (2006). Sphingosine-1-phosphate lyase potentiates apoptosis via p53- and p38- dependent pathways and is down-regulated in colon cancer. *Proc Natl Acad Sci USA*. 103(46):17384-9.

Park, J.H., Schuchman, E.H. (2006). Acid ceramidase and human disease. *Biochimica et Biophysica Acta*. 1758:2133-2138.

Raman, M., Allard, J. (2006). Non alcoholic fatty liver disease: A clinical approach and review. *Can J Gastroenterol*. 20(5):345-349.

Ruvolo, P. (2003). Intracellular signal transduction pathways activated by ceramide and its metabolites. *Pharm Res*. 47:383-392.

Ruvolo, P.P., Deng, X., Ito, T., Carr, B.K., May, W.S. (1999). Ceramide induces Bcl-2 dephosphorylation via a mechanism involving mitochondrial PP2A. *J Biol Chem*. 274(29):20296-300.

Samad, F., Hester, K.H., Yang, G., Hannun, Y.A., Bielawski, J. (2006). Altered adipose and plasma sphingolipid metabolism in obesity: a potential mechanism for cardiovascular and metabolic risk. *Diabetes*. 55(9):2579-2587.

Sathyanarayana, P., Barthwal, M., Kundu, C., Lane, M., Bergmann, A., Tzivion, G., Rana, A. (2002). Activation of the Drosophila MLK by ceramide reveals TNF-alpha and ceramide as agonists of mammalian NLK3. *Mol Cell*.10:1527-1533.

Schissel, S., Jiang, X., Tweedie-Hardman, J., Jeong, T., Camejo, E., Najib, J., Rapp, J., Williams, K., Tabas, I. (1998). Secretory sphingomyelinase, a product of the acid sphingomylinase gene, can hydrolyze atherogenic lipoproteins at neutral pH:implications for atherosclerotic lesion development. *J Biol Chem*.273(5):2738-2746.

Schissel, S., Tweedie-Hardman, J., Rapp, J., Graham, G., Williams, K., Tabas, I. (1996). Rabbit aorta and human atherosclerotic lesions hydrolyze the sphingomyelin of retained low-density lipoprotein. Proposed role for arterial-wall sphingomyelinase in subendothelial retention and aggregation of atherogenic lipoproteins. *J Clin Invest*. 98(6):1455-1464.

Schmelz, E.M., Bushnev, A.S., Dillehay, D.L., Liotta, D.C., Merrill, A.H. (1997). Suppression of aberrant colonic crypt foci by synthetic sphingomyelins with saturated or unsaturated sphingoid base backbones. *Nutr Cancer*.28:81-85.

Schmelz, E.M., Bushnev, A.S., Dillehay, D.L., Sullards, M., Liotta, D., Merrill, A. (1999). Ceramide-beta-D glucuronide:synthesis, digestion, and suppression of early markers of colon carcinogenesis. *Cancer Res*.59:5768-5672.

Segui, B., Andreieu-Abadi, N., Jaffrezou, J.P., Benoist, H., Levade, T. (2006). Sphingolipids as modulators of cancer cell death: Potential therapeutic targets. *Biochim et Biophysica Acta*. 1758:2104-2120.

Selzber, M., Bielawska, A., Morse, M.A., Rudiger, H.A., Sindram, D., Hannun, Y.A., Clavien, P.A. (2001). Induction of apoptotic cell death and prevention of tumor growth by ceramide analogues in metastatic human colon cancer. *Cancer Res*. 61(3):1233-1240.

Shanmugathasan, M., Jothy, S. (2000).Apoptosis, anoikis and their relevance to the pathobiology of colon cacner. *Pathology International*. 50(4):273-279.

Smith, E.R., Merrill, A.H., Obeid, L.M., Hannun, Y.A. (2000). Effects of sphingosine and other sphingolipids on protein kinase C. *Methods Enz*. 312:361-373.

Spiegel, S., Milstien, S. (2003). Sphingosine-1-Phosphate: an enigmatic signaling lipid. *Nat Rev Mol Cell Biol*.4(5):397-407.

Strelow, A., Bernardo, K., Adam-Klages, S., Linke, T., Sandhoff, K., Kronke, M., Adam, D. (2000). Overexpression of acid ceramidase protects from tumor necrosis factor-induced cell death. *J Exp Med*. 192(5):601-12.

Sugiura, M., Kono, K., Liu, H., Shimizugawa, T., Minekura, H., Spiegel,S, Kohama, T. (2002). Ceramide kinase, a novel lipid kinase. Molecular cloning and functional characterization. *J. Biol. Chem.* 277:23294-23300.

Suzuki, E., Handa, K., Toledo, M.S., Hakamori, S. (2004). Sphingosine-dependent apoptosis: a unified concept based on multiple mechanisms operating in concert. *Proc Natl Acad Sci USA*. 101 (41):14788-93.

Tani, M., Katsuhiro, K., Hironobu, K., Tetsuto, N., Ito, M. (1998). Enzymatic Synthesis of ϖ-Amino-Ceramide: Preparation of a Sensitive Fluorescent Substrate for Ceramidase. *Analytical Biochemistry*. 263:183-188.

Vogelstein, B., Fearon E.R., Hamilton, S.R. Kern, S.E.M., Preisinger, A.C., Leppert, M., Nakamura Y., White R., Smits, A.M., Bos, J.L. (1988). Genetic alterations during colorectaltumor development. *New England Journal of Medicine.* 319(9):525-532.

Wang, F., Van Brocklyn, J.R., Hobson, J.P., Moyafagh, S., Zukowska-Grojec, Z., Milstien, S., Spiegel, S. (1999). Sphingosine 1-phosphate stimulates cell migration through a G_i-coupled cell surface receptor. *J Biol Chem*. 274:35343-35350.

Weber, R.V., Stein, D. E., Scholes, J., Kral, J.G. (2000). Obesity potentiates AOM-induced colon cancer. 45(5):890-5.

Woodcock, J. (2006). Sphingosine and ceramide signaling in apoptosis. *Life*. 58(8):462-466.

Xu, R., Jin, J., Hu, W., Sun, W., Bielawski, J., Szulk, Z., Taha, T., Obeid, L., Mao, C. (2006). Gogi alkaline ceramidase regulates cell proliferation and survival by controlling levels of sphingosine and S1P. *FASEB J*. 20(11):1813-1825.

Yetukuri, L., Katajamaa, M., Medina-Gomez, G., Seppanen-Laakso, T., Vidal-Puig, A., Oresic, M. (2007). Bioinformatics strategies for lipidomics analysis: characterization of obesity related hepatic steatosis. *BMC Syst Biol*. 1:12.

Young, B., Heath, J. (2000).Wheater's functional histology 4th ed. London: Churchhill Livingstone.

Young, N., Van Brocklyn, J.R. (2006). Signal transduction of sphingosine-1-phosphate G protein coupled receptors. *Sci World J*. 6:946-966.

Zhang, Z., Lapolla, S.M., Annis, M.G., Truscott, M., Roberts, G. J, Miao, Y., Shao, Y., Tan, C., Peng, J., Johnson, A. E., Zhang, X. C., Andrews, D. W., Lin J. (2004). Bcl-2 homodimization involves two distinct binding surfaces, a topographic arrangement that provides an effective mechanism for Bcl-2 to capture activated Bax. 279(42):43920-8.

Zucker, L., Zucker, T. (1961). Fatty, a new mutation in the rat. *J Hered*. 51-52: 275-278.

Appendix A
Abbreviations

Apaf-1	apoptotic protease activating factor 1
ATP	adenosine triphosphate
Bax	Bcl-2 associated X protein
Bcl-2	B cell lymphoma-2
C1P	ceramide-1-phosphate
CAPP	ceramide-activated protein phosphatase
CerK	ceramide kinase
DNA	deoxyribonucleic acid
Edg receptor	endothelial differentiation gene receptor
HPLC	high-performance liquid chromatography
JNK	Jun kinase
IGF	insulin-like growth factor
IL-1β	interleukin-1 beta
LC-MS	liquid chromatography-mass spectroscopy
MAPK	mitogen-activated protein kinase
MLK	mixed lineage kinase
MS	mass spectroscopy
NAFL	nonalcoholic fatty liver
NASH	nonalcoholic steatohepatitis
PGDF	platelet-derived growth factor
PKB	protein kinase B
PKC	protein kinase C
PP1	protein phosphatase 1
PP2a	protein phosphatase 2a
ROS	reactive oxygen species
S1P	sphingosine-1-phosphate
SAPK	stress-activated protein kinase
SDS-PAGE	sodium dodecyl sulfate-polyacrylamide gel electrophoresis
SM	sphingomyelin

SMase	sphingomyelinase
SK	sphingosine kinase
TNF-α	tumor necrosis factor alpha
VLDL	very low density lipoproteins
WHO	World Health Organization

Appendix B
Additional Liver and Colon Result Figures

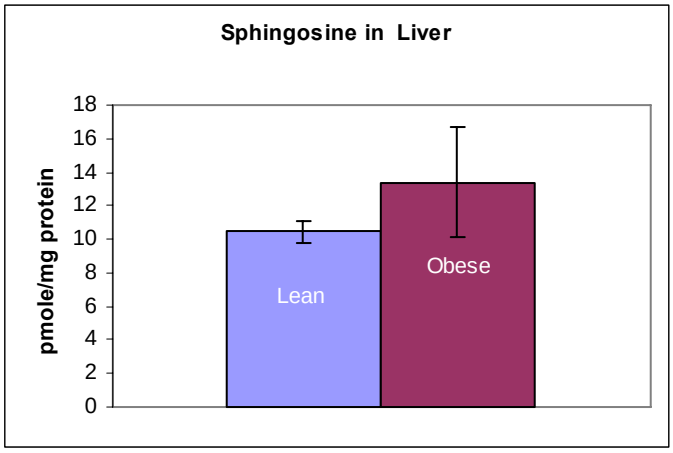

Figure B1: Sphingosine levels in lean and obese liver tissue

Sphingosine levels are shown in pmole/mg protein ± s.e.m. N=5 per group. Sphingosines were quantified by HPLC-MS. 17C-sphingosine was used as an internal standard. After sphingolipid extraction, samples containing 1mg of protein were analyzed using TSQ 7000 LC/MS system.

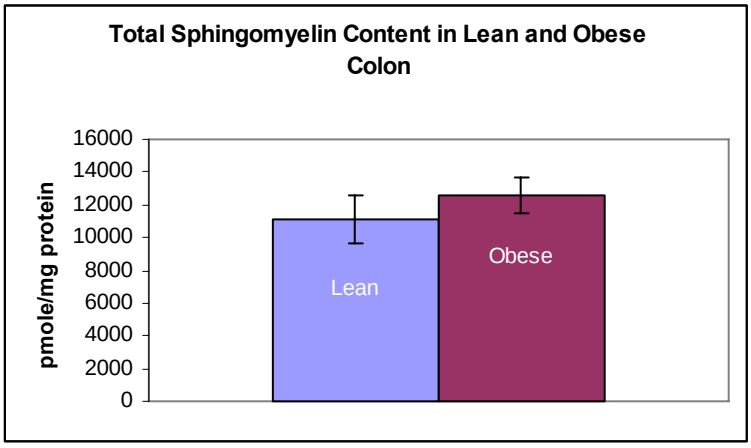

Figure B2: Total sphingomyelin content in lean and obese colon tissue

SM levels are shown in pmole/mg protein ± s.e.m. N=5 per group. SMs were quantified by HPLC-MS. 18C17-SM was used as an internal standard. After sphingolipid extraction, samples containing 1mg of protein were analyzed using TSQ 7000 LC/MS system.

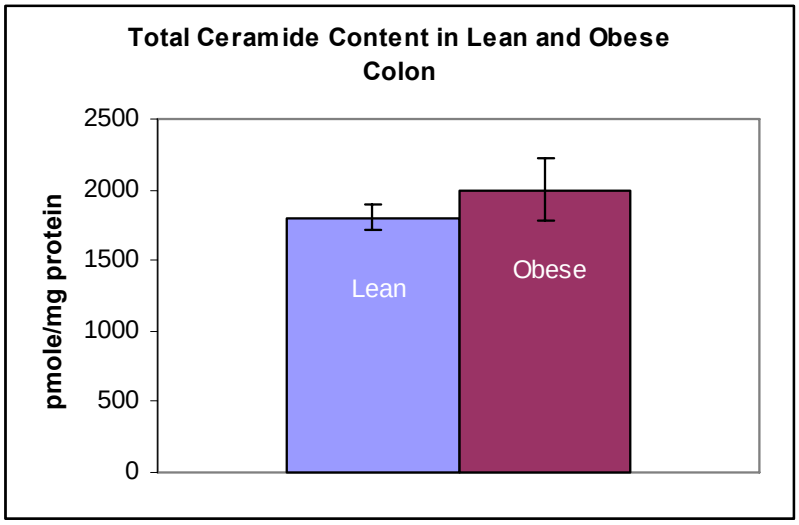

Figure B3: Total ceramide content in lean and obese colon tissue

Ceramide levels are shown in pmole/mg protein ± s.e.m. N=5 per group. Ceramides were quantified by HPLC-MS. 17C16-ceramide was used as an internal standard. After sphingolipid extraction, samples containing 1mg of protein were analyzed using TSQ 7000 LC/MS system.

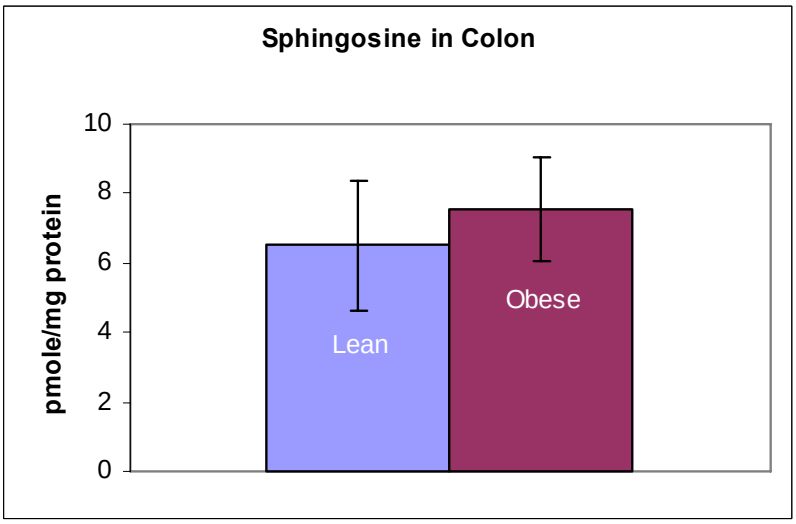

Figure B4: Sphingosine levels in lean and obese colon

Sphingosine levels are shown in pmole/mg protein ± s.e.m. N=5 per group. Sphingosines were quantified by HPLC-MS. 17C-sphingosine was used as an internal standard. After sphingolipid extraction, samples containing 1mg of protein were analyzed using TSQ 7000 LC/MS system.

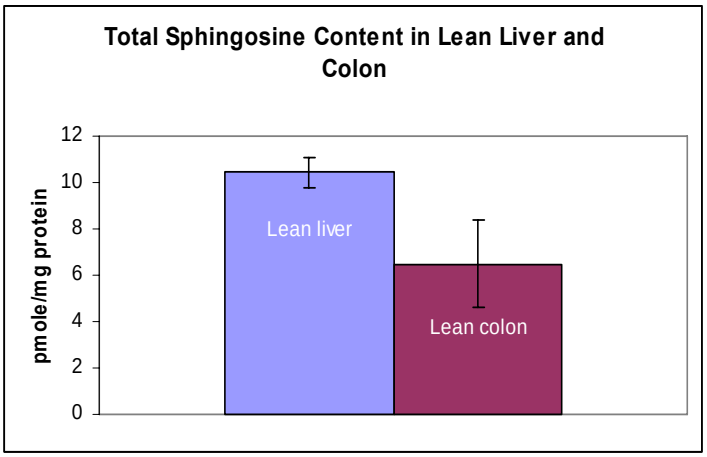

Figure B5: Total sphingosine content in lean liver and colon

Sphingosine levels are shown in pmole/mg protein ± s.e.m. N=5 per group. Sphingosines were quantified by HPLC-MS. 17C-sphingosine was used as an internal standard. After sphingolipid extraction, samples containing 1mg of protein were analyzed using TSQ 7000 LC/MS system.

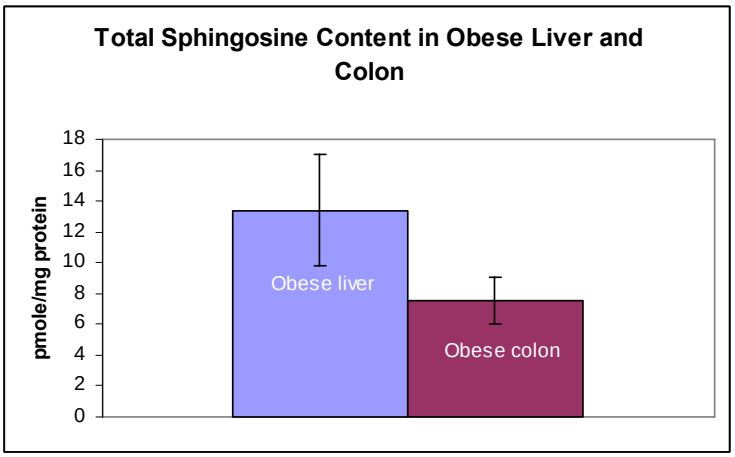

Figure B6: Total sphingosine content in obese liver and colon

Sphingosine levels are shown in pmole/mg protein ± s.e.m. N=5 per group. Sphingosines were quantified by HPLC-MS. 17C-sphingosine was used as an internal standard. After sphingolipid extraction, samples containing 1mg of protein were analyzed using TSQ 7000 LC/MS system.

Appendix C

Sphingolipid Data Tables

The following tables consist of the raw data quantification values for ceramide, SM, C1P, sphingosine and S1P in obese liver and colon.

Table C1:Ceramide Concentration (pmole/mg pro)[b]

Sample ID	C18:1-Cer	C14-Cer	C16-Cer	C18-Cer	C20-Cer	C20:1-Cer	C20:4-Cer	C22-Cer	C22:1-Cer	C24-Cer	C24:1-Cer	C26-Cer	C26:1-Cer
LC 1 L	10.7	0.4	238.8	13.8	22.2	1.8	1.9	96.9	20.2	711.3	223.0	0.2	1.7
LC 2 L	13.4	0.7	468.9	23.4	22.4	2.1	2.1	75.0	19.6	657.6	241.3	6.1	7.6
LC 3 L	8.4	0.3	184.4	14.2	14.0	1.2	0.7	46.8	10.2	445.6	253.5	4.5	2.8
LC 4 L	11.0	0.3	116.0	13.8	13.0	1.8	0.6	59.0	8.3	429.3	320.9	4.1	2.7
LC 5 L	9.6	0.2	232.5	15.8	14.7	1.4	1.0	50.4	12.3	439.7	261.6	3.6	4.3
OC 1 L	7.0	0.4	69.7	15.2	15.9	1.7	5.3	98.5	10.0	492.5	450.7	6.3	2.7
OC 2 L	11.9	0.4	142.3	40.6	27.8	2.1	13.0	105.4	20.2	489.3	499.2	4.3	5.1
OC 3 L	13.8	1.4	103.8	53.8	30.0	2.4	6.7	143.6	20.5	516.9	723.2	2.4	1.9
OC 4 L	13.4	1.3	86.7	59.1	31.7	2.4	7.5	114.6	21.7	410.6	554.1	2.9	2.1
OC 5 L	8.2	0.6	98.1	48.2	27.4	1.9	7.4	126.6	17.6	519.9	583.9	3.4	1.9
LC 1 Col	71.1	1.4	651.2	191.0	142.3	66.4	1.0	51.4	19.3	173.8	262.7	2.1	1.4
LC 2 Col	59.5	2.1	691.0	145.3	140.6	82.4	2.5	51.2	15.4	128.7	229.6	1.8	1.0
LC 3 Col	87.1	7.6	646.0	214.3	158.9	119.1	0.6	71.6	17.0	176.7	322.8	5.1	1.9
LC 4 Col	114.2	3.8	537.9	245.7	113.3	80.4	0.6	50.7	18.3	152.5	287.0	1.6	2.2
LC 5 Col	120.4	5.7	454.7	377.7	172.2	110.1	0.5	70.3	15.2	192.9	393.0	2.9	2.7
OC 1 Col	105.0	5.0	860.6	273.7	173.5	76.8	1.2	66.7	19.9	192.2	463.1	3.2	3.0
OC 2 Col	102.9	2.3	1022	274.8	226.8	104.5	0.8	80.5	22.1	158.8	535.8	2.0	1.6
OC 3 Col	94.7	7.3	647.8	226.5	145.2	96.7	0.5	63.2	23.5	115.9	364.9	1.5	1.3
OC 4 Col	50.9	3.1	559.2	94.8	82.5	42.8	2.2	52.9	7.6	145.3	348.9	1.8	1.8
OC 5 Col	82.3	3.5	586.6	197.3	75.4	51.4	0.6	48.8	14.3	106.6	350.6	1.1	1.9

[b]Cer = ceramide; LC*L = lean control liver sample; OC*L = obese control liver sample; LC*Col = lean control colon sample; OC*Col = obese control colon sample.

Table B2: SM Concentration (pmole/mg pro)[c]

Sample ID	C14-SM	C16-SM	C18-SM	C18:1-SM	C20-SM	C20:1-SM	C22-SM	C22:1-SM	C24-SM	C24:1-SM	C26-SM	C26:1-SM
LC 1 L	2.7	555.0	518.0	5.7	195.8	6.4	1028.2	120.1	3359.2	1632.6	56.8	25.6
LC 2 L	3.3	690.0	535.0	4.6	202.6	6.6	925.3	140.0	3281.6	1516.9	78.2	50.9
LC 3 L	2.8	760.0	462.0	4.0	175.7	5.8	825.0	111.4	3149.3	1619.9	57.1	40.3
LC 4 L	2.6	832.0	524.0	4.9	187.6	7.0	945.6	122.6	3045.8	1602.2	68.6	41.6
LC 5 L	1.9	710.0	422.0	4.1	132.6	5.2	803.5	87.7	3324.4	1445.2	52.9	37.1
OC 1 L	42.5	3630.0	1710.0	78.8	784.6	95.9	507.7	97.6	713.5	1105.7	8.6	7.4
OC 2 L	7.6	1470.0	680.0	6.9	158.8	6.8	658.2	90.0	1656.4	1718.8	13.9	18.5
OC 3 L	7.1	1590.0	684.0	6.3	155.2	6.0	691.0	76.4	1571.8	1601.1	10.2	11.6
OC 4 L	6.2	1230.0	782.0	7.0	185.9	6.5	695.8	94.2	1539.8	1599.8	10.2	13.2
OC 5 L	6.4	1360.0	551.0	5.1	142.3	4.7	674.1	65.3	1698.6	1424.6	12.1	9.8
LC 1 Col	0.0	4760.0	2240.0	131.0	922.3	143.3	578.3	137.9	700.6	1330.1	7.0	7.5
LC 2 Col	4.3	1200.0	393.0	4.3	116.6	5.0	614.1	68.0	1673.3	1293.1	13.1	10.9
LC 3 Col	67.3	6540.0	2030.0	122.0	896.6	128.3	607.6	128.7	913.5	1277.1	10.4	8.8
LC 4 Col	32.7	5240.0	2860.0	192.0	1126.1	195.0	706.5	177.0	885.7	1697.8	8.7	9.3
LC 5 Col	37.8	5560.0	2680.0	210.0	1034.2	176.5	711.2	160.3	982.6	1691.6	7.0	8.1
OC 1 Col	36.9	5610.0	2430.0	147.0	938.4	139.8	576.3	132.5	640.6	1837.7	5.1	7.1
OC 2 Col	30.3	6080.0	3610.0	182.0	1471.0	180.6	863.4	217.8	1131.1	3003.0	8.4	12.8
OC 3 Col	32.1	4080.0	2550.0	132.0	1034.2	144.3	633.2	160.3	771.2	1961.8	5.7	8.7
OC 4 Col	39.0	4310.0	1850.0	74.6	793.7	92.0	537.3	113.1	807.8	1820.4	7.3	8.6
OC 5 Col	31.5	5570.0	2310.0	120.0	816.6	116.2	498.9	112.3	646.6	1603.3	6.2	7.5

[c] LC*L = lean control liver sample; OC*L = obese control liver sample; LC*Col = lean control colon sample; OC*Col = obese control colon sample.

Table B3: C1P Concentration (pmole/mg pro)[d]

Sample ID	C14-C1P	C16-C1P	C18-C1P	C18:1-C1P	C20-C1P	C22-C1P	C24-C1P	C24:1-C1P	C26-C1P	C26:1-C1P
LC 1 L	BDL	51.3	664.7	56.1	2.5	BDL	0.1	BDL	0.2	0.3
LC 2 L	BDL	92.3	988.5	28.3	2.0	BDL	0.1	BDL	BDL	0.1
LC 3 L	BDL	55.7	917.0	12.3	BDL	BDL	0.1	BDL	BDL	BDL
LC 4 L	BDL	62.3	956.4	14.1	2.7	BDL	0.1	BDL	0.2	0.1
LC 5 L	BDL	49.9	725.2	7.4	BDL	BDL	BDL	BDL	BDL	BDL
OC 1 L	BDL	62.0	429.3	1.4	BDL	BDL	BDL	BDL	BDL	BDL
OC 2 L	BDL	55.7	251.0	1.4	1.6	BDL	0.0	BDL	BDL	BDL
OC 3 L	BDL	28.3	569.3	1.2	1.1	BDL	BDL	BDL	BDL	BDL
OC 4 L	BDL	33.8	301.5	0.6	0.1	BDL	BDL	BDL	BDL	BDL
OC 5 L	BDL	46.1	663.7	1.3	0.5	0.2	BDL	BDL	BDL	BDL
LC 1 Col	BDL	57.9	179.1	0.6	0.1	BDL	BDL	BDL	BDL	BDL
LC 2 Col	BDL	52.4	742.5	BDL	0.8	BDL	BDL	BDL	0.0	BDL
LC 3 Col	BDL	51.7	685.7	BDL	0.5	BDL	BDL	BDL	BDL	BDL
LC 4 Col	BDL	72.0	658.5	0.8	BDL	BDL	BDL	BDL	BDL	0.1
LC 5 Col	BDL	50.2	660.3	0.5	0.7	BDL	BDL	BDL	BDL	0.1
OC 1 Col	BDL	46.4	126.6	0.1	BDL	BDL	BDL	BDL	BDL	BDL
OC 2 Col	BDL	61.0	301.6	0.3	0.0	BDL	0.3	BDL	BDL	BDL
OC 3 Col	BDL	50.1	198.1	0.1	BDL	0.0	0.0	BDL	BDL	BDL
OC 4 Col	BDL	37.7	105.6	BDL	0.1	BDL	0.0	BDL	0.0	BDL
OC 5 Col	BDL	61.7	241.1	0.0	BDL	BDL	BDL	BDL	BDL	BDL

[d] BDL= below detection level; LC*L = lean control liver sample; OC*L = obese control liver sample; LC*Col = lean control colon sample; OC*Col = obese control colon sample.

Table C4: Sphingosine and S1P[e] Concentration (pmole/mg pro)		
Sample ID	**Sph**	**S1P**
LC 1 L	11.9	BDL
LC 2 L	11.4	BDL
LC 3 L	11.0	BDL
LC 4 L	9.5	0.7
LC 5 L	8.4	BDL
OC 1 L	7.6	BDL
OC 2 L	26.4	BDL
OC 3 L	17.0	0.9
OC 4 L	7.7	BDL
OC 5 L	8.3	1.2
LC 1 Col	4.3	BDL
LC 2 Col	3.6	BDL
LC 3 Col	14.0	1.9
LC 4 Col	5.4	BDL
LC 5 Col	5.2	BDL
OC 1 Col	4.6	BDL
OC 2 Col	11.8	BDL
OC 3 Col	10.5	8.6
OC 4 Col	6.3	BDL
OC 5 Col	4.5	4.4

[e] Sph = sphingosine; BDL = below detection level; LC*L = lean control liver sample; OC*L = obese control liver sample; LC*Col = lean control colon sample; OC*Col = obese control colon sample.

Appendix D

Animal Diet Composition

Table D1: Diet Composition (g/Kg) for Lean and Obese Zucker Rats:

Ingredients	g/Kg
Casein	400.0
L-Cysteine	3.0
Corn Starch	214.536
Maltodextrin	132.0
Sucrose	109.74
Corn Oil	50.0
Cellulose	50.0
Mineral Mix AIN-93-G	35.0
Calcium Carbonate	5.8
Niacin	0.03
Calcium Pantothenate	0.016
Pyridoxine-HCl	**0.007**
Thiamin HCl	0.006
Riboflavin	0.006
Folic Acid	0.002
Biotin	0.0002
Vitamin B_{12} (0.1% in mannitol)	0.025
Vitamin A Palmitate	0.008
Vitamin D_3, cholecalciferol	0.002
DL-Alpha Tocopheryl Acetate	0.15
Vitamin K, phylloquinone	0.0008
Choline Bitartrate	2.5
TBHQ (antioxidant)	0.014